

UNCLASSIFIED

<b>AD NUMBER</b>
AD818532
<b>NEW LIMITATION CHANGE</b>
<b>TO</b> Approved for public release, distribution unlimited
<b>FROM</b> Distribution: Controlled: All requests to Army Materiel Command, Attn: AMCRD-TE, Washington, DC 20315.
<b>AUTHORITY</b>
USAMC ltr 22 Jul 1971

THIS PAGE IS UNCLASSIFIED

AD818532

# ENGINEERING DESIGN HANDBOOK

STATEMENT #5 UNCLASSIFIED

This document may be further distributed by any holder only with  
specific prior approval of *Army Materiel Comd*

*attn: AMCPD-3E  
Wash. DC 20315*

## SPECTRAL CHARACTERISTICS OF

## MUZZLE FLASH

REC'D D D C  
AUG 17 1967  
RECEIVED

HEADQUARTERS  
UNITED STATES ARMY MATERIEL COMMAND  
WASHINGTON, D.C. 20315

AMC PAMPHLET  
No. 706-255

8 June 1967

ENGINEERING DESIGN HANDBOOK  
SPECTRAL CHARACTERISTICS OF MUZZLE FLASH

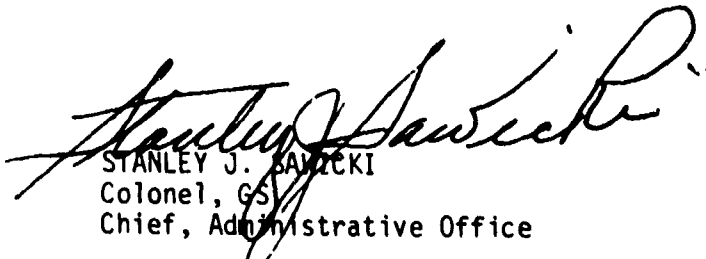
This pamphlet is published for the information and guidance of  
all concerned.

(AMCRD-R)

FOR THE COMMANDER:

K. H. BAYER  
Major General, USA  
Acting Chief of Staff

OFFICIAL:

  
STANLEY J. SAMICKI  
Colonel, GS  
Chief, Administrative Office

DISTRIBUTION:  
Special

## PREFACE

The Engineering Design Handbook Series of the Army Materiel Command is a coordinated series of handbooks containing basic information and fundamental data useful in the design and development of Army materiel and systems. The handbooks are authoritative reference books of practical information and quantitative facts helpful in the design and development of Army materiel so that it will meet the tactical and the technical needs of the Armed Forces.

During the past several years information on the spectral characteristics of muzzle flash has grown considerably in importance, particularly for those concerned with the design of devices for locating the source of weapon fire. The purpose of this handbook is to gather into a single document as much as possible of the information available on the subject. In order to keep this document unclassified some recent classified work (notably that in Ref. 30) has been omitted.

Most of the information was obtained from approximately 75 progress reports on gun flash studies conducted at The Franklin Institute Research Laboratories, between 1946 and 1961. The main purpose of the studies was to determine whether the visible radiation from gun flash could be substantially reduced or eliminated by causing a shift of energy to non-visible portions of the spectrum. While this did not prove to be an effective way to eliminate flash, many of the results are of current interest.

The instruments used for the spectral measurements had less accuracy and fewer capabilities than instruments available now. The handbook therefore includes sections on apparatus and test procedures which should aid the reader in evaluating limitations of the data. In some cases it has been possible to reinterpret the data, making use of new information to modify earlier conclusions.

This handbook was prepared by The Franklin Institute, Philadelphia, Pennsylvania, for the Engineering Handbook Office of Duke University, prime contractor to the Army Research Office—Durham.

Elements of the U. S. Army Materiel Command having need for handbooks may submit requisitions or official requests directly to the Publications and Reproduction Agency, Letterkenny Army Depot, Chambersburg, Pennsylvania 17201. Contractors should submit such requisitions or requests to their contracting officers.

Comments and suggestions concerning this handbook are welcome and should be addressed to Army Research Office—Durham, Box CM, Duke Station, Durham, North Carolina 27706.

## TABLE OF CONTENTS

	Page
PREFACE .....	i
LIST OF ILLUSTRATIONS .....	v
LIST OF TABLES .....	viii
CHAPTER 1. GENERAL DESCRIPTION OF MUZZLE FLASH AND ITS SUPPRESSION .....	1-1
1-1 Muzzle Events Associated with Formation of Weapon Flash .....	1-1
1-2 Description of Different Types of Flash .....	1-2
1-3 Physical Suppression of Muzzle Flash .....	1-3
1-4 Chemical Suppression of Muzzle Flash .....	1-4
CHAPTER 2. SPECTROSCOPIC STUDIES WITH A CALIBER .50 WEAPON .....	2-1
2-1 Introduction .....	2-1
2-2 The Ultraviolet Spectrum of Secondary Flash .....	2-2
2-3 The Visible Spectrum .....	2-2
2-3.1 Visible Spectrum of Intermediate Flash .....	2-2
2-3.2 The Spectral Distribution of the Two Components of Intermediate Flash Observed with an 85-inch Barrel .....	2-4
2-3.3 The Visible Spectrum of Secondary Flash .....	2-6
2-4 The Infrared Spectrum .....	2-6
2-4.1 Introduction .....	2-6
2-4.2 Secondary Flash .....	2-8
2-4.3 Intermediate Flash .....	2-10
2-5 Effect of Propellant Load on Flash Intensity and Other Performance Parameters .....	2-13
2-6 Effect of Barrel Length on Flash .....	2-15
2-7 Summary .....	2-16

## TABLE OF CONTENTS (Cont.)

	Page
CHAPTER 3. SPECTRAL CHARACTERISTICS OF FLASH FROM LARGE-CALIBER WEAPONS .....	3-1
3-1 Introduction .....	3-1
3-2 Relative Spectral Intensity of Flash from 155-mm Artillery Weapon at different distances from gun .....	3-1
3-3 Spectral Emittance of Flash from 155-mm Gun .....	3-3
3-3.1 Test Conditions and Procedure .....	3-3
3-3.2 Calculations .....	3-4
3-3.3 Results .....	3-4
3-3.4 Conclusions .....	3-7
3-4 Additional Data on Flash from 155-mm Gun Obtained with Modified Equipment and Procedure .....	3-9
3-5 Spectral Emittance of Flash from Various Large Caliber Weapons Investigated with an 18-Channel Spectrometer .....	3-9
3-5.1 Introduction .....	3-9
3-5.2 Test Conditions and Procedure .....	3-11
3-5.3 Spectral Emittance of Flash from 280-mm Gun .....	3-12
3-5.4 Data on Spectral Emittance of Flash from Other Large- Caliber Weapons .....	3-12
3-6 Summary .....	3-40
CHAPTER 4. SPECIAL TOPICS .....	4-1
4-1 Variation of Spectra with Time as Studied with an Orthicon Specirograph .....	4-1
4-2 Variations of Breech Pressure and Flash Intensity with Time .....	4-3
4-3 Radiation and Temperature Measurements .....	4-4
4-3.1 Procedure .....	4-4
4-3.2 Results .....	4-5
4-3.3 Conclusions .....	4-5

## TABLE OF CONTENTS (Cont.)

	Page
4-4 Measurements of Flash Temperature by the Line Reversal Technique .....	4-7
4-5 Measurements of Flash Temperature as a Function of Time .....	4-9
4-6 Summary .....	4-11
REFERENCES .....	R-1
GLOSSARY .....	G-1
APPENDICES	
A INSTRUMENTATION .....	A-1
A-1 Introduction .....	A-1
A-2 Special Caliber .50 Test Gun .....	A-1
A-3 Commercial Instruments .....	A-1
A-4 The Image Orthicon Tube .....	A-2
A-5 Infrared Monochromator with Photothermal Detector .....	A-2
A-6 Large-Aperture Spectrograph for Visible and Near-Infrared Radiation .....	A-4
A-7 Ten-Channel Infrared Spectrometer .....	A-4
A-8 Modified Ten-Channel Infrared Spectrometer .....	A-8
A-9 Eighteen-Channel Infrared Spectrometer .....	A-10
B COMPUTATION FOR DATA IN FIGURE 3-1 .....	B-1
C TABLE OF PROPELLANT PROPERTIES .....	C-1/C-2
INDEX .....	I-1/I-2

## LIST OF ILLUSTRATIONS

<u>Fig. No.</u>		<u>Page</u>
1-1	Flow Pattern at a Gun Muzzle .....	1-1
1-2	Primary, Intermediate, and Pre-flash .....	1-2
1-3	Development of Muzzle Glow from Special Caliber .50 Test Gun .....	1-3
2-1	Comparison of Visible Spectral Distribution of Intermediate and Secondary Flash .....	2-3
2-2	Visible Spectrum of Two Components of Intermediate Flash .....	2-5
2-3	Effect of Projectile Material on Visible Spectrum of Secondary Flash .....	2-7
2-4	Spectral Distribution of Infrared Radiation from Secondary Flash .....	2-9
2-5	Spectral Distribution of Infrared Radiation from Secondary Flash. (Plotted against wave number.) .....	2-10
2-6	Spectral Distribution of Radiant Energy from Flash Obtained with Various Propellants and Barrel Lengths .....	2-12
2-7	Effect of Load on Velocity, Pre-flash, Intermediate Flash, Muzzle Pressure, and Maximum Chamber Pressure .....	2-14
2-8	Variation of Peak Radiant Intensity with Barrel Length for Various Charges .....	2-17
3-1	Variation of Spectral Distribution of Radiation from Secondary Flash with Distance from the Gun .....	3-2
3-2	Arrangement of Field-Test Equipment for Observing Gun Flash .....	3-3
3-3	Spectral Emittance of Unsuppressed Flash from 155-mm Gun .....	3-8
3-4	Examples of Spectrographic Records for Unsuppressed Flash .....	3-9
3-5	Spectral Emittance of Suppressed Flash from 155-mm Gun .....	3-10
3-6	Examples of Spectrographic Records for Suppressed Flash .....	3-11
3-7(A)	Spectrograms of Flash from 280-mm Gun .....	3-13
3-7(B)	Spectrograms of Flash from 280-mm Gun .....	3-14

## LIST OF ILLUSTRATIONS (Cont.)

<u>Fig. No.</u>		<u>Page</u>
3-8	Apparent Spectral Emittance of Unsuppressed Flash from 280-mm Gun .....	3-15
3-9	Comparison of Apparent Spectral Emittances of Unsuppressed Flash from 155-mm and 280-mm Guns .....	3-17
3-10(A)	Apparent Spectral Emittance of Flash from Large-Caliber Weapons .....	3-20
3-10(B)	Apparent Spectral Emittance of Flash from Large-Caliber Weapons .....	3-21
3-10(C)	Apparent Spectral Emittance of Flash from Large-Caliber Weapons .....	3-22
3-10(D)	Apparent Spectral Emittance of Flash from Large-Caliber Weapons .....	3-23
3-10(E)	Apparent Spectral Emittance of Flash from Large-Caliber Weapons .....	3-24
3-11(A)	Spectrometer Traces .....	3-29
3-11(B)	Spectrometer Traces .....	3-30
3-11(C)	Spectrometer Traces .....	3-31
3-11(D)	Spectrometer Traces .....	3-32
3-11(E)	Spectrometer Traces .....	3-33
3-11(F)	Spectrometer Traces .....	3-34
3-11(G)	Spectrometer Traces .....	3-35
3-11(H)	Spectrometer Traces .....	3-36
3-11(I)	Spectrometer Traces .....	3-37
3-11(J)	Spectrometer Traces .....	3-38
3-11(K)	Spectrometer Traces .....	3-39
4-1	Variation of the Spectral Distribution of Secondary Flash With Time .....	4-2
4-2	Variation of Breech Pressure and Intensity of Muzzle Glow With Time .....	4-3
4-3	Variation of Breech Pressure and Flash Intensity With Time .....	4-4
4-4	Spectral Distribution of Secondary Flash Superimposed on Continuous Background from Tungsten Filament at 1900°K .....	4-10
4-5	Spectral Distribution of Secondary Flash Superimposed on Continuous Background from Tungsten Filament at Various Temperatures .....	4-12

## LIST OF ILLUSTRATIONS (Cont.)

<u>Fig. No.</u>		<u>Page</u>
4-6	Variation in Temperature of Secondary Flash With Time.....	4-13/4-14
A-1	Special Artillery-Type, Banded Steel Projectile .....	A-1
A-2	Schematic Diagram of Monochromator .....	A-3
A-3	Schematic Diagram of Large Aperture Spectrograph .....	A-5
A-4	Optical System of Infrared Spectrograph .....	A-6
A-5	Beam Splitting Mirrors for Infrared Spectrograph .....	A-7
A-6	Optical System of the Modified Ten-Channel Spectrometer .....	A-9
A-7	Optical System of the 18-Channel Spectrometer .....	A-10
A-8	Block Diagram of the Detecting and Recording System of the 18-Channel Spectrometer .....	A-11/A-12

## LIST OF TABLES

<u>Table No.</u>		<u>Page</u>
2-1	Spectral Distribution of Visible Energy in Secondary Flash .....	2-6
2-2	Wavelength-Intensity Data for Infrared Radiation of Secondary Flash .....	2-11
2-3	Influence of Barrel Length on Frequency of Secondary Flashes .....	2-15
2-4	Influence of Barrel Length on Intensity of Muzzle Glow .....	2-16
3-1	Apparent Spectral Emittance of Unsuppressed Flash From 155-mm Gun .....	3-5
3-2	Spectral Emittance as a Function of Time for Rounds that are Representative of Unsuppressed Flash from 155-mm Gun .....	3-5
3-3	Spectral Emittance of Suppressed Flash from 155-mm Gun .....	3-7
3-4	Comparison of Wavelengths of Flash Emittance Peaks and of CO <sub>2</sub> and H <sub>2</sub> O Absorption Bands .....	3-7
3-5	Spectrographic Data for 280-mm Gun .....	3-16
3-6	Explanation of Maxima and Minima of Spectral Emittance Curves in Figure 3-8 .....	3-16
3-7	Summary of Emittance Data on Flash from Large-Caliber Weapons .....	3-18
3-8(A)	Average Values of the Apparent Spectral Emittance of Flash from Large-Caliber Weapons .....	3-25
3-8(B)	Average Values of the Apparent Spectral Emittance of Flash from Large-Caliber Weapons .....	3-26
3-8(C)	Average Values of the Apparent Spectral Emittance of Flash from Large-Caliber Weapons .....	3-27
4-1	Summary of Flash Temperature Measurement Data .....	4-6
4-2	Flash Temperature Measured by the Line Reversal Method .....	4-8
B-1	Relative Intensity of Radiation from Secondary Flash Produced by 155-mm Gun as a Function of Wavelength and Distance from Source .....	B-2
C-1	Table of Propellant Properties .....	C-1/C-2

## CHAPTER 1

## GENERAL DESCRIPTION OF MUZZLE FLASH AND ITS SUPPRESSION \*

1-1 MUZZLE EVENTS ASSOCIATED WITH FORMATION OF WEAPON FLASH.<sup>14\*\*†</sup>

The sequence of events at the muzzle of a gun after the projectile leaves the barrel is briefly as follows:

(a) Since none of the common propellants contain sufficient oxygen for complete combustion, the gases which emerge from the gun muzzle contain considerable amounts of the combustible gases, CO and H<sub>2</sub>, along with CO<sub>2</sub>, N<sub>2</sub>, H<sub>2</sub>O, oxides of nitrogen, and a few other minor constituents, including various inorganic residues from small amounts of salts present in the propellant and from the projectile and the barrel. These gases continue to escape from the gun muzzle for an appreciable length of time after the projectile has left the muzzle; and the physical and chemical effects which accompany this escape determine the nature of the muzzle flash. The propellant gases are at a high temperature and pressure at the gun muzzle and are moving with a velocity which is probably close to the local velocity of sound. The temperature at this point is sufficiently high to cause the emission of visible radiation which appears on photographs as a small spot of light just at the muzzle. This is referred to as *primary flash*.

(b) Since the pressure of the emergent gases near the muzzle is greater than atmospheric pressure, the gases acquire a component of motion radially outward from the axis of the gun. Thus, as the gases leave the muzzle, they expand adiabatically and are cooled so that they cease to radiate visible light. The velocity of the gases increases somewhat during expansion, while the cooling causes the local velocity of sound to fall so that the gases are then moving at a supersonic velocity. The radial momentum actually causes an overexpansion to below atmospheric pressure before the pressure of the surrounding atmosphere causes the gases to turn radially inward toward the axis. The

inward turning is accomplished by the generation of stationary compression waves, at the boundary between muzzle gas and air, which build up into a shock wave oriented normal to the direction of flow and located at a considerable distance from the muzzle.

(c) The flow pattern at a gun muzzle—as deduced from photographic techniques, pressure measurements, and composition measurements—is indicated in Figure 1-1. The region bounded by the muzzle, the normal shock front, and weak lateral shocks is called the shock bottle. Within the shock bottle and extending partly beyond the normal shock, there is a region (bounded by the inner dashed line in Figure 1-1) which

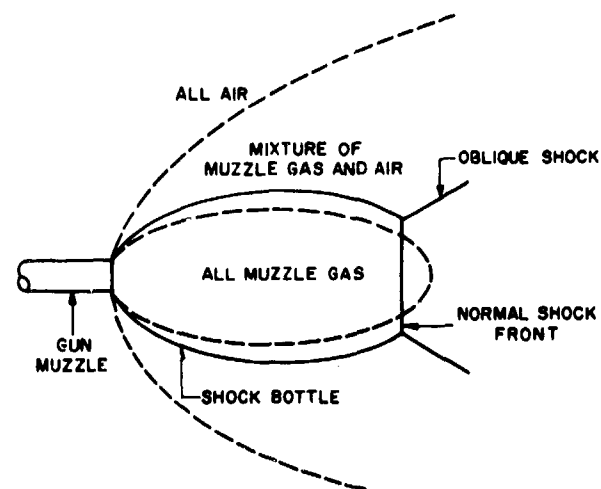


FIGURE 1-1—FLOW PATTERN AT A GUN MUZZLE (FROM REF. 11b)

(DASHED LINES INDICATE COMPOSITION BOUNDARIES)

\*This handbook was written by S. P. Carfagno, The Franklin Institute Research Laboratories. It has been reviewed for technical content and style, respectively, by G. P. Wachtell and G. Cohn, also of FIRL.

\*\*Superscript numbers indicate items in the Reference list following Chapter 4.

†In order to be consistent with the terminology of the source data used in the preparation of this handbook, the word "flash" includes radiation in the visible, ultraviolet, and infrared spectrum.

is not penetrated by atmospheric air during the period of approximately steady flow following the initial emergence of muzzle gases.

(d) On passing through the normal shock front, the gases are decelerated to a subsonic velocity, compressed, and consequently heated to a temperature of the same order as that at the gun muzzle (and possibly even higher). This temperature is sufficiently high to cause the gases and smoke particles in this region to radiate, giving rise to what is termed *intermediate flash*. This flash is usually characterized by a sharp boundary which corresponds to the normal shock on the side toward the gun. Finally, the muzzle gases—having been heated in the region of intermediate flash and mixed with the surrounding air—ignite and burn with a large, luminous flame. This flash, which is called the *secondary flash*, is much more voluminous than the intermediate flash and is responsible for the bulk of the visible radiation from gun flash. Burning of the combustible gas releases an amount of energy that is actually comparable to that released in the original propellant burning inside the gun. It is therefore not surprising that, in the case of artillery weapons, the resultant secondary muzzle flash is not only visible for miles and blinding to the gunners but also produces an excessive amount of noise and blast near the gun.

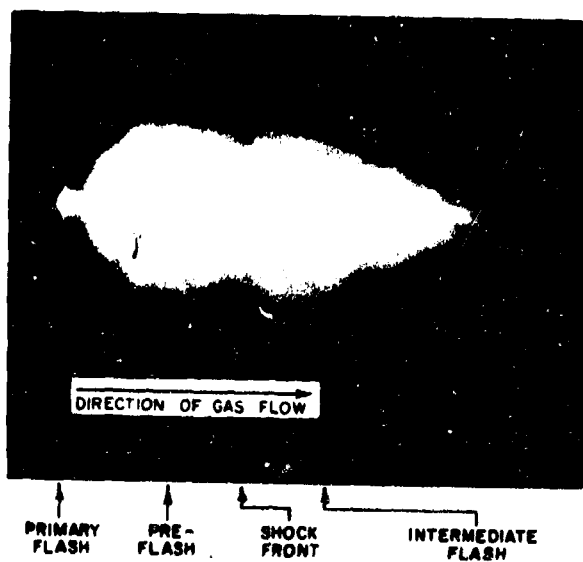


FIGURE 1-2—PRIMARY, INTERMEDIATE, AND PRE-FLASH (FROM REF. 5c)

In summary, muzzle flash results from a sequence of events in which overexpansion of the muzzle gases causes the formation of a normal shock wave. The shock wave causes a considerable elevation in the temperature of the muzzle gases and the consequent formation of intermediate flash. When they mix with the ambient air, the heated muzzle gases may ignite—giving rise to the voluminous flame called secondary flash. In addition, there is evidence that, when there is considerable leakage of propellant gases past the projectile while the latter is still in the barrel, these gases give rise to a muzzle flash occurring before the projectile emerges from the muzzle.

## 1-2 DESCRIPTION OF DIFFERENT TYPES OF FLASH

The various types of flash, Figures 1-2 and 1-3, that have been observed can be described as follows:

(a) Primary Flash — A small zone immediately adjacent to the muzzle of the gun, being simply an extension of the flash inside the barrel. It may exist before or after projectile emergence, or at both times, depending upon whether an appreciable amount of leakage of the propellant gases around the projectile occurs. It may be a white flash, indicative of actual burning, or it may be a reddish glow due to incandescent solids being present in a hot, compressed volume of gas.

(b) Pre-flash — A low-pressure burning of gases which have leaked around the projectile before its emergence from the barrel. Experiments have shown that the combustion is supported by oxygen within the barrel before a round is fired. <sup>5(c), 7(a)</sup> While pre-flash is initiated before projectile emergence, its time duration may vary considerably—depending upon the amount of gas leakage and the resulting temperature and pressure of the gases responsible for pre-flash. In fact, although it *starts* before projectile emergence, in cases of excessive leakage the pre-flash may extend in time beyond projectile emergence, and extend in size sufficiently to ignite secondary flash some distance from the muzzle.

(c) Intermediate Flash — A usually triangular-shaped incandescent zone which

GUN MUZZLE →  
DIRECTION OF GAS FLOW →

AMCP 706-255

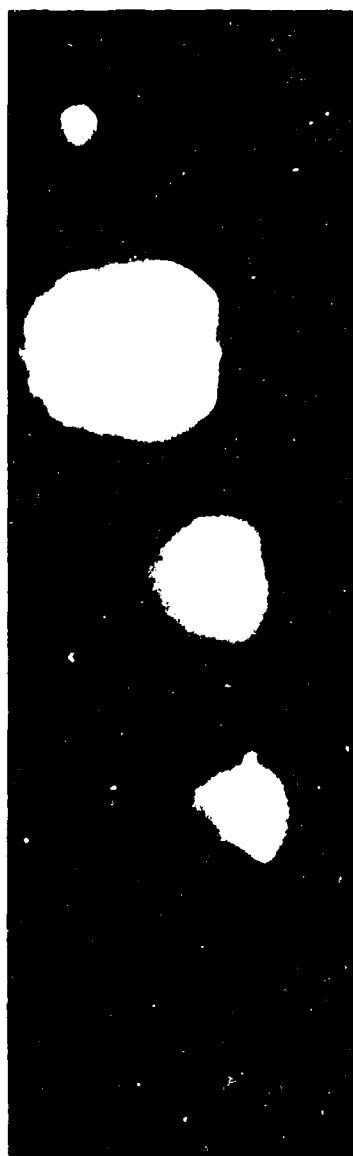


FIGURE 1—3—DEVELOPMENT OF MUZZLE GLOW FROM SPECIAL CALIBER .50 TEST GUN (FROM REF. 5c)

BARREL LENGTH, 85 IN.  
CHAMBERED FOR 20-MM CASES

appears approximately 20 calibers ahead of the muzzle. The base of the triangular zone has been found to coincide with the strong shock front forming the nearly flat forward boundary of the shock bottle; the apex of the triangle points away from the gun. The color of this flash is usually red or reddish-orange and the temperature is roughly 1200° to 1500°K. This is to be contrasted with secondary flash which appears as a bright-

yellow flash with a temperature of approximately 2200°K.

(d) Muzzle Glow— An illumination of the zone enclosed by the shock bottle. This zone extends from the muzzle to the shock front responsible for intermediate flash and has lateral boundaries coincident with the shock bottle. This is a very weak, rarely observed flash.

(e) Secondary Flash— A large voluminous flash which is initiated in or near the intermediate flash region and spreads in all directions. This flash is a low-pressure burning of combustible gases which have issued from the muzzle of the gun and mixed with atmospheric air.

### 1-3 PHYSICAL SUPPRESSION OF MUZZLE FLASH

Since it appears that the normal shock wave serves as a means for raising the temperature of muzzle gas to the point where it may ignite when mixed with air, it would seem that it ought to be possible to eliminate flash by devising mechanical means for preventing the formation of shock fronts. The function of the flash suppressor is to control the process by which the hot combustible muzzle gases mix with the cool air surrounding the gun so that conditions of temperature, composition, and pressure under which the gas would ignite are avoided. The best that a mechanical suppressor can do is to cause this mixing to take place at atmospheric pressure.\* Thus, the *ideal* suppressor is regarded as a device for controlling the escape of muzzle gases so that they are released at atmospheric pressure. Real suppressors do not accomplish this; it is believed that their effectiveness results largely from their ability to prevent formation of the normal shock wave which otherwise develops at some distance downstream of the muzzle.

As described in par. 1-4, chemical flash suppression has the disadvantage of producing large quantities of smoke. While mechanical suppressors do not have this tendency, a major difficulty is that an adequate device may prove cumbersome and be unacceptable because of size and weight.

\*See page 74 of Ref. 13.

A fairly successful mechanical method for suppressing flash utilizes a cone-shaped *bider*.<sup>1,3</sup> The cone, which is attached to a gun at the muzzle, is regarded as a device for expanding the muzzle gases to near atmospheric pressure before allowing them to mix with the surrounding air. In this case, the emerging gases do not overexpand and there should be no consequent formation of a shock wave.

Another type of mechanical suppressor consists of muzzle attachments which include two or more bars extending beyond the muzzle, arranged symmetrically about the gun axis.<sup>10(a to d)</sup> Very effective suppression was obtained with such devices in a variety of small arms. Studies using the shadowgraph technique indicated that the effectiveness of the bar-type suppressor is a consequence of its preventing formation of the normal shock wave which gives rise to the intermediate flash. Attempts to apply the bar-type suppressor to larger caliber weapons have been only partially successful. The lower effectiveness is thought to involve several differences between artillery weapons and small arms. The smaller barrel length-to-caliber ratio in artillery weapons results in less expansion of the muzzle gases prior to projectile emergence; consequently, less cooling occurs. Also, the longer times involved in large guns for any process, such as the time of outflow of gases from the muzzle, allow more opportunity for the induction times of chemical reactions to be exceeded; and this facilitates initiation of the combustion associated with secondary flash.

A generalized theory of mechanical flash suppressors was developed without making any assumptions about the shape or size of the suppressor.<sup>11(a), 15</sup> With this theory it is possible to calculate the temperature of the muzzle gas-air mixture outside a gun equipped with an *ideal* suppressor. It was learned that in some weapons these temperatures exceed the minimum ignition temperatures of the muzzle gas-air mixture at atmospheric pressure, so that even an *ideal* suppressor could not eliminate flash from such weapons. A theory was also developed for the design of *ideal* mechanical suppressors to accomplish the aim of permitting muzzle gas to mix with air only at atmospheric

pressure.<sup>12</sup> The theory applies to the period of approximately steady conditions that follows projectile emergence. Whenever secondary flash occurs, it is almost certain that ignition starts during this period. The highly transient nature of events preceding and following the steady period makes it impractical to design a single device which will be completely satisfactory over the entire range of conditions. It was found that the theoretically *ideal* suppressor would be a cumbersome device even for small calibers. Empirically, much simpler devices have been found to be adequate for caliber .30 and caliber .50 weapons. For large-caliber weapons, however, the use of mechanical devices to prevent flash has not proved feasible.

One of the physical approaches to the problem of suppressing gun muzzle flash involves modification of the propelling charge itself. The object is to lower the temperature of the muzzle gases so that they remain below their ignition temperature. Within limits, this temperature can be lowered by increasing the thermodynamic efficiency of the weapon. The case may be stated simply thus:

The burning of a given weight of propellant releases a certain amount of energy. Part of this energy is transferred to the projectile. If minor losses are neglected, the remainder of the energy appears in the propellant gases. If a greater fraction of this available energy is given to the projectile, then less will remain in the gases. Thus they will be cooler and less susceptible to ignition.

There are, of course, limitations to this method of eliminating gun muzzle flash. For example, one frequently encounters difficulty in keeping the chamber pressure within reasonable limits when attempting to increase the thermodynamic efficiency of a weapon.

#### 1-4 CHEMICAL SUPPRESSION OF MUZZLE FLASH

Another approach to the solution of the flash problem is chemical rather than physical. The most common chemical method involves the addition of about one percent of an alkali metal salt, usually potassium sulfate, to the propellant. Various studies have

indicated that this method functions by providing a chain-breaking mechanism in the scheme of muzzle gas-air reactions.<sup>14</sup> The gross effect of the chemical additive may be to increase the ignition limits and/or the ignition delays of the muzzle gas-air mixtures sufficiently to prevent ignition. This eliminates the secondary flash but not the intermediate flash which results from the radiation of heated gases and particles instead of a combustion process.

The principal objection to the use of chemical suppressants is that they contribute to the generation of excessive gun smoke.

From the difficulties encountered with physical approaches it is evident that a chemical suppressant would provide the ideal solution to the problem if one could be found that was effective, did not have any undesirable effects on the weapon's performance, and did not produce smoke. Although hundreds of substances have been added to propellants in the attempt to find superior chemical suppressants, the performance of the best ingredients has not been appreciably different from that of potassium sulfate.<sup>18</sup> It is thought that organic suppressants might be less likely to generate excessive smoke; however, their use has been hampered by other difficulties, such as their inability to survive gun conditions.

## CHAPTER 2

## SPECTROSCOPIC STUDIES WITH A CALIBER .50 WEAPON

## 2-1 INTRODUCTION

Until World War II, most of the work on the spectrum of gun flash had been done by British investigators.\* For several years, beginning in 1946, a substantial effort directed partly toward prevention of gun flash was conducted in this country. One of the principal aims of the early U. S. effort was to determine whether propellant and projectile could be modified in ways that would cause radiant energy emitted by the muzzle gas in the visible region to be diverted into non-visible regions of the spectrum. Although this effort was eventually judged to be unfeasible and more practical methods of suppressing gun flash were investigated, the data obtained on the spectral characteristics of gun flash have acquired considerable importance in recent years. Such data are of particular interest to those who need to devise methods for locating the source of gun firing.

This chapter records the information obtained on flash from caliber .50 guns. An extensive investigation of secondary and intermediate flash was conducted. The weapon that was used in most of the tests was a special caliber .50 gun that was chambered for 20-mm cartridge cases. (See Appendix A-2.)

From emission spectra it was determined that the emitters responsible for practically all of the visible radiation superimposed on the continuum radiation are potassium, sodium, and calcium and copper compounds. All of these emitters are impurities in the propellant gases. The main source of the copper responsible for the copper oxide and copper hydroxide bands is the gilding metal jacket on the projectile. The visible radiation from intermediate flash is principally continuum and sodium-line radiation. There is some CaOH radiation, but the CuO and CuOH bands are not excited in the intermediate flash region even when powdered copper oxide is added to the propellant.\*\* By

far the largest portion of radiation from gun flash lies in the infrared region, where it is characterized by the emission bands of CO<sub>2</sub> and H<sub>2</sub>O. In tests with a caliber .50 gun it was found that less than 1 percent of the radiation energy was in the visible range of the spectrum.

A wide-aperture, image-orthicon visible spectrograph was constructed to obtain the variation of the spectral distribution of gun flash with time. While no new emitters were detected by the use of this instrument, with the exception of a water-vapor band in the vicinity of 9400 Å, it helped show that the peak intensity from the potassium-line radiation is reached at a different time from that corresponding to sodium and some of the other emitters. This was one of the earliest clues to the action of potassium atoms as inhibitors of secondary flash. Chemical kinetic studies later established that the role of potassium as a flash suppressor rests in its action as a breaker of one or more of the chain reactions which ultimately lead to the explosion associated with secondary flash.<sup>14</sup>

Practically all of the radicals involved in the hydrogen-oxygen and carbon monoxide-oxygen chain-reaction system have emission and absorption spectra in the near visible or ultraviolet regions of the spectrum. The ultraviolet emission spectrum of secondary flash, recorded on an ultraviolet sensitized plate by means of the quartz spectrograph, verified the presence of the ultraviolet line and band structure.

---

\*Some of the highlights of this work are summarized in Section VII of Ref. 17.

\*\*Note that some of the compounds which contribute to flash radiation are high temperature species which do not exist at ordinary temperatures.

## 2-2 THE ULTRAVIOLET SPECTRUM OF SECONDARY FLASH

Very little information is available on the ultraviolet radiation of gun flash. A few measurements were made with the intention of determining what radicals are present in the muzzle gas and what role they play in the combustion reactions.<sup>5(c), 9(a)</sup> Because of the limitations of the available instruments, however, the measurements were limited to the near ultraviolet region; and the work did not proceed very far.

Three spectrographs were used for these studies: A Hilger medium quartz, a Hilger small quartz and a large-aperture glass instrument constructed at The Franklin Institute (see Appendix A-6). The lower wavelength limit of the large-aperture spectrograph was about 4000 Å, not low enough for the observation of ultraviolet spectra; but the dispersion of 20 Å/mm at 4000 Å proved useful in the identification of the potassium doublet at 4044 and 4047 Å. Eastman Kodak plates 103-O, especially sensitized to ultraviolet radiation, were used throughout this work. The plates were taped in place in the plate holders, and all movable parts of the spectrographs were fixed in position in order to withstand the repeated blasts of the gun fire during exposure. Since the radiation emitted by secondary flash is comparatively weak in this region, it was necessary to integrate the radiation from many rounds — up to 2000 being necessary to give sufficient exposure for identification of some of the bands. For longer exposures, a caliber .50 HB Browning machine gun was used with unsalted IMR-type propellant, the firing being in bursts of 50 rounds. For shorter exposures, the special caliber .50 test gun\* was used, firing unsalted IMR-type propellant and Ball M2 projectiles. An iron-arc comparison spectrum was photographed together with all the flash spectra to aid in wavelength measurement.

The spectra showed the following emitters superimposed on a rather weak continuum:

- (a) Strong lines of atomic potassium at 4047—4044 Å;
- (b) Medium strength atomic copper at 3274—3248 Å;

- (c) Strong bands of CuCl which, according to Pearse & Gaydon,<sup>19</sup> belong to the B, C, D, and E systems. These extended between approximately 4300 Å and 4900 Å;
- (d) Two fairly strong bands which were identified as the (0, 0) and (1, 0) bands of CuH at 4280 and 4005 Å, respectively;
- (e) Weak OH bands, (0, 0) and (1, 0), at 3064 and 2811 Å, respectively; and
- (f) Very weak NH bands, (0, 0) and (1, 1), at 3360 and 3370 Å, respectively.

A careful examination of the plates failed to reveal the presence of the following radicals which are often present in flames: C<sub>2</sub> Swan bands, CN, CH, and HCO.

## 2-3 THE VISIBLE SPECTRUM

### 2-3.1 THE VISIBLE SPECTRUM OF INTERMEDIATE FLASH<sup>4(e), 9(a)</sup>

A photograph of the spectrum of intermediate flash was obtained by firing 200 rounds of IMR propellant in the special caliber .50 test gun (with 20-mm chamber). Ball M2 projectiles were used. The length of the barrel was 85 in., which is too long to allow the production of secondary flashes under normal conditions of firing.

A spectral distribution curve for intermediate flash obtained from the spectrum plate, with a curve for secondary flash included for comparison, appears in Figure 2-1. The data were corrected for plate sensitivity. The sharp peak near 5890 Å is due to sodium emission. The other peaks are due to emission by CaOH, CuO, and CuOH.\*\* It should be emphasized that, although these curves appear to be fitted together near the sodium line, no wavelength adjustment was made. The ratio of intensities on the two curves at a given wavelength is dependent

\*See Appendix A-2.

\*\*Some of the bands initially thought to be those of CaO and CuO are now thought, on the basis of newer measurements, to be those of CaOH and CuOH.<sup>31</sup>

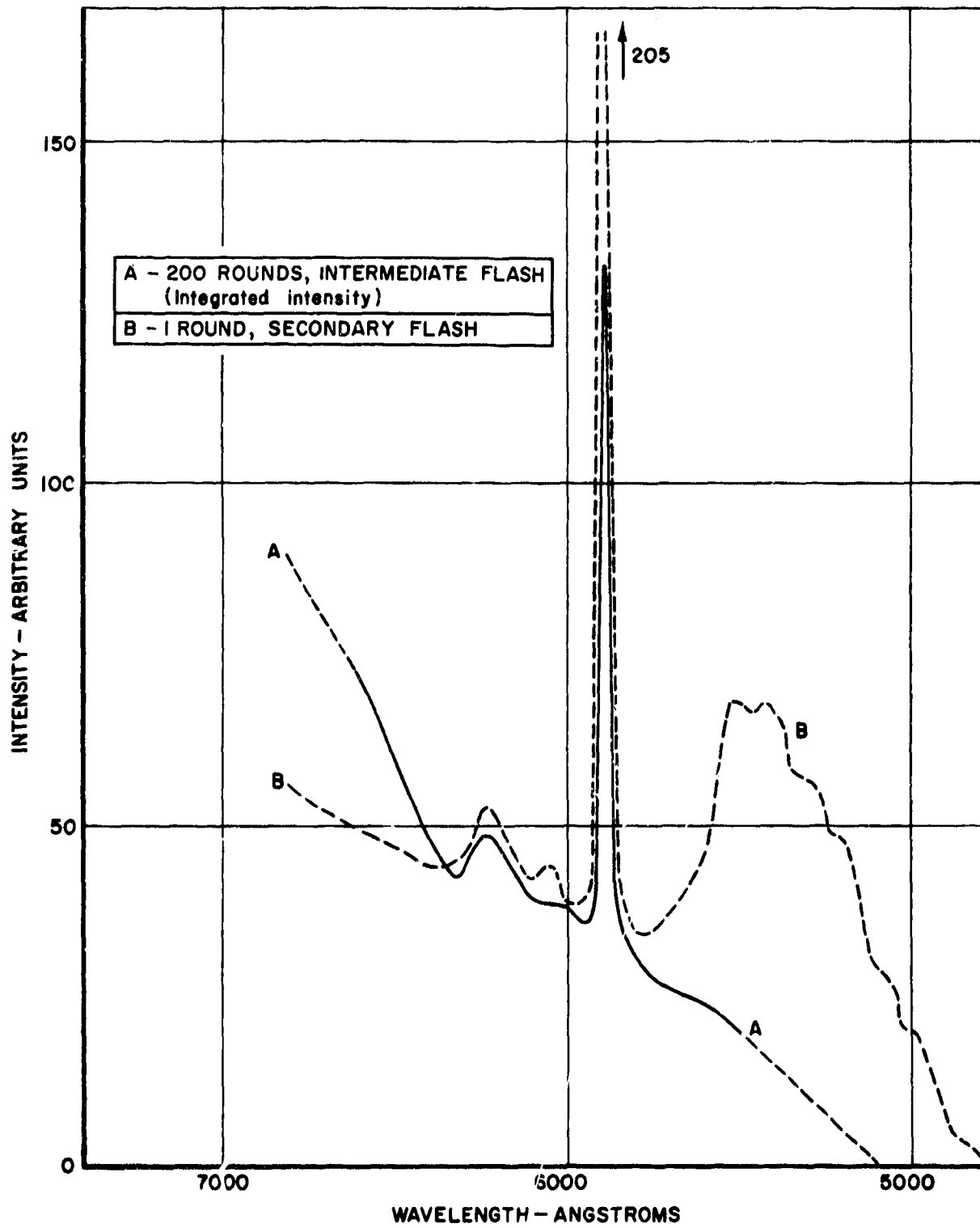


FIGURE 2-1 — COMPARISON OF VISIBLE SPECTRAL DISTRIBUTION OF INTERMEDIATE AND SECONDARY FLASH (FROM REF. 4a)

TEST CONDITIONS: SPECIAL CALIBER .50 GUN WITH 30-MM CHAMBER,  
BARREL LENGTH 85 IN., IMR PROPELLANT, BALL M2 PROJECTILES

on the fact that one curve represents 1 round of secondary flash while the other represents the integrated intensity from 200 rounds of intermediate flash.

An examination of the curves shows that the intermediate flash has a small peak at 6230 Å due to CaOH emission; but no CuO or CuOH radiation was observed. This was probably due to the fact that the temperature in the region of intermediate flash is considerably lower than the temperature generated when the combustion associated with secondary flash occurs. It is also possible that the copper particles pass through the intermediate flash region too rapidly to react. Further tests showed that the CuO and CuOH bands are not excited in the intermediate flash region even when powdered copper oxide is added to the propellant.<sup>5(b)</sup>

In summary, it was found that intermediate flash from a caliber .50 gun, using IMR propellant, is principally continuum—with some Na and CaOH radiation, but no radiation due to copper compounds. The observed prominence of the continuum supports the attribution of the major part of the luminosity of intermediate flash to incandescent solids.

### 2-3.2 SPECTRAL DISTRIBUTION OF THE TWO COMPONENTS OF INTERMEDIATE FLASH OBSERVED WITH AN 85-INCH BARREL.<sup>5(a)</sup>

Studies of intermediate flash obtained by firing an IMR type propellant in a caliber .50 gun with an 85-in. barrel indicated that the continuum was relatively more predominant in intermediate than in secondary flash; that while there was some calcium hydroxide and sodium radiation, it was fairly weak; and that radiation due to copper compounds was absent (see par. 2-3.1).

It was also observed that the intermediate flash often consisted of two distinct parts: (a) a small comparatively intense part, designated Part A for convenience, the center of which was approximately 5 in. from the gun muzzle; and (b) a large hazier portion, designated Part B, which started approximately 8 in. from the muzzle—the center of the region being about 11 or 12 in. from the muzzle. The smaller part tended to merge with the larger portion as firing of a run progressed,

particularly when copper-banded artillery-type projectiles\* were used. By using a condensing lens in connection with the large-aperture spectrograph, spectra were obtained of both parts of the intermediate flash.

The wavelength vs intensity curve of Part A is shown in Figure 2-2. This spectrum was obtained from 150 rounds of EX6332 propellant (coated nitrocellulose, 0.7% K<sub>2</sub>SO<sub>4</sub>) in an 85-in. gun with artillery-type projectiles. In order to avoid merging of the two parts of the flash, which took place if firing was too prolonged, the rounds were fired in groups of about 30 rounds each. A similar curve for Part B, obtained by firing 350 rounds of EX6332 propellant in the same gun and using the same type of projectiles, is also shown in Figure 2-2.

From a comparison of the two curves in Figure 2-2, taking into consideration the number of rounds fired\*\*, certain conclusions are indicated:

- (a) The intensity of Part A of the flash, as indicated by the spectrograph, is approximately 4 or 5 times that of Part B. It should be noted that these intensities do not refer to total intensity, but only to that portion of each part of the flash which lies within the field of the spectrograph. Since the volume occupied by Part B of the flash is larger than the volume of Part A, it is possible that the total intensities are of the same order.
- (b) The continuum radiation in both cases is relatively more predominant than in the case of secondary flash. For comparison, a typical curve for secondary flash is shown in Figure 2-1.
- (c) Emission by calcium hydroxide and sodium is relatively weak in intermediate flash. This is particularly true of Part B where calcium hydroxide radiation was not detected, and that of sodium was very weak.

\*See Figure A-1, Appendix A-2.

\*\*The curve for Part A in Figure 2-2 should be multiplied by the ratio 350/150 to make it comparable with the curve for Part B.

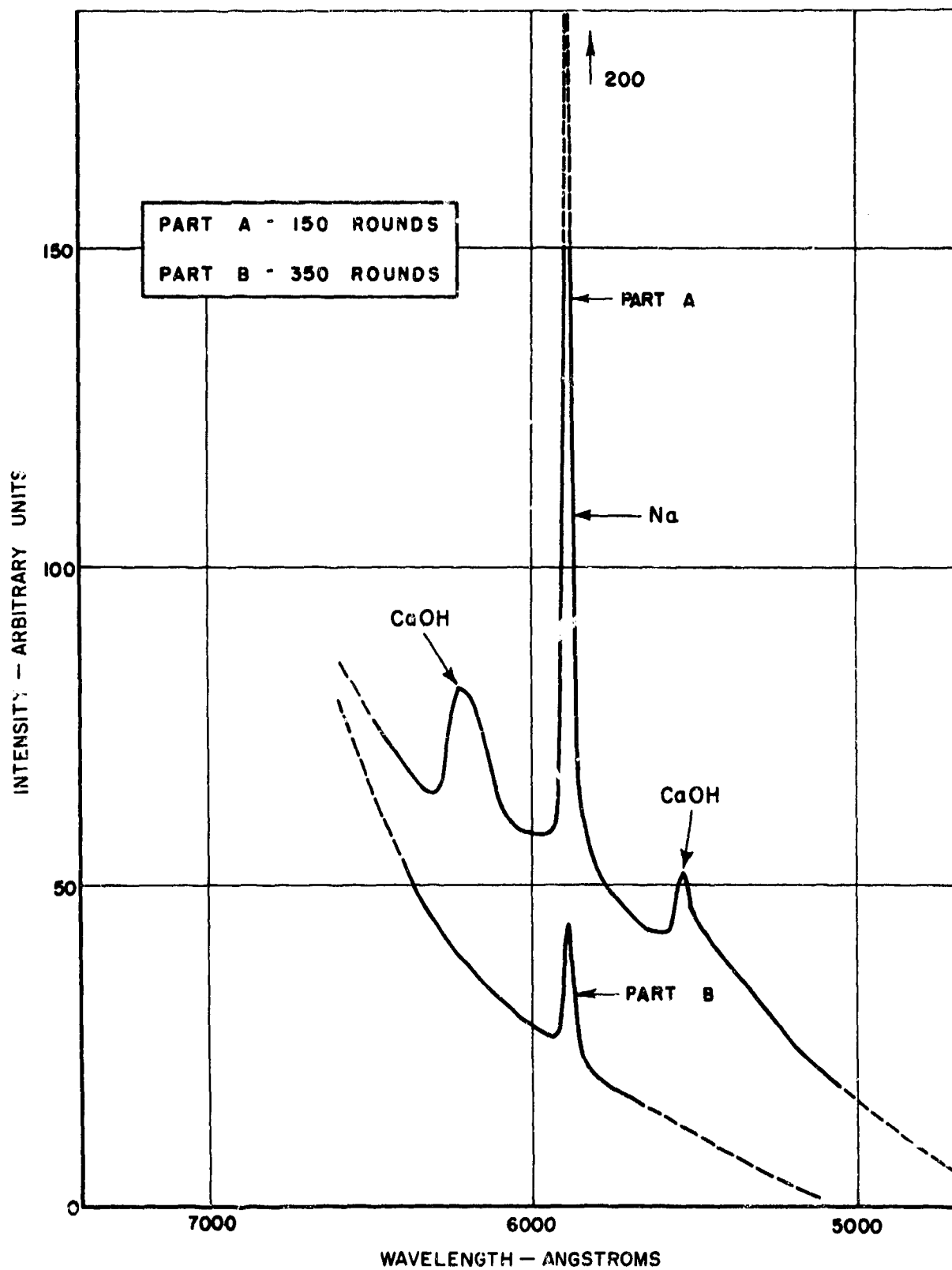


FIGURE 2 - 2 - VISIBLE SPECTRUM OF TWO COMPONENTS OF INTERMEDIATE FLASH (FROM REF. 5a)

- (d) Radiation due to copper compounds was not detected in either part of the intermediate flash. Two possible explanations for the absence of this radiation are (1) that, while copper may be present in the gases in the intermediate flash region, it does not react until the gases are mixed with atmospheric oxygen in the secondary flash region; (2) that copper compounds may be present but are not excited under the conditions of pressure and temperature which obtain in the intermediate flash region.

Since the radiation from both parts of the intermediate flash appears to be mostly continuum, comparatively free from the influence of discrete band radiation, a calculation of temperature based on Wien's radiation law\* for a black body should give at least an approximation of the temperatures involved. Such calculations were carried out using the ratio of intensities at several different wavelengths. The temperature so calculated for Part A varied between 2200° and 2500° K, and for Part B between 1200° and 1500° K. These results are difficult to reconcile with the geometry of the two types of flash, which indicated that the more intense Part A was probably located within the shock bottle and that Part B was located downstream of the normal shock wave—where intermediate flash is usually located. In the absence of combustion, temperatures would be expected to be higher in region B (downstream of the shock wave) than in region A (upstream of the shock wave). While its high temperature would indicate that combustion was responsible for Part A, it is difficult to understand how combustion could occur inside the shock bottle where there is no oxygen from the atmosphere (see par. 1-1). If the combustion were a continuation of burning within the barrel, instead of resulting from ignition outside the gun, one would have expected the flame to stream directly out of the muzzle.

#### 2-3.3 THE VISIBLE SPECTRUM OF SECONDARY FLASH 4(•)

Curve B, Figure 2-3, shows the distribution of energy in a secondary flash obtained

by firing nitrocellulose propellant (EX6333, DNT coated) in the caliber .50 test gun with Ball M2 projectiles. Curves obtained from spectrum plates by use of the Leeds & Northrup recording microphotometer were corrected for plate sensitivity before being plotted in the above figure. An analysis of these curves indicated that the energy emitted in the visible region by a normal secondary flash can be attributed to the sources which are listed in Table 2-1 together with the average values of their relative contributions.

TABLE 2-1  
SPECTRAL DISTRIBUTION OF VISIBLE ENERGY  
IN SECONDARY FLASH \*\*

CuO and CuOH	50%
CaOH	25%
Na	7%
Miscellaneous (Probably Continuum)	18%

When steel bullets with steel rotating bands were used in place of Ball M2 projectiles, the character of the distribution curve for secondary flash was altered. This is indicated by Curve A in Figure 2-3. Note that, while calcium hydroxide radiation persisted, radiation due to copper compounds disappeared.\*\*\* The color of the flash changed slightly and the visual brightness decreased noticeably.

#### 2-4 THE INFRARED SPECTRUM 6(b, d, •)

##### 2-4.1 INTRODUCTION

By far the largest portion of the radiation from gun flash lies within the infrared region of the spectrum. The spectral distribution of radiation from secondary flash obtained in tests with the special caliber .50 gun is described in par. 2-4.2. The changes that occurred when the secondary flash was suppressed in several ways are described in par. 2-4.3.

\*See *Radiation law, Wien's* in Glossary.

\*\*See footnote for par. 2-3.1.

\*\*\*CuO has band heads at 6045.1, 6059.3, 6146.8, and 6161.5 Å; and CuOH has broad diffuse maxima at 5220, 5400, 5660, and 5760 Å.<sup>31</sup>

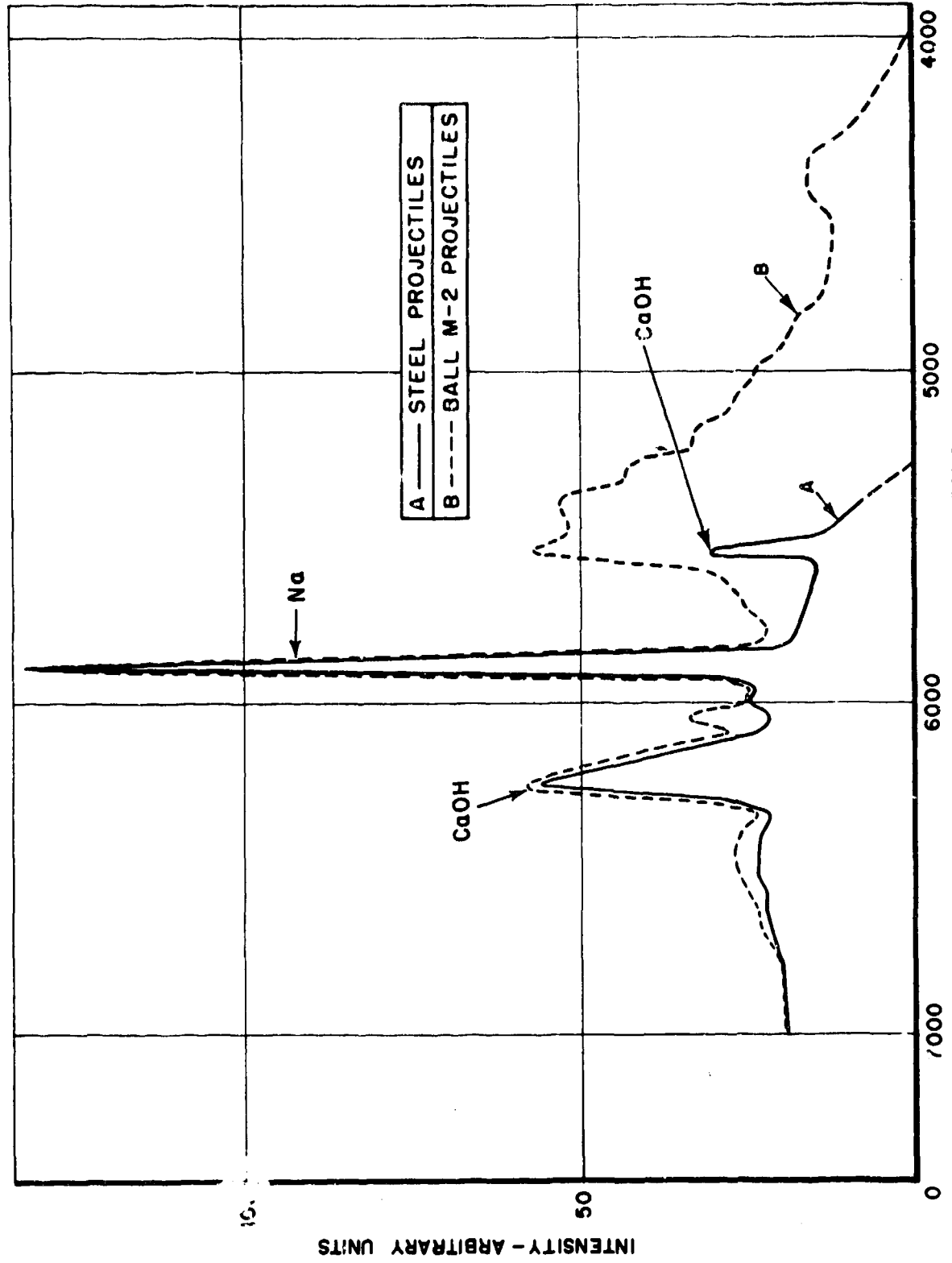


FIGURE 2-3 — EFFECT OF PROJECTILE MATERIAL ON VISIBLE SPECTRUM OF SECONDARY FLASH (FROM REF. 4e)

## 2-4.2 SECONDARY FLASH

The infrared spectrum of secondary flash described in this paragraph was obtained from tests conducted with the special caliber .50 gun which has a 20-mm chamber. A 36-in. barrel was used. The rounds had a load of 390 grains of EX6333 propellant. The spectral distribution was determined by means of the monochromator-photothermal detector combination using a prism of potassium bromide which is transparent to approximately 25 microns.

The results are shown in Figure 2-4. The spectral distribution curve in Figure 2-4 was corrected for the overlapping effect due to the use of a wide slit. (In this figure, the visible component of radiation could be represented as a small tail at the left end of the curve.) A more revealing analysis of the distribution curve is made possible by plotting wave number instead of wavelength for the abscissa. The curve plotted in this manner is shown in Figure 2-5. The principal advantage derived from plotting the results as a function of wave number is that the emission peaks assume a symmetrical shape and their influence on the intensity of radiation at a given wavelength is more readily ascertained.

In Figures 2-4 and 2-5 the gray-body curve for a temperature of 136° K is shown. This seemed to be the most logical gray-body curve over the entire spectral range. By making use of Planck's radiation law\*,

$$W_{\lambda} = \frac{C_1}{\lambda^5 \left( e^{C_2/\lambda T} - 1 \right)}$$

the shape of the curve was calculated by matching the corrected intensity curve at 1.0  $\mu$  and 1.5  $\mu$ ,\*\* as follows:

$$\frac{I_{1.5}}{I_{1.0}} = \frac{1.77}{0.20} = \frac{(1)^5}{(1.5)^5} \left[ \frac{\left( \frac{14320}{T \times 1} - 1 \right)}{\left( \frac{14320}{T \times 1.5} - 1 \right)} \right]$$

The value of T which satisfies this equation is 136° K; but because of errors in the

values of I, this temperature is accurate to at most three significant figures.

The corrected intensity curve in Figure 2-5 consists of a number of emission peaks superimposed upon a background of thermal radiation. The wavelength and wave number of the emission peaks and their corresponding intensities are listed in Table 2-2.

It can be seen that the principal contributors to the intensity from the flash are the emission peaks at 2.8 and 4.54  $\mu$ , although some of the other peaks such as those at 1.90, 2.31, and 3.91  $\mu$  contribute considerable amounts when compared to the thermal radiation at the same wavelengths.

The position of the peaks at 5.56, 7.41 and 12.50  $\mu$  do not seem to agree with the commonly accepted rotational absorption bands of water vapor and carbon dioxide. The fact that these are emission bands, not absorption bands, might have caused some shift in their position. The peaks at 12.50  $\mu$  might be due to ammonia, rather than carbon dioxide, since the rotational ammonia bands are in this spectral range.

No appreciable amounts of radiation in excess of thermal radiation appear beyond the broad band due to water vapor in the vicinity of 7.0  $\mu$ .

In the range of 0.5 to 13.0  $\mu$ , only approximately 0.25 percent of the radiant energy emitted from the flash caused by firing 390 grains of EX6333 propellant in the special caliber .50 gun is visible radiation. Of the remaining (infrared) radiation, approximately 20 percent is concentrated in the region 2.65 to 3.15  $\mu$ , and approximately 14 percent is in the region 4.15 to 4.65  $\mu$ . These two concentrated regions of emission are thought to be due to emission from carbon dioxide and water-vapor molecules, although it is possible that an appreciable part of the emission in the 2.65 - 3.15  $\mu$  region may be due to the OH radical.

\*See *Radiation law, Planck's*, in Glossary.

\*\*It was assumed that the emissivity of the flash was the same as these two wavelengths.

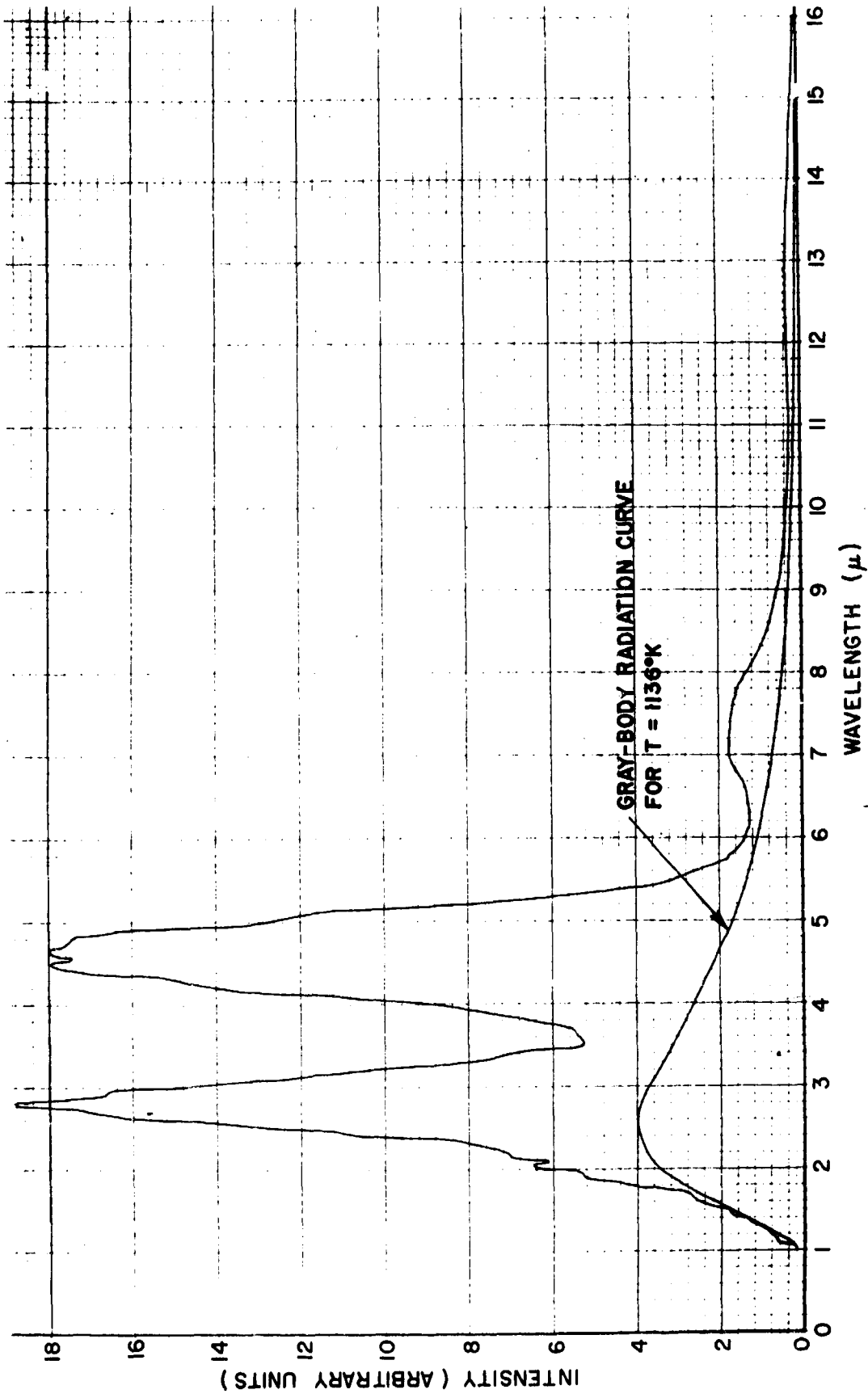


FIGURE 2-4 — SPECTRAL DISTRIBUTION OF INFRARED RADIATION FROM SECONDARY FLASH (FROM REF. 6a)  
SPECIAL CALIBER .50 GUN WITH 20-MM CHAMBER  
BARREL LENGTH = 36 IN.  
390 GRAINS EX6333

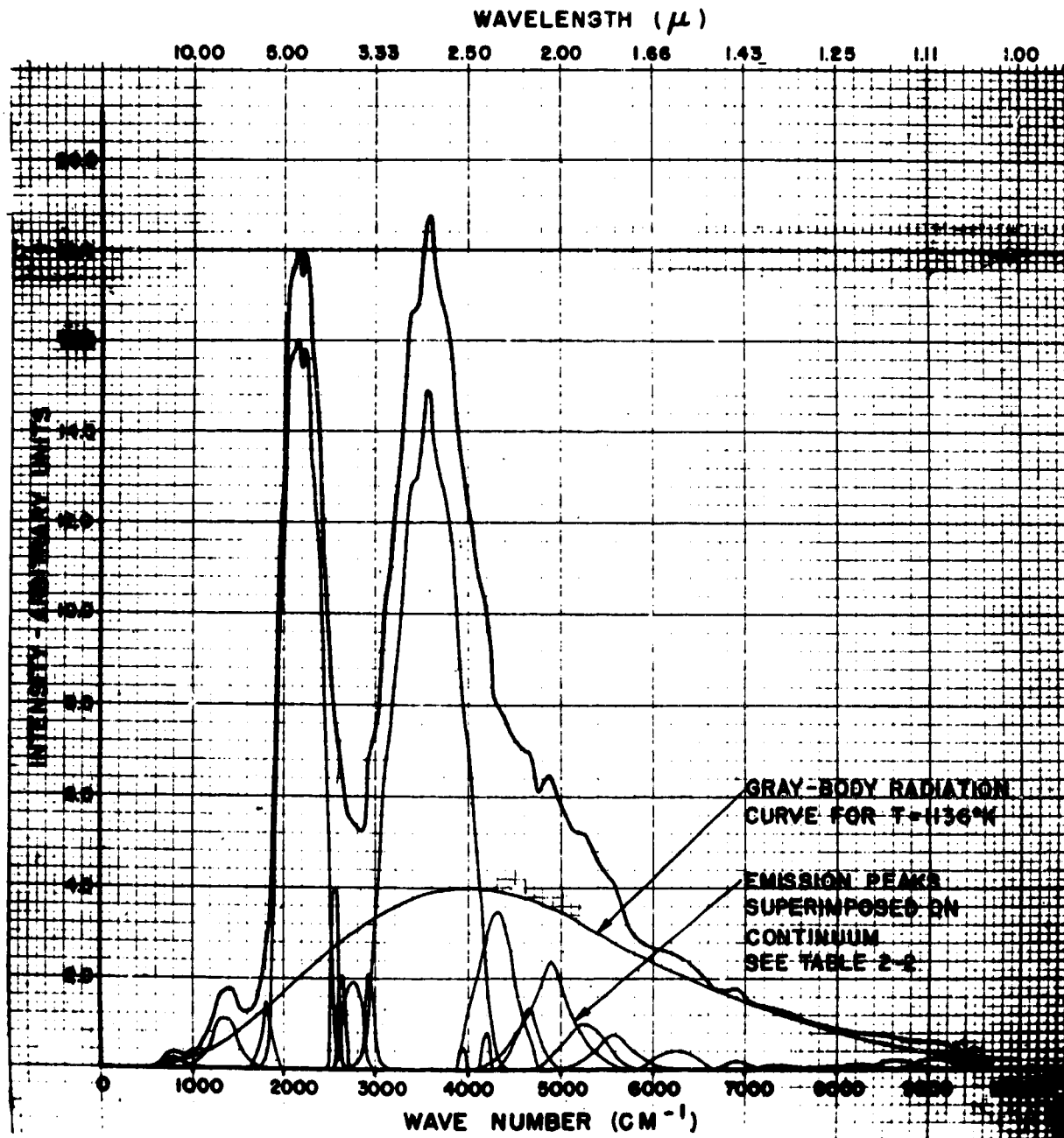


FIGURE 2-5—SPECTRAL DISTRIBUTION OF INFRARED RADIATION FROM SECONDARY FLASH  
(PLOTTED AGAINST WAVE NUMBER) (FROM REF. 6e)  
FIRING CONDITIONS SAME AS THOSE FOR FIGURE 2-4

#### 2-4.3 INTERMEDIATE FLASH

The caliber .50 gun with 20-mm chamber used to study the spectral radiation of secondary flash was also used to study intermediate flash. The radiation was analyzed with the special low-dispersion monochromator having a photothermal detector.\* The spectral

distribution of the flash was determined for each of the combinations of propellant and barrel length in the following list, which also indicates the type of flash produced in each case:

\*See Appendix A-5.

TABLE 2-2  
WAVELENGTH-INTENSITY DATA FOR INFRARED RADIATION OF SECONDARY FLASH  
(From Ref. 6e)

Wavelength ( $\lambda$ ) ( $\mu$ )	Wave Number ( $1/\lambda$ ) ( $\text{cm}^{-1}$ )	Emission Peak Intensity (Arbitrary units)	Thermal Radiation Intensity for $T = 1136^\circ\text{K}$ (Arbitrary units)
1.10	9080	0.24	0.35
1.15	8700	0.17	0.49
1.21	8260	0.11	0.68
1.26	7920	0.06	0.87
1.30	7720	0.04	0.98
1.36	7360	0.10	1.23
1.45	6900	0.17	1.58
1.60	6250	0.41	2.13
1.79	5580	0.76	2.78
1.90	5270	1.00	3.16
2.04	4900	2.36	3.56
2.15	4650	1.34	3.74
2.31	4320	3.48	3.90
2.38	4200	0.80	3.96
2.54	3940	0.46	4.00
2.80	3570	14.90	3.88
3.41	2930	2.10	3.26
3.64	2750	1.92	3.00
3.80	2630	2.08	2.82
3.91	2560	4.00	2.72
4.54	2200	15.60	2.06
5.56	1800	1.48	1.32
7.41	1350	1.10	0.60
12.50	800	0.22	0.12

- (a) 390 grains EX6333, 45-in. barrel, fired into inert atmosphere of nitrogen and carbon dioxide; fairly bright intermediate flash.
- (b) 390 grains EX6333 + 4% to 5%  $\text{K}_2\text{SO}_4$ , 36-in. barrel; large intermediate flash with incipient secondary flash.
- (c) 375 grains EX212 Cordite, 36-in. barrel; fairly bright intermediate flash.
- (d) 410 grains EX6333, 85-in. barrel; small intermediate flash.

The infrared spectra of the last three combinations listed above are shown in Figure 2-6. For comparison, the figure involves the spectrum of secondary flash produced with EX6333 propellant (without additive) and a 36-in. barrel.

The spectral distribution of energy in the flash from each of these combinations of propellant, barrel length, and type of atmosphere showed the existence of strong maxima in the vicinity of 2.8 and 4.5 $\mu$ . The first peak is due to the radiation from both water-vapor and carbon-dioxide molecules, and

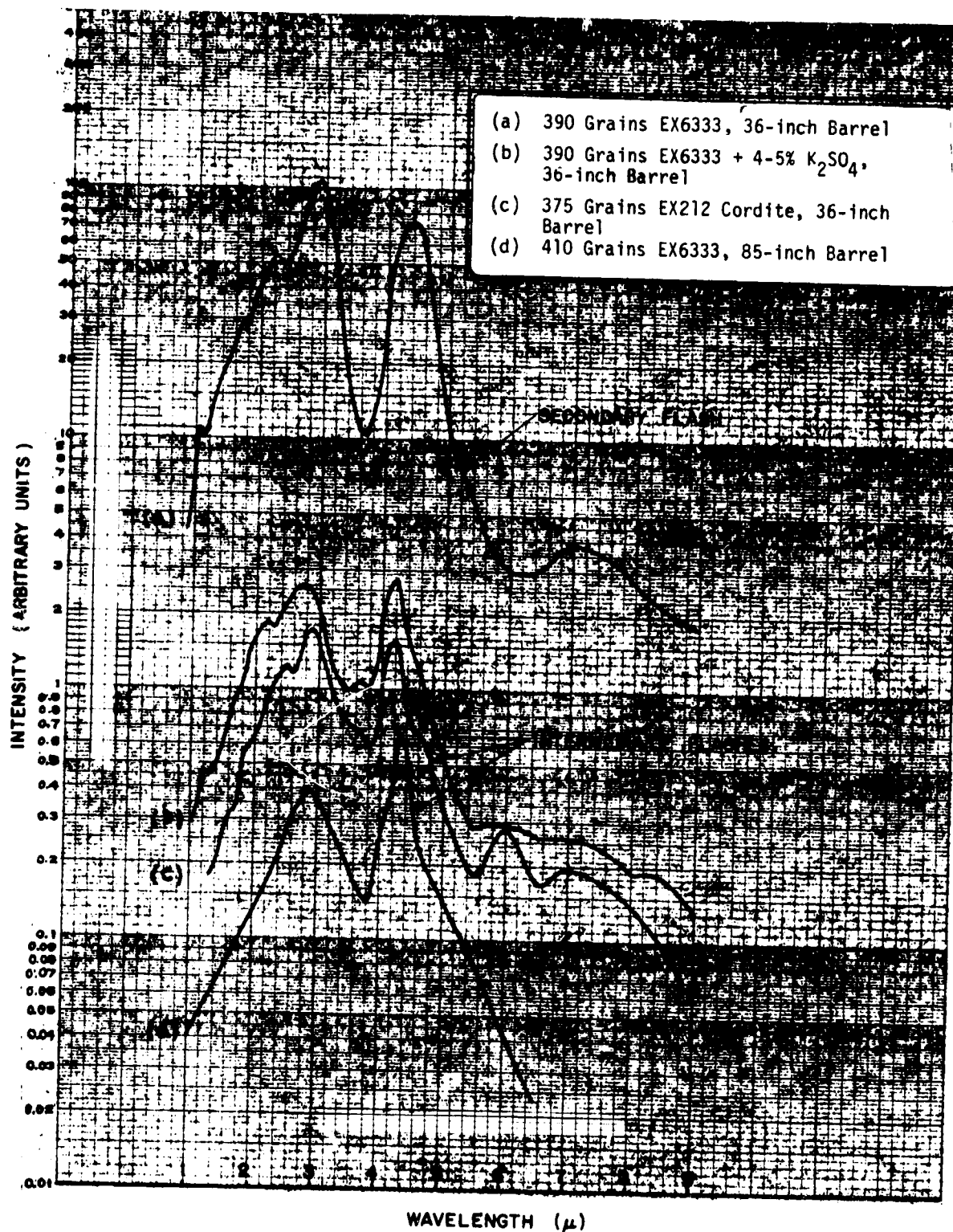


FIGURE 2 — 6 — SPECTRAL DISTRIBUTION OF RADIANT ENERGY FROM FLASH OBTAINED WITH VARIOUS PROPELLANTS AND BARREL LENGTHS (FROM REF. 6c)  
SPECIAL CALIBER .50 GUN WITH 20-MM CHAMBER

the second is due to carbon dioxide alone. Their relative intensity depends upon the composition, temperature, and pressure of the issuing gas.

A study of the infrared flash spectra from the above propellant-weapon combinations led to the following conclusions:

- (a) When secondary flash is suppressed—whether by the addition of potassium sulfate, by lengthening the barrel, or by firing a cool propellant—the emission bands of water-vapor and carbon dioxide, at or near 2.9 and 4.3 $\mu$ , still exist and account for a large percentage of the total infrared radiation.
- (b) The addition of potassium sulfate, with the resulting suppression of secondary flash from the EX6333 propellant, caused a reduction of intensity to approximately 2 percent of the value for the secondary flash produced by the same propellant in a 36-in. barrel (par. 2-4.2).
- (c) Of the four propellant-weapon combinations tried, firing of EX6333 propellant in the 85-in. barrel produced the least intense flash. The intensity of the flash was approximately 1 percent of that of the unsuppressed flash from the EX6333 propellant in the 36-in. barrel (par. 2-4.2). This was to be expected because the muzzle gas emerges at a lower temperature when the barrel length is increased.
- (d) The infrared flash from the Cordite propellant had lower intensity than the suppressed flash produced by the addition of potassium sulfate to EX6333 propellant. This was not surprising because the barrel lengths were the same and the loads approximately equal, but the Cordite propellant is cooler than the EX6333 propellant.

## 2-5 EFFECT OF PROPELLANT LOAD ON FLASH INTENSITY AND OTHER PERFORMANCE PARAMETERS. <sup>9(a and b)</sup>

The characteristics of flash are dependent on the propellant load because of its influence on the pressure, temperature, and composition of the propellant gases. Figure 2-7 indicates how the peak pre-flash and intermediate flash intensities, the peak muzzle pressure, and a few other weapon parameters depend on the propellant load in a particular weapon. The addition of 5% of  $K_2SO_4$  to each of the loads caused the flashes to be generally of the intermediate type, although some variations occurred and at least one secondary flash was observed with the 450-grain load. The peak intermediate flash intensity increased by approximately an order of magnitude as the load was nearly doubled, from 200 to 375 grains; but it decreased considerably when the load was further increased to 475 grains. Increasing the load always resulted in an increase of the muzzle pressure.

It is possible to explain the reduction in flash intensity at the highest loads by considering the change in efficiency of the weapon as the load was increased. Computations making use of the projectile velocity curve in Figure 2-7 show that the projectile kinetic energy per grain of propellant increased as the load was increased; it was nearly doubled, in fact, as the load was increased from 300 to 450 grains. Having done more work per grain of propellant, the emerging muzzle gas had a lower stagnation temperature at the higher loads. The higher pressures at the higher loads had the tendency to cause stronger shock waves and, therefore, greater increase in the temperature of the gas following its expansion out of the muzzle. These opposite tendencies could cause the peak flash intensity to occur at an intermediate load.

An explanation offered in Ref. 9(a) is that the reduction in flash intensity at the highest loads is a consequence of excessive gas leakage before projectile emergence. This possibility was supported by photographic evidence showing the appearance of pre-flash

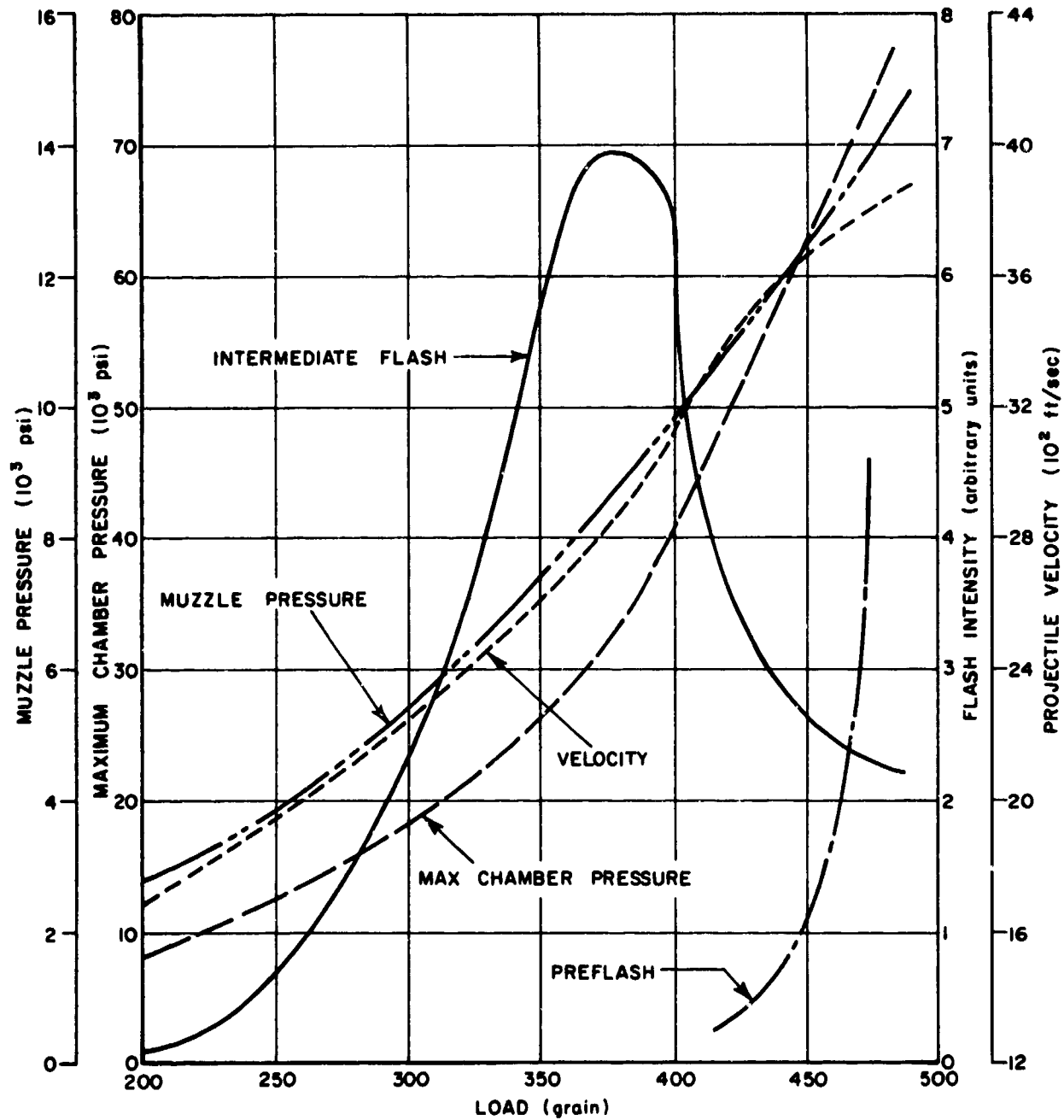


FIGURE 2-7—EFFECT OF LOAD ON VELOCITY, PRE-FLASH, INTERMEDIATE FLASH, MUZZLE PRESSURE, AND MAXIMUM CHAMBER PRESSURE, (FROM REF. 9b)  
 SPECIAL CALIBER .50 GUN WITH 20-MM CHAMBER  
 BARREL LENGTH, 45 IN.  
 LOAD, EX6451 PROPELLANT AND 5% K<sub>2</sub>SO<sub>4</sub>

between the muzzle and the region of intermediate flash at loads of 425 grains or more. It was thought that the pre-flash was probably due to burning propellant gases emerging ahead of the projectile. The pre-flash was observed to be of short duration, but of a brilliant white by comparison with the more reddish intermediate flash. One might expect that, with a higher load, the conditions following some gas leakage would be just as conducive to flash as they are at a lower load in the absence of leakage. However, the leakage gases might displace the air in front of the barrel so that, subsequently, the shock-heated gases contain too little oxygen for ignition to occur.

#### 2-6 EFFECT OF BARREL LENGTH ON FLASH 4(b), 6(c)

The effect of barrel length on the appearance and intensity of secondary flash and on the intensity of the muzzle glow was determined with a caliber .50 gun, 85 in. long, shortened in successive increments of 6 inches. With the 85-in. barrel, EX6333 propellant gave no secondary flashes. As the barrel was shortened, secondary flashes appeared sporadically until, at a sufficiently short length, all rounds gave fully developed secondary flashes.

Information on the number of flashing rounds for each length of barrel is presented

in Table 2-3. Note that the 79-in. length gave a number of secondary flashes, whereas the 73-in. length gave none. It was not possible to discover any reason for this behavior.\* Rounds were fired with the 79-in. barrel on two successive days; on the first day nearly half the rounds gave full secondary flashes, while on the second day no secondary flashes were observed. Breech pressure, bullet velocities, relative humidity, temperature, and barometric pressure were nearly the same on both days. The rate of fire was also the same on both days. It was noted, however, that in *flashless* rounds with EX6333 propellant and the 79-in. barrel the muzzle glow was considerably brighter than would be expected from a consideration of muzzle glow intensities from the 85-in. and the 73-in. lengths, a fact which may possibly be ascribed to the same cause which produced a number of unexpected secondary flashes on one of the days when the 79-in. barrel was fired.

Cordite N propellant gave no secondary flashes in the test gun even for barrel lengths as short as 36 inches. It produced a muzzle glow, the maximum intensity of which increased, as expected, as the barrel was shortened. This increase was apparent in the visible region (photocell measurements) and also in the near infrared region (infrared detector). Data on relative intensities from muzzle glow are presented in Table 2-4.

TABLE 2-3  
INFLUENCE OF BARREL LENGTH ON FREQUENCY OF SECONDARY FLASHES  
(From Ref. 4b)  
Propellant EX6333

Barrel Length (in.)	Number of Rounds	Number of Secondary Flashes	Percent of Rounds Giving Secondary Flash
85	15	0	0
79	136	11	8.1
73	36	0	0
67	30	26	86.5
61	20	20	100
55	25	25	100

\*It may be deduced from the given information that a considerably larger number of rounds were fired the second day the 79-in. barrel was used than on any other day. While this may have been expected to produce greater heating of the gun, a condition more conducive to flashing, no flashes occurred on that day.

TABLE 2-4  
 INFLUENCE OF BARREL LENGTH ON  
 INTENSITY OF MUZZLE GLOW  
 (From Ref. 4b)  
 Propellant - Cordite N, EX195

Barrel Length (in.)	Number of Rounds	Average Maximum Intensity (Arbitrary Units)
79	15	0.71
73	15	0.77
67	15	1.08
61	13	2.17
55	15	2.53

Additional tests were conducted to determine the effect of barrel length on the peak intensity of radiation from suppressed flash for the three loads indicated in Figure 2-8. For all three charges tested, the peak radiant intensity (in the absence of secondary flash) generally decreased as the barrel length was increased. However, in the case of the EX6333 propellant a local reversal of this trend appeared in going from the 73-in. to the 79-in. barrel length. The effect was less prominent when potassium sulfate was added to the propellant (Curve a). The effect was thought to be real and not due to experimental error. It is possible that the reversal in the trend of flash intensity might have been caused by an unnoticed extraneous condition, such as a burr being left on the end of the 73-in. barrel after the cutting operation. It is possibly a correlative fact that the visible and infrared radiations from the non-oxidative portion of the flash were inordinately intense when secondary flash was incipient. For the particular set of conditions existent in this case, the phenomenon is believed to have taken place with the 79-in. barrel. It was at these barrel lengths (73 in. and 79 in.) that a peculiarity in the number of secondary flashes was noticed (Table 2-3).

Other points to be noted in Figure 2-8 are the very regular decrease in intensity with increased barrel length for the Cordite N propellant and the consistently larger values

of peak radiant intensity, at all barrel lengths, for EX6333 propellant plus potassium sulfate by comparison with those for EX6333 propellant alone. It is to be remembered, however, that all of the data in Figure 2-8 were recorded without the presence of secondary flash. Curve b is not extended below a barrel length of 67 in. because secondary flash appeared with the 63-in. barrel.

## 2-7 SUMMARY

Most of the results reported in this chapter were obtained with a special caliber .50 gun that was chambered for 20-mm cartridge cases. Usually, Ball M2 projectiles were used with a propellant of the IMR type.

The *ultraviolet spectrum* of secondary (un-suppressed) gun flash was observed over a wavelength range extending down to 2800 Å. Because of the weakness of the radiation in this region and the low sensitivity of the spectrographic equipment, it was necessary to integrate the effect of up to 2000 rounds to obtain spectra of adequate intensity. Superimposed on a weak continuum the following emitters were observed: strong lines of atomic potassium (4044-4047 Å), medium strength lines of atomic copper (3248-3274 Å), strong bands of CuCl (4300 to 4900 Å), fairly strong bands of CuH (4005 and 4280 Å), weak OH bands (2811 and 3064 Å), and very weak NH bands (3360 and 3370 Å).

The *visible spectrum of intermediate (suppressed) flash* consists principally of continuum radiation with some Na (5890 Å) and CaOH (6230 Å) emission superimposed. The major part of the luminosity of intermediate flash may be attributed to incandescent solids. It is approximately two orders of magnitude less intense than the radiation from secondary flash which is characterized by combustion and a much higher temperature.

Under some conditions, intermediate flash was observed to consist of two parts: a small, relatively intense part near the muzzle and a larger part further from the muzzle. The spectrum of both parts was very similar to that of the usual intermediate flash.

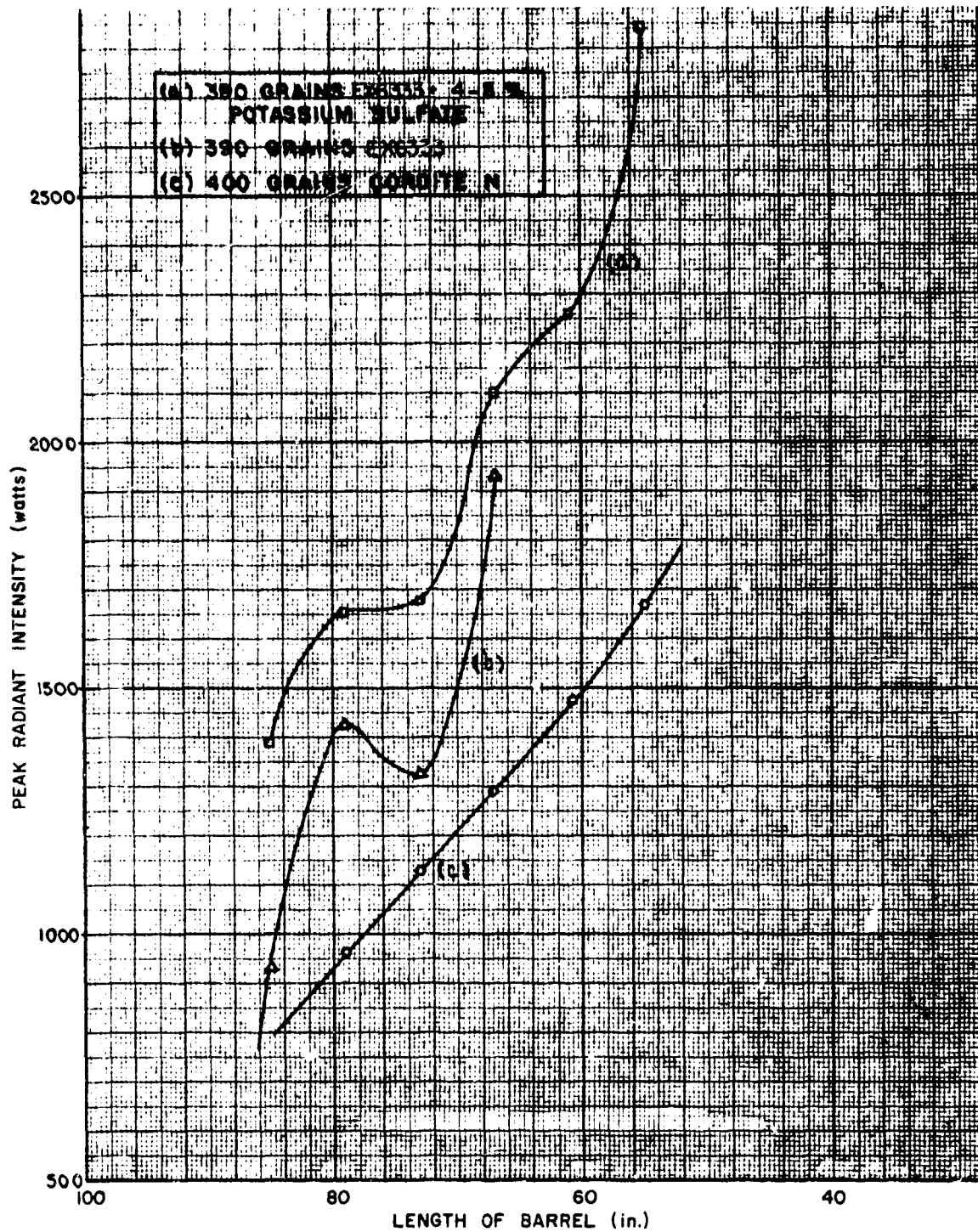


FIGURE 2—8 — VARIATION OF PEAK RADIANT INTENSITY WITH BARREL LENGTH FOR VARIOUS CHARGES (FROM REF. 6c)

SPECIAL CALIBER .50 GUN WITH 20-MM CHAMBER  
 FOR THE BARREL LENGTHS INCLUDED IN THE ABOVE GRAPH THE FLASH  
 WAS OF THE SUPPRESSED TYPE.

The energy in the *visible spectrum of secondary flash* consisted mostly of continuum (18%) and radiation due to copper compounds (50%), CaOH (25%), and Na (7%). When the copper jacketed Ball M2 projectiles were replaced by steel projectiles with steel rotating bands, the radiation due to copper compounds disappeared.

More than 99 percent of the radiation from gun flash was observed to be in the *infrared* region of the spectrum. In addition to a continuum, the infrared radiation of both intermediate and secondary flash consists largely of emission from carbon dioxide and water-vapor, with possible contributions from ammonia and the OH radical. The intensity of the infrared radiation from intermediate flash may vary considerably, depending on the firing conditions; however, it is always much less intense than the radiation from secondary flash—by one to two orders of magnitude.

The maximum intensity of intermediate flash was observed at an intermediate load when the propellant load was increased in a sequence of steps, a constant percentage of chemical suppressant being added to prevent secondary flash. This was probably a consequence of the opposing influences of increasing gun efficiency and increasing muzzle pressure as the load was increased.

For gun barrels sufficiently long to cause suppression of secondary flash, it was observed that the intensity of the flash from a cool propellant (Cordite N) increased as the barrel was shortened. With an IMR propellant there was a local reversal of the trend; but for any given barrel length, the intensities of flash from the IMR propellant were always substantially greater than those observed with the cool propellant. With the addition of 4 to 5 percent of  $K_2SO_4$  to the IMR propellant, the flash intensities were further increased substantially; and the local reversal in the trend of increasing flash intensity as the barrel was shortened became practically absent.

## CHAPTER 3

## SPECTRAL CHARACTERISTICS OF FLASH FROM LARGE-CALIBER WEAPONS

## 3-1 INTRODUCTION

In this chapter, spectral data are presented for the flash from a number of weapons ranging in caliber from 75 mm to 8 inches. A 10-channel infrared spectrometer with photothermal detectors was used to obtain the relative spectral distribution of radiation emitted by the flash from a 155-mm gun, as observed at distances of 200, 500, and 1350 ft from the gun. After the spectrometer was modified by replacing the photothermal detectors with lead sulfide (Ektron) detectors, the spectral emittance was obtained for flash from a 155-mm gun using both normal and super propellant charges. Finally, an 18-channel infrared spectrometer with Ektron detectors was used to obtain the spectral emittance of flash from a number of other weapons.

3-2 RELATIVE SPECTRAL INTENSITY OF FLASH FROM 155-MM ARTILLERY WEAPON AT DIFFERENT DISTANCES FROM GUN <sup>7(b)</sup>

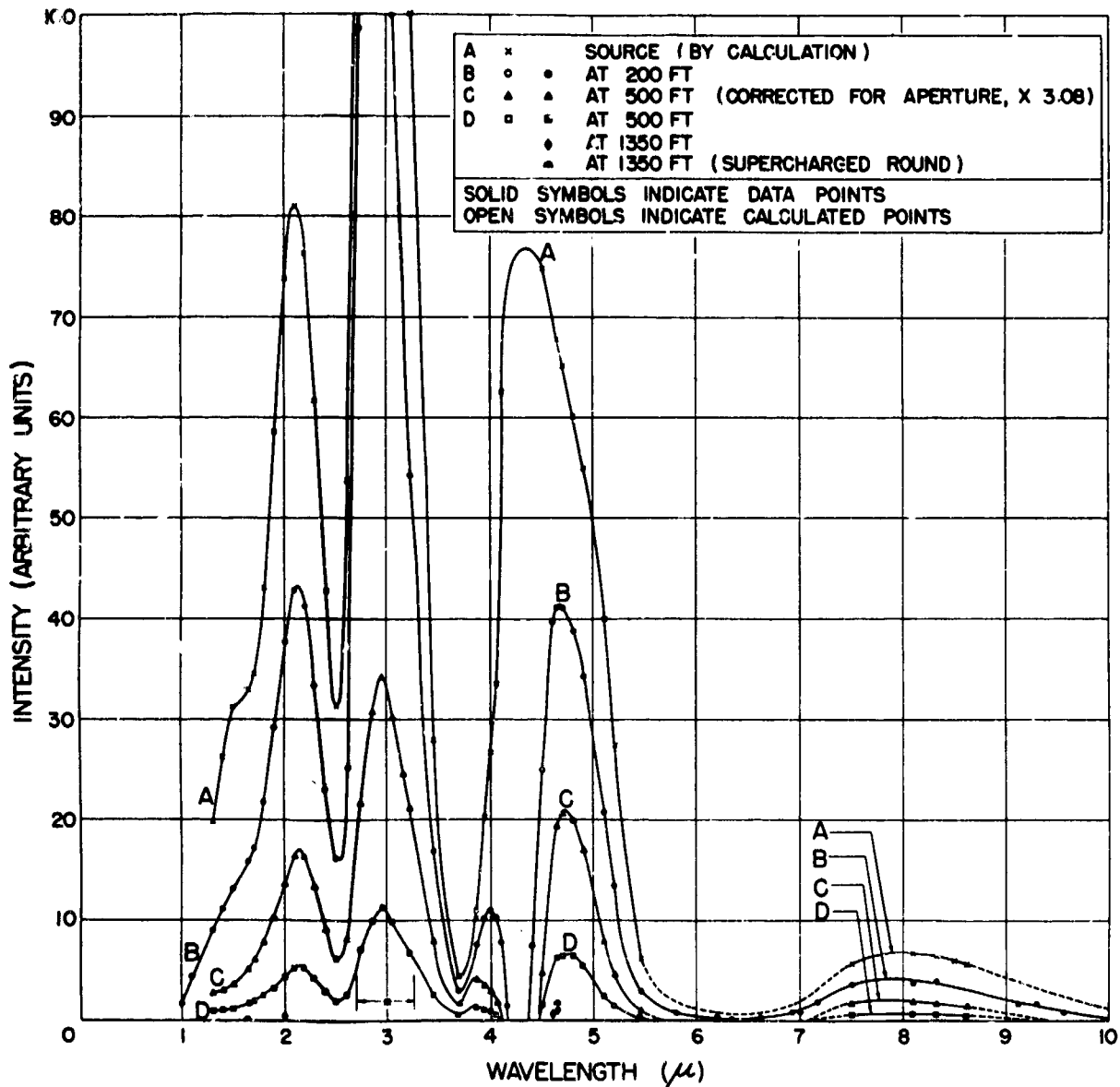
The secondary flash produced by firing a normal charge of 21 lb of M6 propellant in the 155-mm M2 artillery weapon was studied by using the infrared spectrometer with photothermal detectors, described in Appendix A-7. The barrel was approximately 40 calibers long, the projectile was a dummy HE projectile (M101) weighing 95 lb, and the muzzle velocity was about 2100 ft/sec. Observation was made at distances of 200, 500, and 1350 ft from the muzzle of the gun. At the farthest distance, some rounds were fired with super charges of 30 lb-7 oz, yielding muzzle velocities of 2800 ft/sec. The secondary flash from a round of normal charges appeared to be approximately 40 ft long and 15 to 18 ft wide. With a super-charged round, both dimensions increased approximately 50 percent. Values of spectral intensity were obtained at 30 wavelengths between 1 and 9.56  $\mu$ . From the 200-ft dis-

tance, observations were also made of the flash suppressed by the addition of black powder and potassium sulfate to the charge; but the radiation was so weak that no signals were obtained at any wavelength.

The purpose of these measurements was to establish the region of the spectrum in which the radiation available for detection would be most intense, taking into account absorption due to the atmosphere and any other factors affecting the radiation reaching a given distance from the weapon. The relationship <sup>7(b)</sup> worked out for calculating the spectral distribution of energy at the source from the spectral data obtained at the observation stations required a determination of the atmospheric absorption of radiation from secondary flash. This was greatest, as expected, in the regions where water-vapor and carbon dioxide have strong absorption bands.

The spectral distribution, shown in Figure 3-1, closely resembled that obtained by observation of the secondary flash produced by a caliber .50 gun in the laboratory. Due to higher resolution, the maxima and minima observed in the field with the 10-channel spectrograph were sharper than those observed in the laboratory with the infrared monochromator. The characteristic emission bands from water-vapor and carbon dioxide at 2.9 and 4.4  $\mu$  were present. The absorption at 2.62  $\mu$  by cold water molecules in the atmosphere was much more pronounced in the field, where the minimum separation of the source from the measuring equipment was 200 ft, than in the laboratory, where the separation was only 10 ft.

The one super-charged round which was successfully tested yielded useful data at only two wavelengths (1.64 and 4.64  $\mu$ ). At 4.64  $\mu$ , the only wavelength at which a direct comparison was possible, the intensity of



\* NOTHING DETECTED IN THIS RANGE AT 1350 FT

FIGURE 3-1 — VARIATION OF SPECTRAL DISTRIBUTION OF RADIATION FROM SECONDARY FLASH WITH DISTANCE FROM THE GUN (FROM REF. 7b)  
WEAPON: 155-MM, M2 ARTILLERY GUN

radiation from the super-charged round was 1.8 times that from the normal round (see Table B-1 in Appendix B).

In general, it was concluded that for distances up to 500 ft, the strongest signal from:

gun flash radiation transmitted through the atmosphere occurs near  $2.9 \mu$ . Between 500 and 1000 ft and beyond, the position of maximum transmitted energy shifts to near  $4.6 \mu$ .

It is possible that most of the energy entering the detection system at the 1350-ft distance did not come directly from the source, but was reflected from surrounding surfaces.\* Since grass is known to have good reflectivity in the near infrared region of the spectrum, it is possible that most of the energy was reflected from the grassy field between the gun and the spectrograph. There seems to be no possibility for strong flash radiation beyond  $10\mu$ , mainly due to the low emissivity of the flash in this range.

The above results emphasize the importance of taking into account the effect of the reflectivity of the terrain and atmospheric absorption in problems concerned with the detection of infrared sources.

### 3-3 SPECTRAL EMITTANCE OF FLASH FROM 155-MM GUN

#### 3-3.1 TEST CONDITIONS AND PROCEDURE <sup>8(a)</sup>

By means of a 10-channel spectrometer with Ektron detectors (Appendix A-8) the apparent values of the spectral emittances of flash were determined for a 155-mm gun firing a normal charge and a normal charge plus a chemical flash suppressant. Unsuppressed flash was produced by firing the normal propelling charge consisting of 21 lb 4 oz of M6 propellant. Suppressed flash was produced by using 14.38 oz of black powder and 9.59 oz of potassium sulfate in addition to the normal charge.

The test arrangement is shown in Figure 3-2. The slit of the spectrometer was located 100 ft and 50 ft, respectively, from the center of unsuppressed and suppressed flash. These values were used in order that the flash might fill the aperture of the spectrometer. The angle  $\alpha$  between the axes of the spectrometer and the gun was kept small to minimize the travel of the flash across the field of view of the spectrometer. To prevent the gun from protruding into the field of view of the spectrometer, the angle could not be zero.

Alignment of the spectrometer, so that the center of the field of view coincided with the center of flash, was accomplished by means

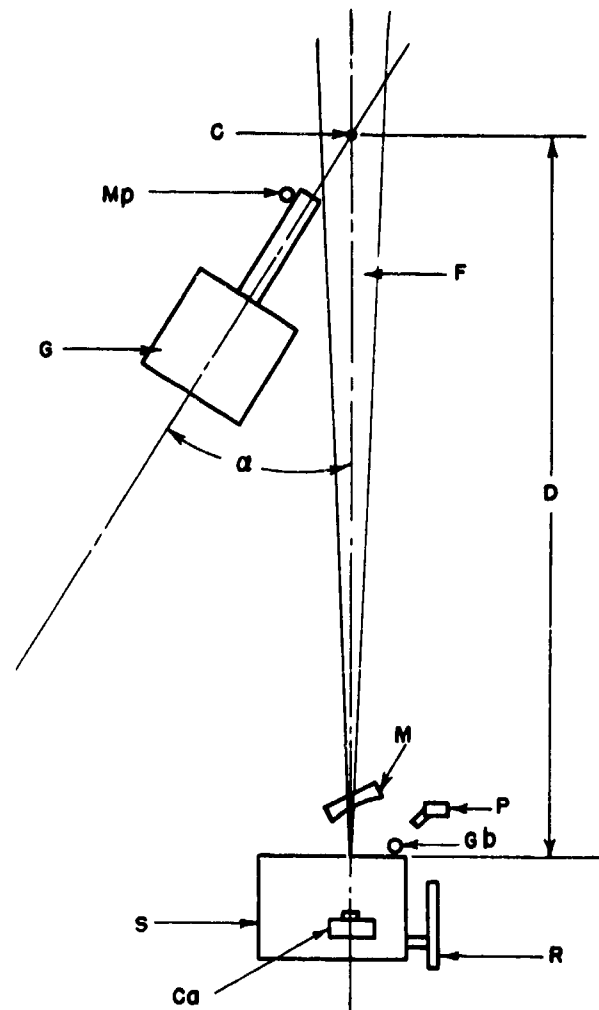


FIGURE 3-2—ARRANGEMENT OF FIELD-TEST EQUIPMENT FOR OBSERVING GUN FLASH (FROM REF. 8a)

- G GUN
- S MULTI-CHANNEL SPECTROMETER
- $\alpha$  ANGLE BETWEEN THE AXES OF THE GUN AND SPECTROMETER
- F FIELD OF VIEW OF THE SPECTROMETER
- D DISTANCE FROM THE CENTER OF FLASH TO SPECTROMETER
- M REMOVABLE FOCUSING MIRROR
- Gb GLOBAR
- P OPTICAL PYROMETER
- Ca CAMERA
- R RING SIGHT
- Mp MICROPHONE

\*The aperture of the 10-channel spectrograph had an  $f$  number of 7.33, which yields a field of view 27 ft wide at a distance of 200 ft. Particularly at the 1350-ft distance, therefore, the spectrometer was capable of receiving radiation reflected from the terrain.

of ring-sight (R) and camera (Ca) as follows. Since the axis of the spectrometer was parallel to, and below that of the camera, the proper horizontal angle was set when an object placed at the center of flash was focused on a vertical line in the center of the focal plane of the camera. The elevation of the spectrometer was adjusted so that the center of flash coincided with a horizontal line in the ring-sight (R), the axis of which was parallel to and in the same plane as that of the spectrometer.

Before each round was fired, the spectrometer was calibrated as follows. Chopped radiation from a Globar source (Gb), usually operated at 1300°K, was focused in the entrance slit of the spectrometer by the removable mirror (M). The *f*-number of this mirror was chosen so that the radiation from the Globar completely filled the aperture of the spectrometer. After completion of the calibration, the test gun was fired. The pressure wave preceding the flash energized the microphone (MP) located at the muzzle of the gun, thereby initiating the sweep of the recording traces which were then deflected by radiation from the flash.

### 3-3.2 CALCULATIONS

The apparent spectral emittance of the flash was computed with the following formula.

$$W_{\lambda F} = \frac{D_F}{D_G} \frac{G_G}{G_F} W_{\lambda B} \quad (3-1)$$

where

- $\lambda$  = wavelength ( $\mu$ )
- $W_{\lambda F}$  = spectral emittance of flash (watt/cm<sup>2</sup> $\mu$ )
- $D_F$  = deflection of the recording trace caused by the flash
- $D_G$  = deflection of the recording trace caused by the Globar
- $G_G$  = spectrometer gain for the Globar
- $G_F$  = spectrometer gain for the flash

3-4

For a black body at 1300°K, we have\*

$$W_{\lambda B} = \frac{3.74 \times 10^4}{\lambda^5} \left[ \exp \left( \frac{14390}{1300\lambda} \right) - 1 \right]$$

The total rate of radiation by the flash in the wavelength interval between  $\lambda_1$  and  $\lambda_2$  was calculated with the following equation:

$$E = A \int_{\lambda_1}^{\lambda_2} W_{\lambda F} d\lambda \quad (3-2)$$

where

A = area of flash projected onto a plane perpendicular to the viewing direction

$\int_{\lambda_1}^{\lambda_2} W_{\lambda F} d\lambda$  = total emittance in the wavelength interval between  $\lambda_1$  and  $\lambda_2$

### 3-3.3 RESULTS

The spectral emittances calculated at the peak deflections of the recording traces are shown in Table 3-1 for unsuppressed flash and in Table 3-3 for suppressed flash. Spectral emittances\*\* of unsuppressed flash are shown as a function of time in Table 3-2, for representative rounds grouped as discussed below.

Those rounds which gave similar results for unsuppressed flash were grouped together and the values of spectral emittances were averaged. The average emittances of each group are plotted as a function of wavelength in Figure 3-3. Test records of representative rounds for two of these groups are shown in Figure 3-4.

\*See *Radiation law, Planck's* in Glossary.

\*\*These values were determined by assuming that the radiation filled the entrance aperture of the spectrometer at all times.

No attempt was made to group rounds in which flash was suppressed. The average emittances are plotted as a function of wavelength in Figure 3-5. The representative

rounds shown in Figure 3-6 were chosen to show the variations in shape and in the location of the peak deflections of the recording traces.

TABLE 3-1

APPARENT SPECTRAL EMITTANCE OF UNSUPPRESSED FLASH FROM 155-mm GUN (From Ref. 8a)  
The Values in the Following Table Were Calculated for the Peak Deflections of the Recording Traces

<u>Wavelength (<math>\mu</math>)</u>	<u>2.32</u>	<u>2.46</u>	<u>2.57</u>	<u>2.72</u>	<u>2.83</u>	<u>3.00</u>	<u>3.15</u>	<u>3.29</u>	<u>3.46</u>	<u>3.60</u>
Spectral Emittance (watt/cm <sup>2</sup> $\mu$ )										
Average of rounds 6, 7, 8, and 11.	3.09	4.80	1.95	5.37	7.40	4.45	3.89	3.70	4.05	4.05
Round 10.	1.32	2.42	1.03	3.14	3.81	2.26	1.93	2.00	2.25	2.54
<u>Wavelength (<math>\mu</math>)</u>	<u>1.00</u>	<u>1.17</u>	<u>1.26</u>	<u>1.49</u>	<u>1.67</u>	<u>1.90</u>	<u>2.09</u>	<u>2.25</u>	<u>2.43</u>	<u>2.59</u>
Spectral Emittance (watt/cm <sup>2</sup> $\mu$ )										
Average of rounds 15, 16, 17, and 22.	1.37	2.67	2.24	3.77	2.81	5.28	4.65	2.50	6.10	2.15
Average of rounds 14 and 19.	1.02	2.01	1.73	2.95	2.19	4.14	3.77	2.00	5.08	1.78
Average of rounds 18 and 21.	0.691	1.56	1.44	2.17	1.73	3.77	3.03	1.45	4.24	1.52

TABLE 3-2

SPECTRAL EMITTANCE AS A FUNCTION OF TIME FOR ROUNDS THAT  
ARE REPRESENTATIVE OF UNSUPPRESSED FLASH FROM 155-mm GUN  
(From Ref. 8a)

Round 7										
<u>Wavelength (<math>\mu</math>)</u>	<u>2.32</u>	<u>2.46</u>	<u>2.57</u>	<u>2.72</u>	<u>2.83</u>	<u>3.00</u>	<u>3.15</u>	<u>3.29</u>	<u>3.46</u>	<u>3.60</u>
Spectral Emittance (watt/cm <sup>2</sup> $\mu$ )										
<u>Maximum emittance</u>	<u>3.20</u>	<u>5.15</u>	<u>1.97</u>	<u>5.52</u>	<u>7.49</u>	<u>4.52</u>	<u>3.96</u>	<u>3.70</u>	<u>4.11</u>	<u>4.11</u>
<u>Time after max. emittance (msec)</u>										
5	2.41	4.27	1.69	4.55	6.44	3.67	3.07	2.95	3.35	3.30
10	2.20	4.01	1.55	4.26	5.97	3.67	3.07	2.80	3.23	3.20
15	1.92	3.73	1.41	3.86	5.52	3.27	2.84	2.55	2.81	2.91
20	1.77	3.49	1.27	3.46	5.18	3.11	2.67	2.55	2.69	2.84
40	1.35	2.68	1.06	2.63	4.03	2.82	2.31	2.30	2.49	2.55
50	0.925	2.01	0.844	2.21	3.58	2.26	1.88	1.92	2.16	2.10

Table is concluded on next page.

TABLE 3-2 (CONCL.)  
SPECTRAL EMITTANCE AS A FUNCTION OF TIME FOR ROUNDS THAT  
ARE REPRESENTATIVE OF UNSUPPRESSED FLASH FROM 155-mm GUN  
(From Ref. 8a)

Round 10										
Spectral Emittance (watt/cm <sup>2</sup> μ)										
<u>Maximum emittance</u>	<u>1.32</u>	<u>2.42</u>	<u>1.03</u>	<u>3.14</u>	<u>3.83</u>	<u>2.26</u>	<u>2.54</u>	<u>2.00</u>	<u>2.25</u>	<u>1.93</u>
Time after max. emittance (msec)										
5	1.24	2.32	0.93	3.01	3.55	2.09	2.41	1.83	2.11	1.80
10	1.11	2.14	0.84	2.65	3.26	1.92	2.29	1.83	1.97	1.67
15	1.06	2.07	0.73	2.31	3.14	1.74	2.16	1.67	1.83	1.54
20	0.93	1.89	0.65	2.15	2.87	1.57	2.03	1.50	1.69	1.41
40	0.61	1.26	0.65	1.57	2.22	0.174	1.55	1.27	1.50	1.31
50	0.43	0.97	0.52	1.05	1.68	0	1.27	1.27	1.20	1.10
Round 14										
Spectral Emittance (watts/cm <sup>2</sup> μ)										
<u>Wavelength (μ)</u>	<u>1.00</u>	<u>1.17</u>	<u>1.49</u>	<u>1.26</u>	<u>1.67</u>	<u>1.90</u>	<u>2.59</u>	<u>2.25</u>	<u>2.43</u>	<u>2.09</u>
<u>Maximum emittance</u>	<u>0.95</u>	<u>2.11</u>	<u>2.82</u>	<u>1.71</u>	<u>2.16</u>	<u>4.27</u>	<u>1.83</u>	<u>2.21</u>	<u>5.15</u>	<u>3.80</u>
Time after max. emittance (msec)										
5	0.68	1.62	2.42	1.40	1.79	3.86	1.66	1.92	4.58	3.42
10	0.53	1.35	2.16	1.21	1.64	3.45	1.49	1.73	4.24	3.23
15	0.42	1.13	1.95	1.13	1.49	3.17	1.41	1.53	3.77	2.95
20	0.38	1.02	1.81	1.06	1.34	3.04	1.33	1.34	3.42	2.85
40	0.17	0.65	1.10	0.61	0.89	2.07	0.92	1.96	1.96	1.90
50	0.08	0.33	0.69	0.34	0.60	1.38	0.67	1.23	1.23	1.24
Round 17										
Spectral Emittance (watt/cm <sup>2</sup> μ)										
<u>Wavelength (μ)</u>	<u>1.00</u>	<u>1.17</u>	<u>1.49</u>	<u>1.26</u>	<u>1.67</u>	<u>1.90</u>	<u>2.59</u>	<u>2.25</u>	<u>2.43</u>	<u>2.09</u>
<u>Maximum emittance</u>	<u>1.35</u>	<u>2.61</u>	<u>3.80</u>	<u>2.24</u>	<u>2.89</u>	<u>5.07</u>	<u>2.16</u>	<u>2.47</u>	<u>6.00</u>	<u>4.78</u>
Time after max. emittance (msec)										
5	0.69	1.47	2.83	1.45	2.01	3.89	1.69	1.75	4.55	3.67
10	0.53	1.20	2.37	1.23	1.71	3.48	1.47	1.59	4.17	3.42
15	0.43	0.95	2.13	1.08	1.55	3.23	1.31	1.35	3.58	3.04
20	0.37	0.85	1.97	1.04	1.55	3.11	1.23	1.27	3.39	2.97
40	0.21	0.57	1.52	0.70	1.20	2.34	1.16	0.96	2.43	2.33
50	0.11	0.28	0.84	0.35	0.72	1.43	0.85	0.64	1.46	1.47
Round 18										
Spectral Emittance (watt/cm <sup>2</sup> μ)										
<u>Wavelength (μ)</u>	<u>1.00</u>	<u>1.17</u>	<u>1.42</u>	<u>1.26</u>	<u>1.67</u>	<u>1.90</u>	<u>2.59</u>	<u>2.25</u>	<u>2.43</u>	<u>2.09</u>
<u>Maximum emittance</u>	<u>0.710</u>	<u>1.54</u>	<u>1.99</u>	<u>1.33</u>	<u>1.59</u>	<u>3.45</u>	<u>1.47</u>	<u>1.29</u>	<u>4.05</u>	<u>2.93</u>
Time after max. emittance (msec)										
5	0.61	1.29	1.84	1.29	1.51	3.30	1.38	1.21	3.7	2.79
10	0.53	1.19	1.77	1.12	1.43	3.17	1.30	1.08	3.48	2.67
15	0.44	1.09	1.66	1.00	1.36	3.17	1.30	1.00	3.36	2.61
20	0.39	0.94	1.58	0.91	1.21	2.87	1.22	0.96	3.10	2.54
40	0.23	0.65	1.24	0.71	1.06	2.30	0.98	0.75	2.20	1.31
50	0.12	0.40	0.96	0.58	0.91	2.02	0.82	0.58	1.68	1.00

TABLE 3-3  
SPECTRAL EMITTANCE OF SUPPRESSED FLASH FROM 155-mm GUN (From Ref. 8a)  
Values were calculated for the peak deflections of the recording traces.  
Units of spectral emittance are ( $10^{-2}$  watt/cm<sup>2</sup>μ).

Wavelength (μ)	<u>1.00</u>	<u>1.17</u>	<u>1.26</u>	<u>1.49</u>	<u>1.67</u>	<u>1.90</u>	<u>2.09</u>	<u>2.25</u>	<u>2.43</u>	<u>2.59</u>
Average spectral emittance for Rounds 4-13	1.06	2.08	3.45	4.67	10.0	15.2	10.6	18.8	21.4	10.6
Wavelength (μ)	<u>2.32</u>	<u>2.46</u>	<u>2.57</u>	<u>2.72</u>	<u>2.83</u>	<u>3.00</u>	<u>3.15</u>	<u>3.29</u>	<u>3.46</u>	<u>3.60</u>
Average spectral emittance for Rounds 18-24	22.8	18.6	10.6	10.0	13.9	9.80	8.70	11.1	9.2	7.34

By integrating the maximum curve for unsuppressed flash and the average curve for suppressed flash, the total emittances shown below were obtained for the region between 1 and 3.6 μ. These values and the projected areas of flash were used to calculate the total rates of radiation according to Eq. 3-2.

Type of Flash	Total Emittance (watt/cm <sup>2</sup> )	Total Rate of Radiation (watt)
Unsuppressed	10.1	$4.73 \times 10^6$
Suppressed	0.28	$4.96 \times 10^4$

In obtaining the above values:

- The area of flash was assumed to be independent of wavelength.
- The projected areas of the flash were calculated from photographs of the flash.
- The total emittance was assumed constant over the entire area of the flash.

### 3-3.4 CONCLUSIONS

The wavelength regions in which peak emittances occur, determined from the curves of Figures 3-3 and 3-5, are listed in Table 3-4 along with the locations of the absorption bands for CO<sub>2</sub> and H<sub>2</sub>O. The peaks at 2.42 and 2.83 μ for unsuppressed flash do not correspond to any of the absorption bands listed for CO<sub>2</sub> and H<sub>2</sub>O. This is also true for the peaks at 2.34 and 2.87 μ for suppressed flash. These peaks may be caused by atmospheric absorption of CO<sub>2</sub> and H<sub>2</sub>O at 2.7 μ.

Inspection of the data indicated that the time for each trace to reach its maximum value was nearly independent of the wavelength. The data also showed that radiation of shorter wavelength had shorter time duration.

The spectral emittances of unsuppressed flash were 10 to 100 times larger than those of suppressed flash.

TABLE 3-4  
COMPARISON OF WAVELENGTHS OF FLASH EMITTANCE PEAKS AND OF CO<sub>2</sub> and H<sub>2</sub>O ABSORPTION BANDS (From Ref. 8a)

Wavelength at Emittance Peaks (μ)		Wavelength of Absorption Bands (μ)	
Suppressed Flash	Unsuppressed Flash	CO <sub>2</sub>	H <sub>2</sub> O
	1.10 to 1.20		1.13
	1.40 to 1.56	1.57, 1.53, 1.43	1.38, 1.45
1.7 to 2.02	1.90 to 2.10	1.96, 2.01, 2.06	1.88
2.2 to 2.48	2.36 to 2.46		
2.8 to 2.93	2.76 to 2.90	2.78, 2.70	2.74

CODE	AVERAGE OF ROUNDS
●	6, 7, 8, 11
X	15, 16, 17, 22
△	14, 19
▲	18, 21
○	10

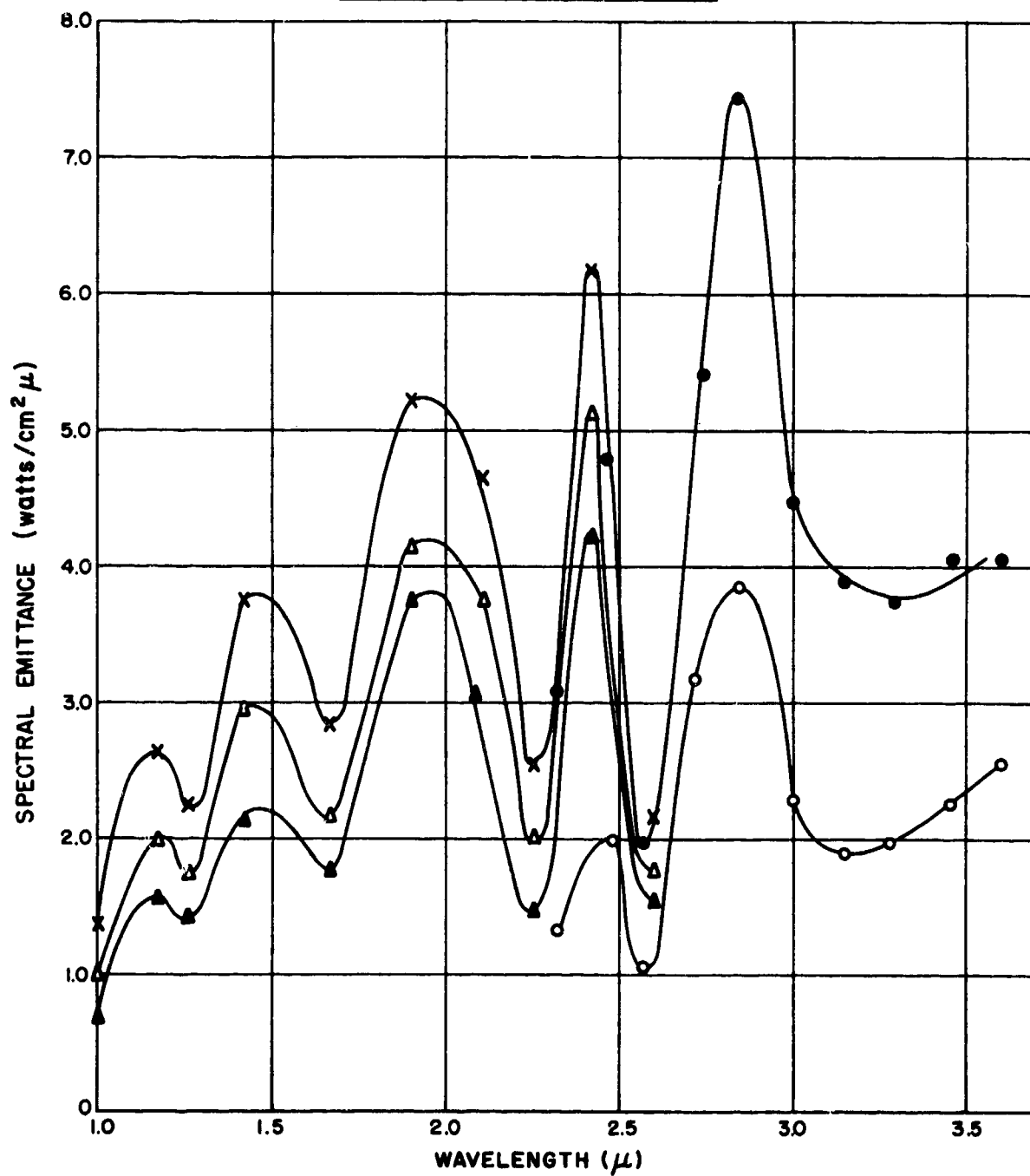


FIGURE 3-3—SPECTRAL EMITTANCE OF UNSUPPRESSED FLASH FROM 155-MM GUN (FROM REF. 8a)

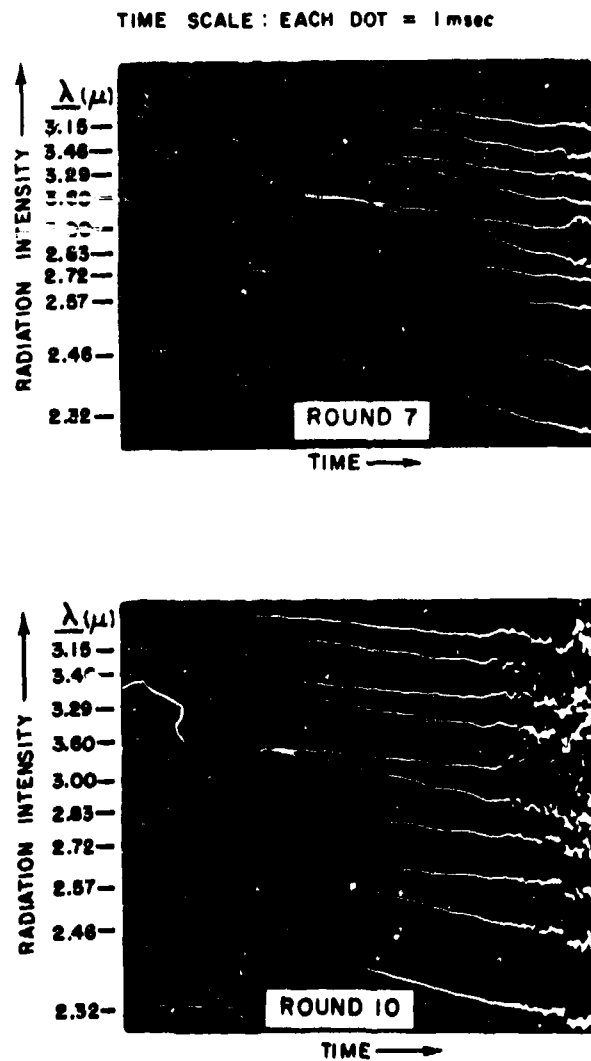


FIGURE 3-4—EXAMPLES OF SPECTROGRAPHIC RECORDS FOR UNSUPPRESSED FLASH (FROM REF. 8a)  
(155-MM GUN)

### 3-4 ADDITIONAL DATA ON FLASH FROM 155-MM GUN OBTAINED WITH MODIFIED EQUIPMENT AND PROCEDURE <sup>8(b)</sup>

Additional data on the spectral emittance of flash from the weapon discussed in par. 3-2 and 3-3, obtained with slightly modified equipment and procedure, were not substantially different from the data given in the above paragraphs.

The test changes were:

- (a) The wavelength bandwidth falling on each Ektron cell was reduced by placing a limiting aperture in front of the Ektron cell assembly (Appendix A-8).
- (b) The procedure for calibrating the spectrometer was modified to include observation of the response of individual channels to a constant electrical input in addition to observing the response to a standard source.

The modified procedure increased the efficiency with which the spectrometer calibration could be checked before each round was fired.

The spectral emittance curve obtained for unsuppressed flash using the modified procedure had the same features as the curves in Figure 3-3; and the values of spectral emittance at any wavelength fell mostly within the range of values displayed in Figure 3-3. Likewise, the spectral emittance curve obtained for suppressed flash was similar to the curve in Figure 3-5, the new values of spectral emittance being somewhat lower for  $\lambda < 2.5 \mu$  and somewhat higher for  $\lambda > 3 \mu$ .

The modified procedure was also used to observe the flash from the 155-mm gun when a super charge (30 lb 8-5/8 oz, without chemical suppressant) of M6 propellant was used. There was no clear distinction between the spectral emittance curves for the normal and super charges. The intensity-vs-time traces for the super-charge rounds had peaks that were typically more rounded and were generally of longer duration by comparison with the traces for rounds of normal charge.

### 3-5 SPECTRAL EMITTANCE OF FLASH FROM VARIOUS LARGE-CALIBER WEAPONS INVESTIGATED WITH AN 18-CHANNEL SPECTROMETER

#### 3-5.1 INTRODUCTION

An 18-channel infrared spectrometer was used to obtain the spectral emittance of flash from various weapons ranging in caliber from 75 mm to 8 inches. The results obtained for a 280-mm gun, which was used in establishing the procedure, are presented separately.

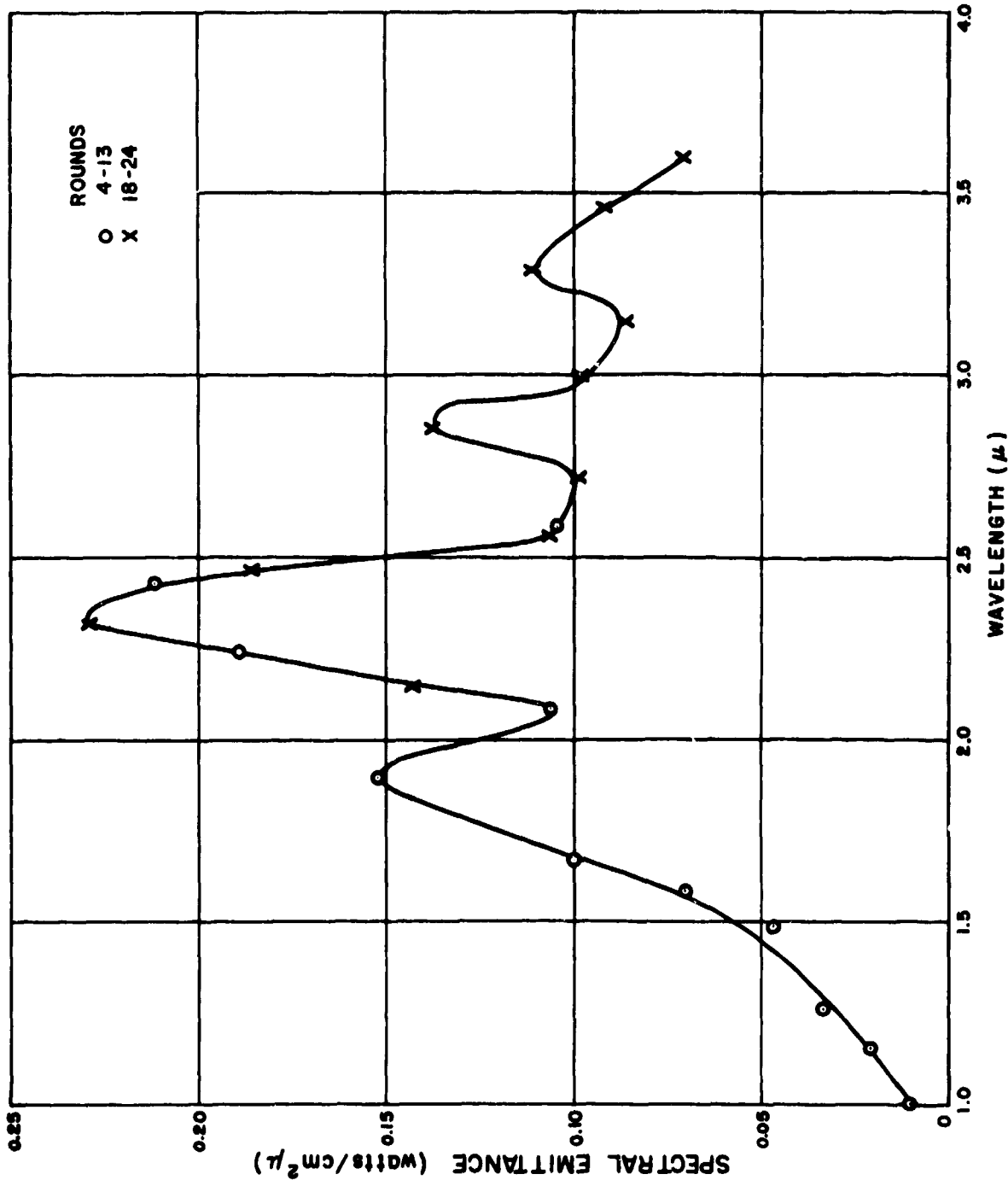


FIGURE 3—5—SPECTRAL EMITTANCE OF SUPPRESSED FLASH FROM 155-MM GUN (FROM REF. 8a)

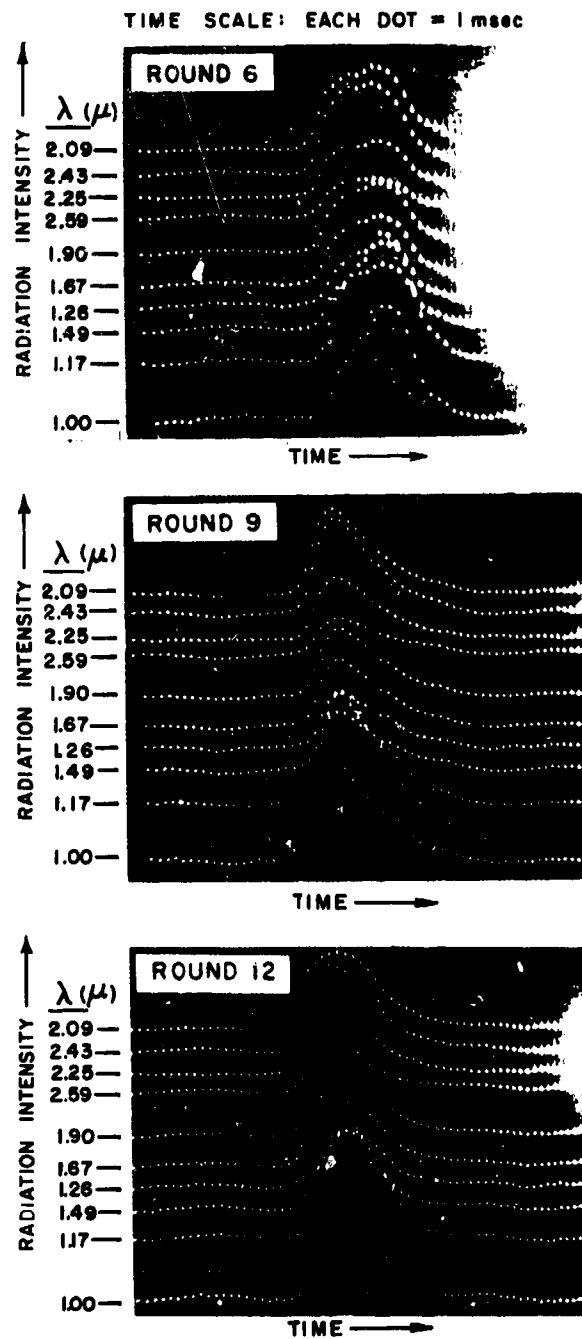


FIGURE 3-6—EXAMPLES OF SPECTROGRAPHIC RECORDS FOR SUPPRESSED FLASH (FROM REF. 8a)  
(155-MM GUN)

### 3-5.2 TEST CONDITIONS AND PROCEDURE 8(e)

The test arrangement was similar to that shown in Figure 3-2. The main difference

was that a telescope, located above and parallel to the axis of the spectrometer, replaced the ring sight for aiming the spectrometer at the flash. The distance between the spectrometer and the flash was varied from 20 ft (for the 75-mm gun) to 150 ft (for the 8-in. gun). These distances were chosen so that the flash would fill the field of view of the spectrometer. As indicated in par. 3-5.4, however, some flashes were too small to satisfy this requirement.

The test procedure for each combination of weapon and propellant consisted in firing a number of rounds at each of three spectrometer prism orientations, yielding data at a total of 54 wavelengths.

The procedure at each prism orientation was as follows:

- (1) Individual flashes were observed, and the gains of the amplifiers were adjusted until satisfactory deflections of the recording traces were obtained.
- (2) The spectrometer was calibrated by recording the deflections caused by the radiation from a Global, the temperature of which (1300°K) was measured by means of an optical pyrometer.
- (3) Five rounds were fired and spectrographic data were recorded.
- (4) The spectrometer was recalibrated.
- (5) Spectrographic data were recorded for five additional rounds.

The spectral emittances of the flashes were calculated from the recorded data by means of Eq. 3-1\*

$$W_{\lambda F} = \frac{D_F}{D_G} \frac{G_G}{G_F} W_{\lambda B} \quad (3-1)$$

\*See Par. 3-3.2.

The total rate of radiation emitted by the flashes in the interval between 0.99 and 3.4  $\mu$  was determined with the following equation:

$$E = A \int_{0.99\mu}^{3.4\mu} W_{\lambda} d\lambda,$$

where  $E$  = total rate of radiation;

$\int_{0.99\mu}^{3.4\mu} W_{\lambda F} d\lambda$  = total emittance in the interval between 0.99 and 3.4  $\mu$ , obtained by integrating under the spectral emittance curves;

$A$  = projected area of flash as determined from flash photographs.\*

The validity of the above equation requires that the radiation from both sources fill the aperture of the instrument so that, aside from the influence of other factors, the galvanometer deflections would have the same proportionality to the spectral intensities of both sources. However, the arrangement was such that flash radiation, particularly, was subject to absorption by the atmosphere. The values obtained for emittance and total radiation must therefore be regarded as apparent values.<sup>8(d)</sup>

### 3-5.3 SPECTRAL EMITTANCE OF FLASH FROM 280-MM GUN

Spectral emittance data for a 280-mm gun are given in Table 3-5 for wavelengths between 0.61 and 3.29  $\mu$ . Spectrograms for four rounds are shown in Figures 3-7 (A) and (B).<sup>8(d)</sup> The apparent spectral emittance of flash from the 280-mm gun has been plotted as a function of wavelength in Figure 3-8.<sup>8(d)</sup> Table 3-6 gives explanations for some of the maxima and minima of the spectral emittance graphs. Most of the maxima can be attributed to emission by CO<sub>2</sub> or H<sub>2</sub>O in the flash; most of the minima can be attributed to absorption by H<sub>2</sub>O in the atmosphere.

The apparent spectral emittances obtained for the 155-mm and 280-mm guns are compared in Figure 3-9.<sup>8(d)</sup> Over most of the range of wavelengths the two curves have similar shape, the values of apparent emittance for the 280-mm gun being somewhat higher than those for the 155-mm gun.

A comparison of the oscillograms for flash from both weapons showed considerable difference in the time scale. The recording traces for flash from a 155-mm gun reached their peak values in approximately 8.0 msec, while those for the 280-mm gun required approximately 70 msec to reach their peak values. The times required for the recording traces to decrease to 50% of their peak values were 35 msec for flash from the 155-mm gun and 140 msec for flash from a 280-mm gun.

### 3-5.4 DATA OF SPECTRAL EMITTANCE OF FLASH FROM OTHER LARGE-CALIBER WEAPONS

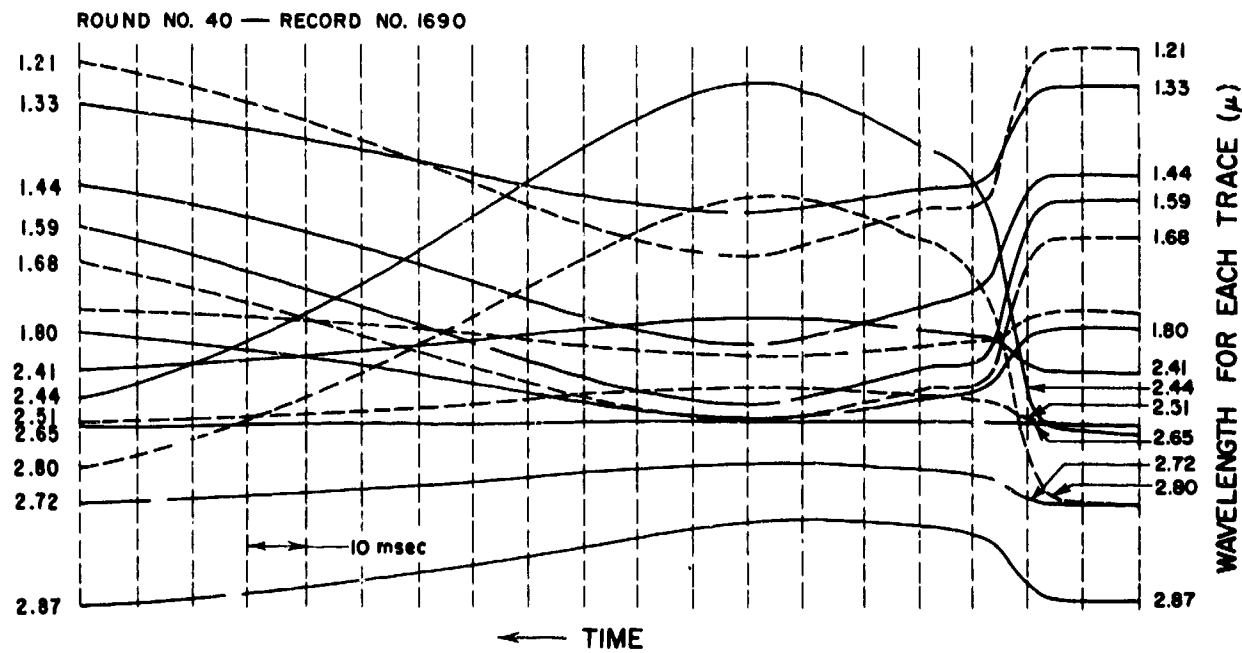
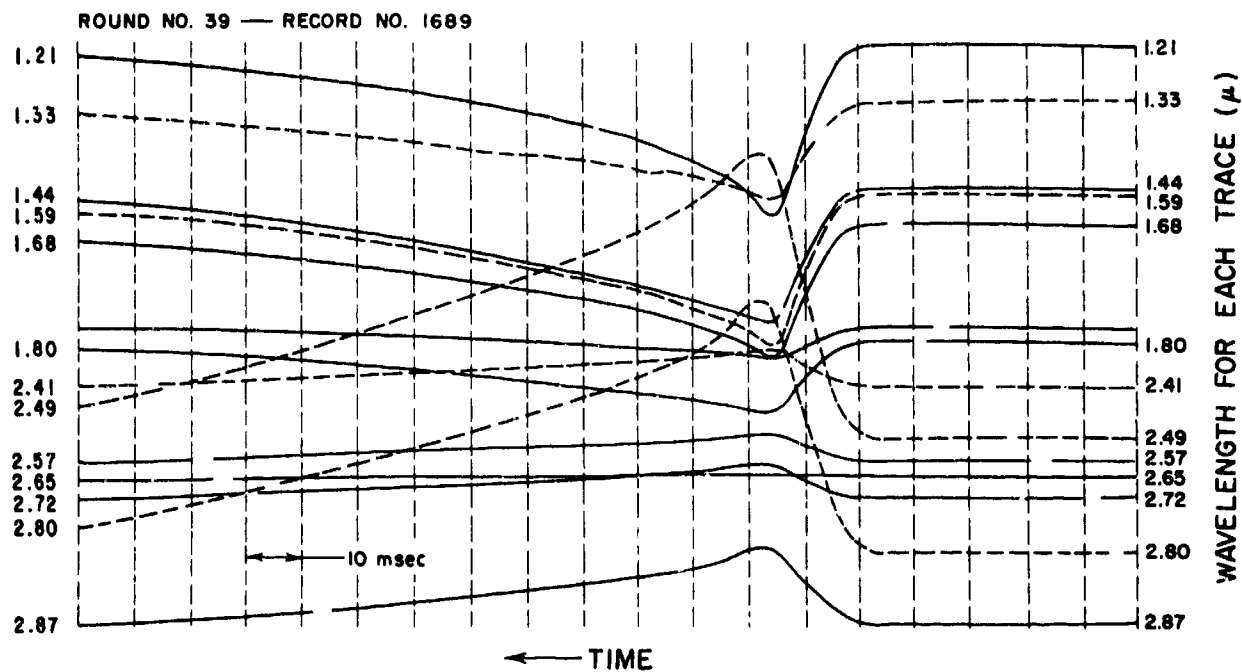
A summary of flash data is given in Table 3-7. Spectral emittance data are presented in Figures 3-10 (A to E) and Tables 3-8 (A to C).

The emittance curves for some of the intermediate flashes are approximate because their projected areas (Table 3-7) were too small to meet the requirement that the flash must cover the field of view of the spectrometer.\*\*

In general, the data show that the radiation from flash is characteristic of H<sub>2</sub>O and CO<sub>2</sub> emission for all of the propellants and weapons tested.

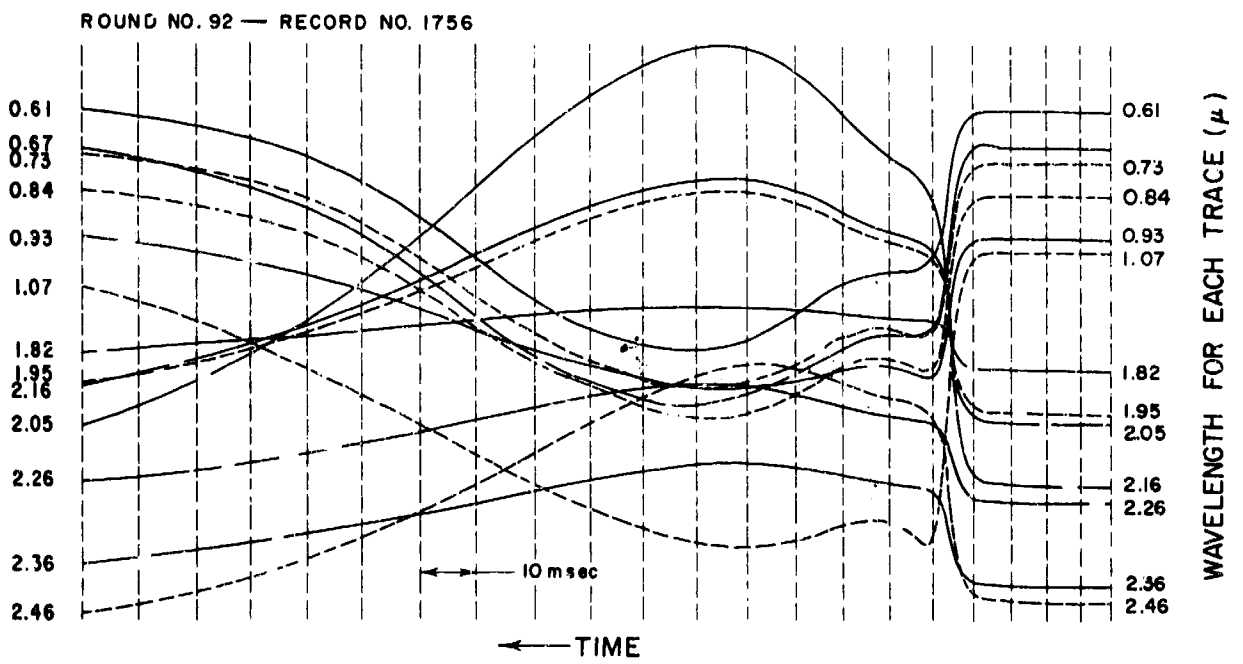
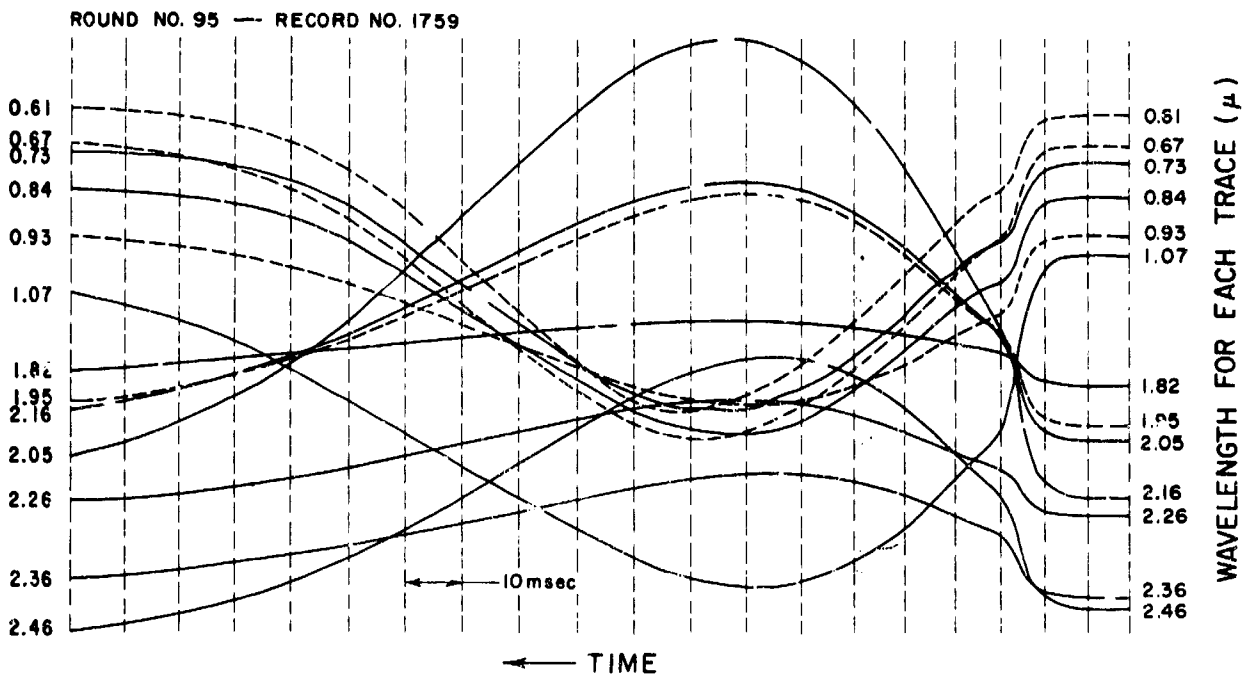
\*Investigation of the boundary of the flash with the spectrometer, with and without an infrared absorbing filter, showed that the boundaries of the regions emitting visible and infrared radiation were approximately the same. Therefore, photographs provided a reasonable indication of the projected area.

\*\*In these cases one could make an approximate correction of the spectral emittances by assuming that the flash radiation was uniform over all portions of its projected area as viewed by the spectrometers, and dividing the uncorrected values of emittance by the fraction of the field of view filled by the flash. The same correction would apply to radiant emittance and to the total radiant energy.



NOTE: BOTH SOLID AND DOTTED CURVES USED FOR CLARITY.

FIGURE 3 — (A) — SPECTROGRAMS OF FLASH FROM 280-MM GUN (FROM REF. 8d)  
 BOTH SOLID AND DOTTED CURVES USED FOR CLARITY. POSITIVE  
 DEFLECTION IS DOWNWARD FOR TRACES HAVING WAVELENGTHS BETWEEN  $1.21\mu$  and  $1.80\mu$ .



NOTE: BOTH SOLID AND DOTTED CURVE LINES USED FOR CLARITY ONLY.

FIGURE 3 — 7(B) — SPECTROGRAMS OF FLASH FROM 280-MM GUN (FROM REF. 8d)  
 BOTH SOLID AND DOTTED CURVES USED FOR CLARITY. POSITIVE DEFLECTION IS DOWNWARD FOR TRACES HAVING WAVELENGTHS BETWEEN 0.61 $\mu$  AND 1.07 $\mu$ .

WEAPON: 280 mm GUN		
TEST NO.	CODE	DIAL SETTING OF SPECTROMETER*
1		2578 - 2728 - 2891
2	---	●    ▲    ○
3	—	●    ⊗    ⊙

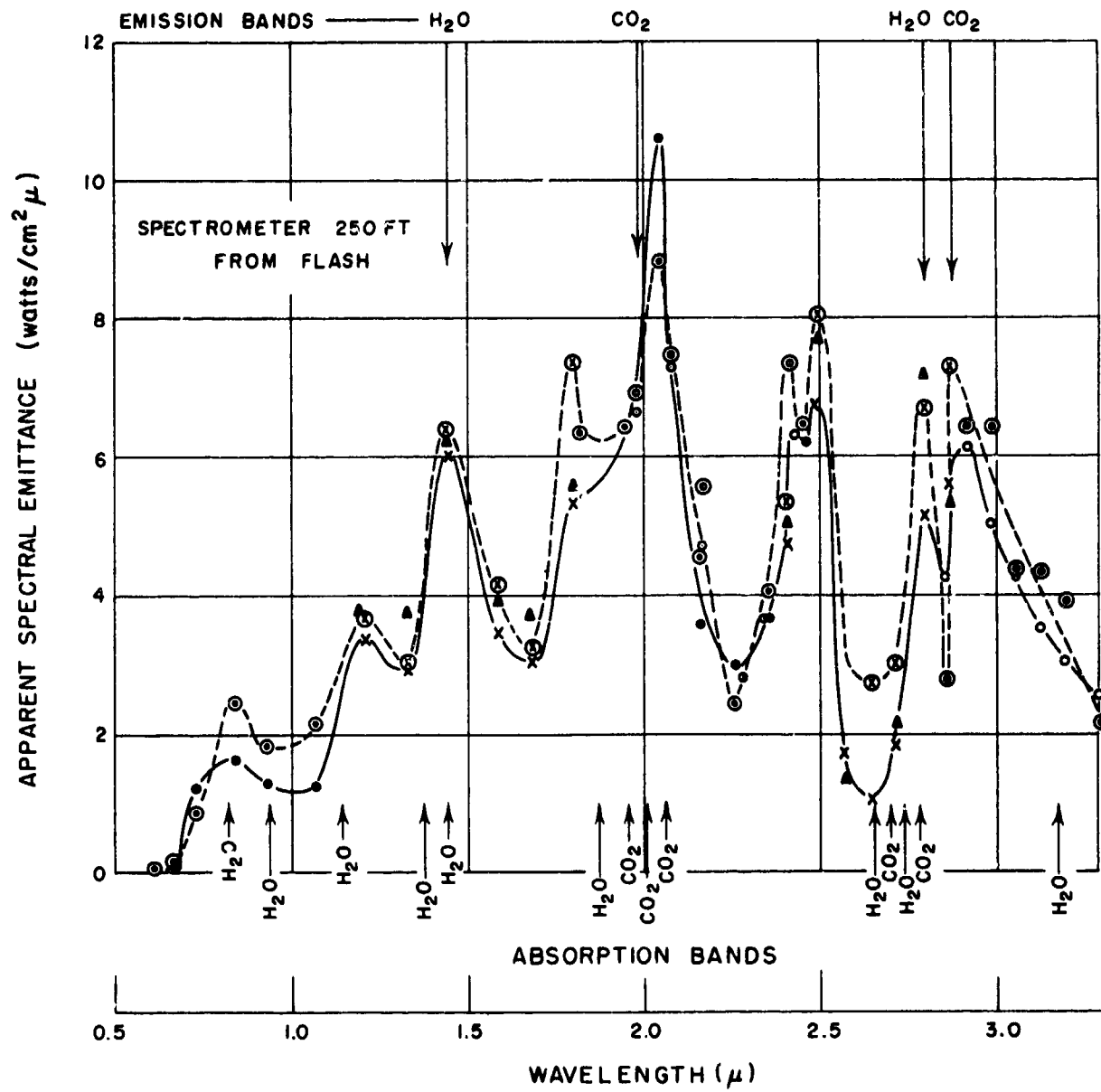


FIGURE 3—8—APPARENT SPECTRAL EMITTANCE OF UNSUPPRESSED FLASH FROM 280-MM GUN (FROM REF. 8d)  
 \*THE DIAL SETTING OF THE SPECTROMETER DETERMINED THE RANGE OF WAVELENGTHS FALLING ON THE DETECTORS

TABLE 3-5  
SPECTROGRAPHIC DATA FOR 280-mm GUN (From Ref. 8d)  
Propellant M6, MP

Charges: Test I - Vary from 156.76 to 171.29 lb.  
Test II - 159.5 lb.  
Test III - Vary from 156.76 to 163.16 lb.

Test No.	Round Nos.													
		<u>0.61</u>	<u>0.67</u>	<u>0.73</u>	<u>0.84</u>	<u>0.93</u>	<u>1.07</u>	<u>1.82</u>	<u>1.95</u>	<u>2.05</u>	<u>2.16</u>	<u>2.26</u>	<u>2.36</u>	<u>2.46</u>
		Average Spectral Emittance (watt/cm <sup>2</sup> μ)												
II	47-50	0.0480	0.108	1.21	1.64	1.30	1.23	5.39	--	10.6	3.57	3.00	3.69	6.25
		(Note 1)												
III	90-95	0.0440	0.135	0.829	2.45	1.82	2.18	6.33	6.42	8.82	4.57	2.45	4.07	6.46
		(Note 3)												
		<u>1.21</u>	<u>1.33</u>	<u>1.44</u>	<u>1.59</u>	<u>1.68</u>	<u>1.80</u>	<u>2.41</u>	<u>2.49</u>	<u>2.57</u>	<u>2.65</u>	<u>2.72</u>	<u>2.80</u>	<u>2.87</u>
		Average Spectral Emittance (watt/cm <sup>2</sup> μ)												
I	39-45	3.74	3.77	6.22	3.92	3.74	5.56	5.09	7.71	1.35	--	2.19	7.20	5.35
		(Note 2)												
II	51-54	3.37	2.92	6.05	3.47	3.07	5.36	4.78	6.76	1.75	1.09	1.84	5.19	5.60
III	97-100	3.70	3.01	6.44	4.17	3.28	7.36	5.35	8.07	--	2.77	3.02	6.71	7.31
		(Note 3) (Note 3)												
		<u>1.98</u>	<u>2.08</u>	<u>2.17</u>	<u>2.28</u>	<u>2.35</u>	<u>2.43</u>	<u>2.86</u>	<u>2.92</u>	<u>2.99</u>	<u>3.06</u>	<u>3.13</u>	<u>3.21</u>	<u>3.29</u>
		Average Spectral Emittance (watt/cm <sup>2</sup> μ)												
II	55, 56	6.63	7.29	4.71	2.82	3.69	6.32	4.27	6.15	5.04	4.25	3.53	3.02	2.59
III	102-107, 109	6.94	7.48	5.54	3.30	4.17	7.32	2.80	6.44	6.45	4.39	4.30	3.95	2.20
		(Note 3)												

Notes: 1. Value obtained for Round 47 only.  
2. Data missing for 3 of the 7 rounds.  
3. Data missing for 1 round.

TABLE 3-6  
EXPLANATION OF MAXIMA AND MINIMA OF SPECTRAL EMITTANCE CURVES IN FIGURE 3-8  
(From Ref. 8d)

Wavelength (μ)	Maximum	Minimum	Explanation
2.89-2.99	X		2.88 μ - Emission characteristic of CO <sub>2</sub> .
2.80	X		2.81 μ - Emission characteristic of H <sub>2</sub> O.
2.65		X	Absorption by atmospheric H <sub>2</sub> O.
2.50	X		Undetermined.
2.46		X	Undetermined.
2.42	X		Undetermined.
2.05	X		1.99 μ - Emission characteristic of CO <sub>2</sub> .
1.90		X	Absorption by atmospheric H <sub>2</sub> O.
1.70		X	This minimum is caused by the overlapping of emission at 1.45 and 2.00 μ.
1.45	X		Emission characteristic of H <sub>2</sub> O.
1.34		X	Absorption by atmospheric H <sub>2</sub> O.
1.20	X		This is an apparent peak caused by absorption at 1.35 μ.

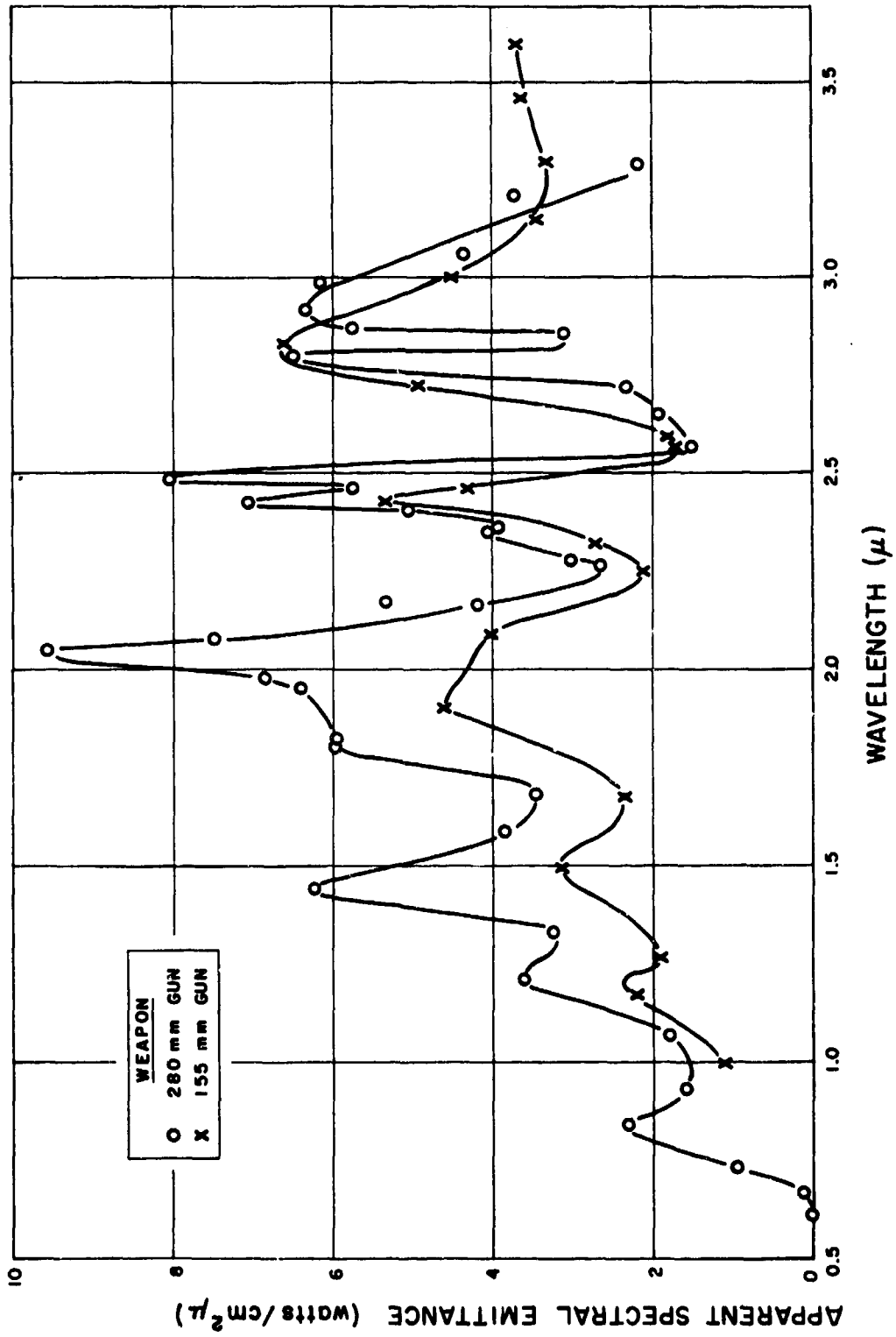


FIGURE 3 -- 9 -- COMPARISON OF APPARENT SPECTRAL EMITTANCES OF UNSUPPRESSED FLASH FROM 155-MM AND 280-MM GUNS (FROM REF. 8d)  
(VALUES OBTAINED FROM WEIGHTED AVERAGES OF DATA IN TABLES 3--1 AND 3--5)

TABLE 3-7  
SUMMARY OF EMITTANCE DATA ON FLASH FROM LARGE-CALIBER WEAPONS  
(From Ref. 8e)

Cannon	Propellant	Charges (lb)	No. of Flashes Secondary	Inter- mediate	Flash Area (ft <sup>2</sup> )	Total Emittance (1) (watts/cm <sup>2</sup> )	Total Rate of Radiation (watts)	% of Field of View Filled by Flash
75-mm Gun (M1897 A4)	M1	1.98	0	40	5	(2) 0.38	1.8x10 <sup>3</sup>	(5) 42
85-mm Gun (Russian)	---	5.47	3	37	30	0.78	2.2x10 <sup>4</sup>	100
90-mm Gun (M2)	M15	6.7	1	39	45	0.55	2.3x10 <sup>4</sup>	100
75-mm Howitzer (M1A1)	M1	0.94	0	40	---	0.11	---	---
105-mm Howitzer (M3)	M1	2.79	0	40	14	0.23	3.0x10 <sup>3</sup>	(5) 56
122-mm Howitzer (Russian)	---	1.44	2	10	24	(3) 0.16	3.5x10 <sup>3</sup>	(5) 50
155-mm Howitzer (M1)	M1	M3 5.54	0	40	4	0.09	3.3x10 <sup>2</sup>	(5) 16
8-Inch Howitzer (M1)	M1	28.2	3	37	50	(4) 0.27	1.3x10 <sup>4</sup>	(5) 70
90-mm Gun (M2)	M6	7.94	40	0	190	8.7	1.5x10 <sup>6</sup>	100
155-mm Howitzer (M1)	M1	M4A1 6.8	40	0	240	5.9	1.3x10 <sup>6</sup>	100
8-Inch Gun (M1)	M6	92.88	40	0	1300	14	1.7x10 <sup>7</sup>	100

INTERMEDIATE

SECONDARY

(1)  $\lambda$  (0.99 to 3.4  $\mu$ )  
 (2)  $\lambda$  (0.99 to 3.2  $\mu$ )  
 (3)  $\lambda$  (0.99 to 2.84  $\mu$ )  
 (4)  $\lambda$  (0.99 to 3.27  $\mu$ )  
 (5) See footnote to par. 3-5.4 for comment concerning cases where field of view was not filled.

Table is concluded on next page.

TABLE 3-7 (CONCL.)  
SUMMARY OF EMITTANCE DATA ON FLASH FROM LARGE-CALIBER WEAPONS  
(From Ref. 8e)

Weapon	No. of Peaks For Each Trace	Time of Peaks (msec.)		Total Time Duration (msec.)	Characteristics
		First	Second		
77-mm Gun (M1897 A4)	1	2.7	--	10	Traces for $\lambda = 0.44$ to $0.9 \mu$ occur sooner than the others.
85-mm Gun (Russian)	1	4.4	--	14	Traces appear more rounded.
90-mm Gun (M2)	1	4.0	--	15	Traces 8 and 9 ( $\lambda = 0.77 \mu$ and $\lambda = 0.9 \mu$ ) have odd shapes.
75-mm Howitzer (M1A1)	2	1.9	3.1	7	Traces for $\lambda = 0.44$ to $0.9 \mu$ do not return to their base lines as the others do.
105-mm Howitzer (M3)	2	2.8	5.4	12	-----
122-mm Howitzer (Russian)	2	2.8	5.1	14	-----
155-mm Howitzer (M1)	2	2.6	7.0	15	-----
8-Inch Howitzer (M1)	2	4.7	8.6	24	-----
90-mm Gun (M2)	Peak varies for each trace	18.0 to 29.0	--	(6) <sub>40</sub>	Peaks are rounded and do not occur at the same place.
155-mm Howitzer (M1)	---	5.1	--	(6) <sub>46</sub>	-----
8-Inch Gun (M1)	---	10.1	--	(6) <sub>107</sub>	Rise to peak signal is fast.

INTERMEDIATE

SECONDARY

(6) Total time from 0 to C on Spectrographic Records (See Fig. 3-11, Parts D, E and J.)

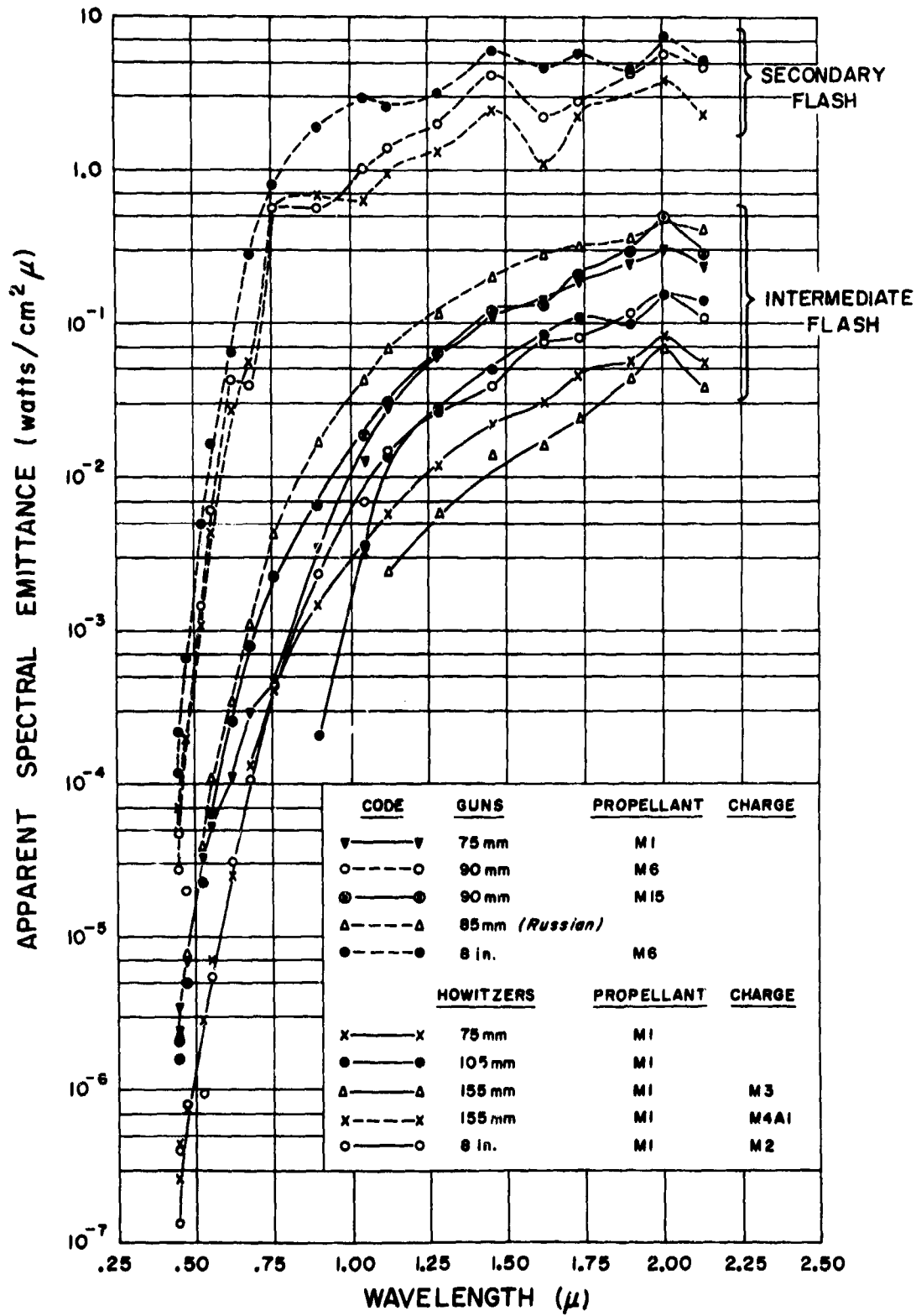


FIGURE 3-10—APPARENT SPECTRAL EMITTANCE OF FLASH FROM LARGE CALIBER WEAPONS (FROM REF. 8a)  
 (A)  $\lambda = 0.41$  TO  $2.13\mu$ . SEE TABLE 3-8(A).

CODE	GUNS	PROPELLANT	CHARGE
▼	75 MM	M1	
⊙	90 MM	M15	
Δ	85 MM (Russian)		
HOWITZERS		PROPELLANT	CHARGE
x	75 MM	M1	
●	105 MM	M1	
▼	122 MM (Russian)		
Δ	155 MM	M2	M3
○	8 IN.	M1	M2

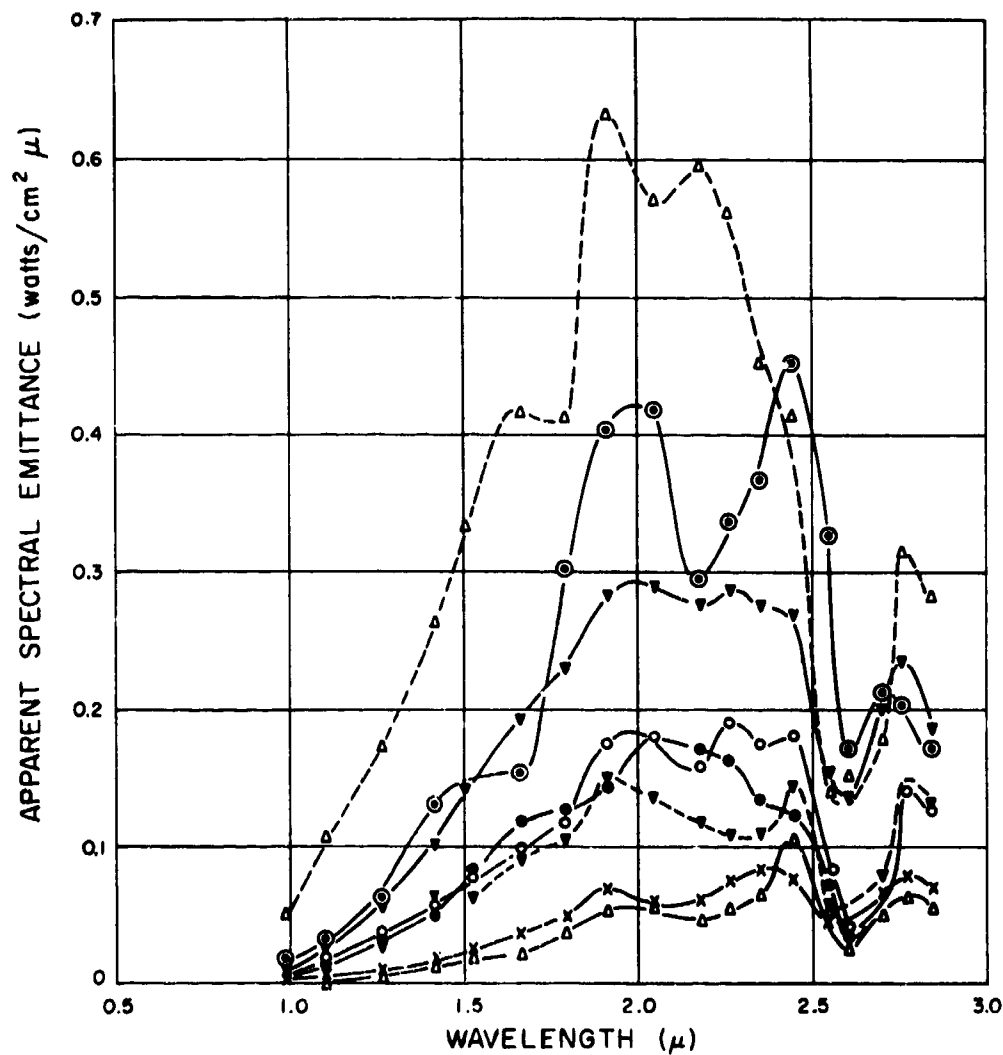


FIGURE 3-10—APPARENT SPECTRAL EMITTANCE OF FLASH FROM LARGE CALIBER WEAPONS (FROM REF. 8a)  
 (B)  $\lambda = 0.99$  TO  $2.84 \mu$ . SEE TABLE 3-8(B)  
 INTERMEDIATE FLASH

CODE	CANNON	PROPELLANT	CHARGE
○—○	90mm GUN	M6	
X—X	155mm (Howitzer)	M1	M4A1
●—●	8 in. GUN	M6	
●- - ●	155 mm GUN	} See Figure 3-9	
⊕- - ⊕	280 mm GUN		

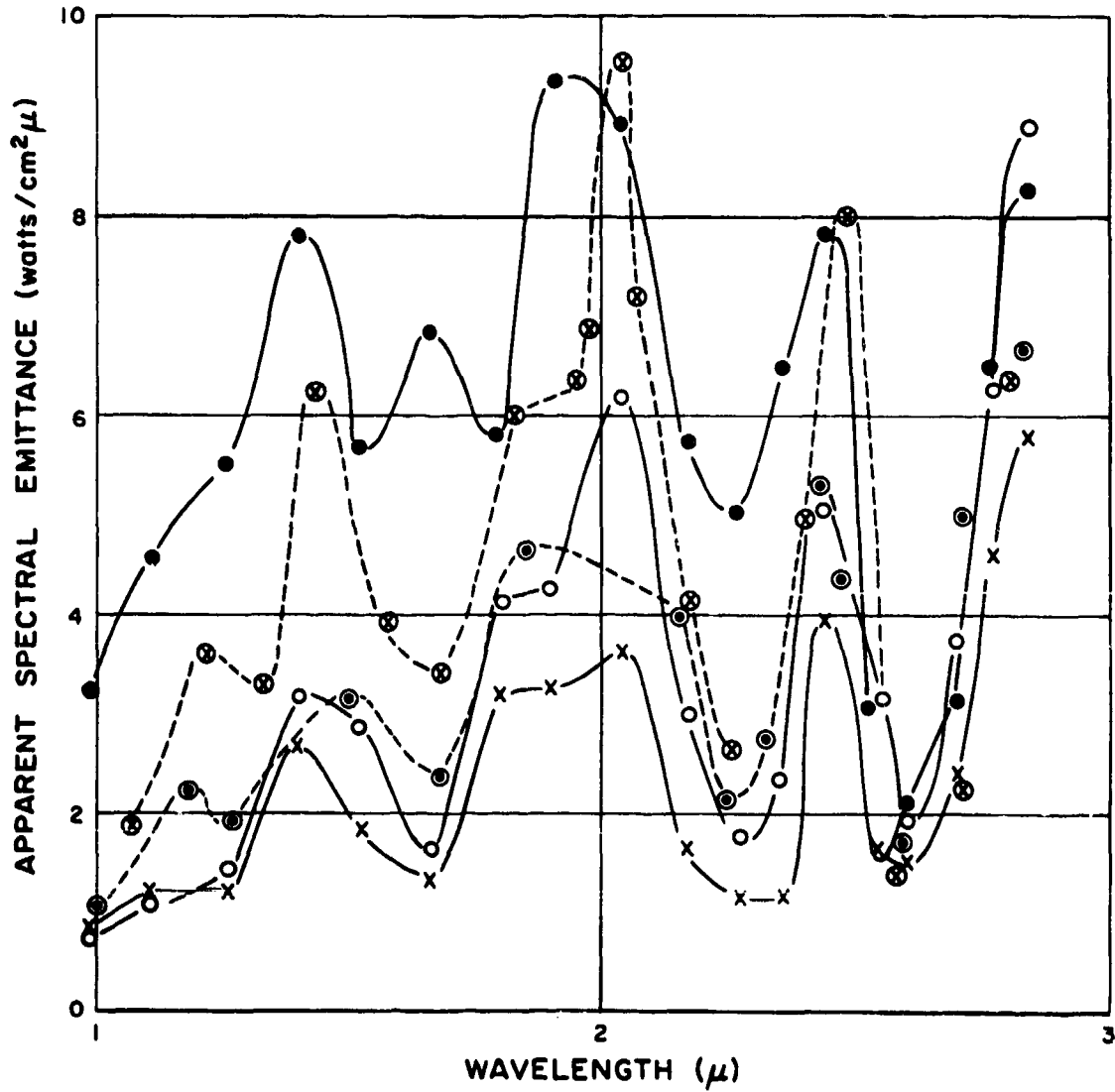


FIGURE 3-10 — APPARENT SPECTRAL EMITTANCE OF FLASH FROM LARGE CALIBER WEAPONS (FROM REF. 8c)  
 (C)  $\lambda = 0.99$  TO  $2.84\mu$ . SEE TABLE 3-8(B)  
 SECONDARY FLASH

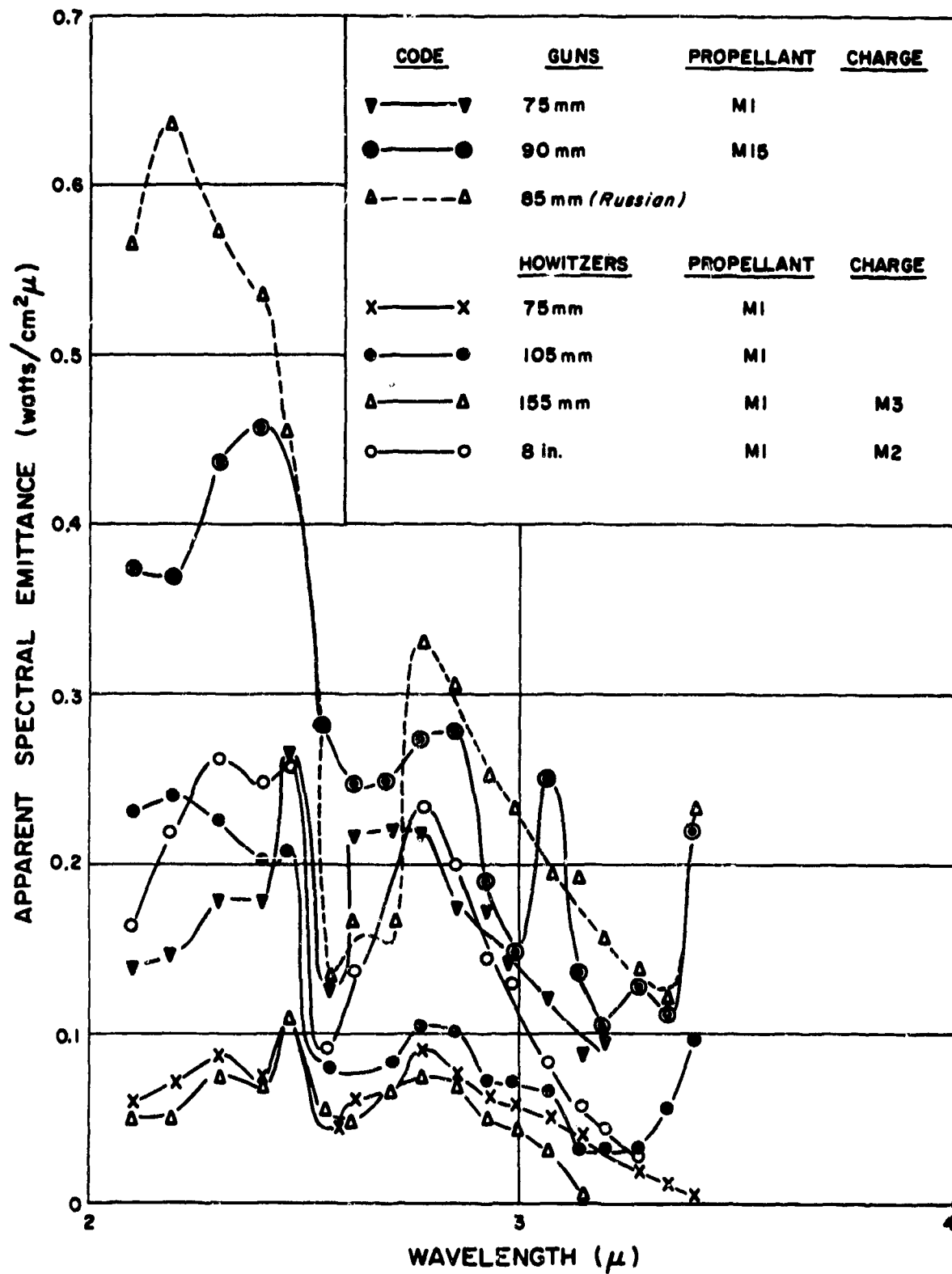


FIGURE 3-10—APPARENT SPECTRAL EMITTANCE OF FLASH FROM LARGE CALIBER WEAPONS (FROM REF. 8e)  
 (D)  $\lambda = 2.1$  TO  $3.40\mu$ . SEE TABLE 3-8(C)  
 INTERMEDIATE FLASH

CODE	CANNON	PROPELLANT	CHARGE
○—○	90 mm GUN	M6	
X—X	155 mm (Howitzer)	M1	M4A1
●—●	8 in. GUN	M6	
●- - -●	155 mm GUN		} See Figure 3-9
⊕- - -⊕	280 GUN		

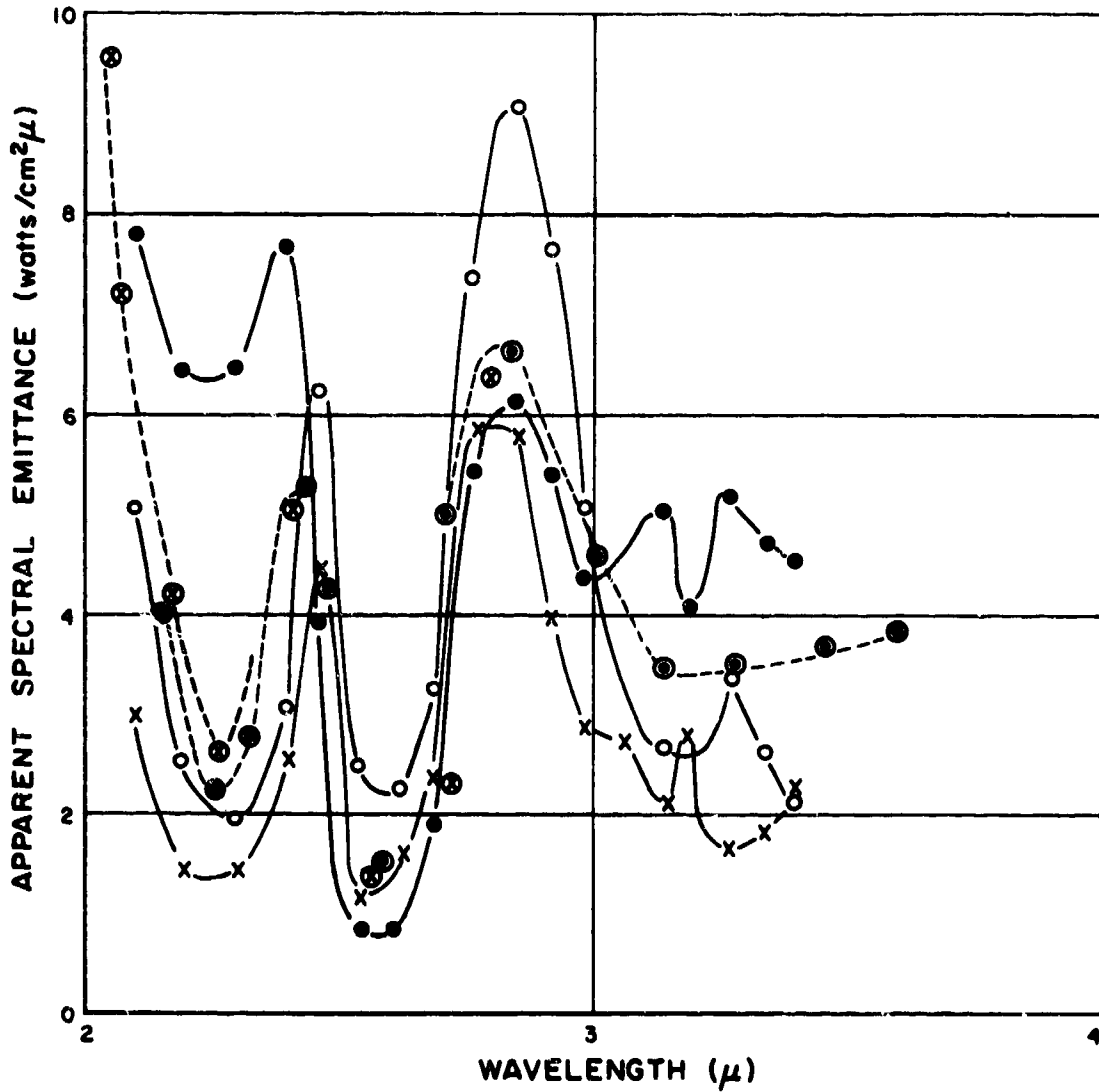


FIGURE 3-10—APPARENT SPECTRAL EMITTANCE OF FLASH FROM LARGE CALIBER WEAPONS (FROM REF. 8c)  
(E)  $\lambda = 2.1$  TO  $3.4\mu$ . SEE TABLE 3-8(C).

SECONDARY FLASH

TABLE 3-8(A)  
 AVERAGE VALUES OF THE APPARENT SPECTRAL EMITTANCE OF FLASH FROM LARGE-CALIBER WEAPONS  
 (From Ref. 8e)

Wavelength ( $\mu$ )	APPARENT SPECTRAL EMITTANCE $\left(\frac{\text{watts}}{\text{cm}^2 \mu}\right)$									
	155-mm Howitzer Charge M3	75-mm Howitzer	8-In. Howitzer	105-mm Howitzer	75-mm Gun	90-mm Gun Propellant M15	90-mm Gun Russian	155-mm Howitzer Charge M4A1	90-mm Gun Propellant M6	8-In. Gun
0.44	--	$4.4 \times 10^{-7}$	$1.4 \times 10^{-7}$	$2.6 \times 10^{-7}$	$2.5 \times 10^{-6}$	$1.6 \times 10^{-6}$	$2.4 \times 10^{-6}$	$4.9 \times 10^{-5}$	$2.7 \times 10^{-5}$	$1.2 \times 10^{-4}$
0.45	--	--	$4.1 \times 10^{-7}$	$6.4 \times 10^{-7}$	$3.5 \times 10^{-6}$	$2.0 \times 10^{-6}$	$3.6 \times 10^{-6}$	$7.0 \times 10^{-5}$	$5.0 \times 10^{-5}$	$2.2 \times 10^{-4}$
0.47	--	$7.5 \times 10^{-7}$	$8.0 \times 10^{-7}$	$4.7 \times 10^{-7}$	$7.0 \times 10^{-6}$	$4.9 \times 10^{-6}$	$7.7 \times 10^{-6}$	$2.0 \times 10^{-4}$	$2.0 \times 10^{-5}$	$6.7 \times 10^{-4}$
0.52	--	$2.9 \times 10^{-6}$	$9.4 \times 10^{-7}$	$7.8 \times 10^{-6}$	$3.3 \times 10^{-5}$	$2.3 \times 10^{-5}$	$3.8 \times 10^{-5}$	$1.1 \times 10^{-3}$	$1.4 \times 10^{-3}$	$5.0 \times 10^{-3}$
0.56	--	$7.2 \times 10^{-6}$	$5.5 \times 10^{-6}$	$9.4 \times 10^{-6}$	$5.3 \times 10^{-5}$	$6.4 \times 10^{-5}$	$1.1 \times 10^{-4}$	$4.3 \times 10^{-3}$	$6.1 \times 10^{-3}$	$1.7 \times 10^{-2}$
0.62	--	$2.5 \times 10^{-5}$	$3.1 \times 10^{-5}$	--	$1.1 \times 10^{-4}$	$2.6 \times 10^{-4}$	$3.4 \times 10^{-4}$	$2.7 \times 10^{-3}$	$4.4 \times 10^{-2}$	$6.5 \times 10^{-2}$
0.68	--	$1.3 \times 10^{-4}$	$1.1 \times 10^{-4}$	--	$2.9 \times 10^{-7}$	$7.8 \times 10^{-4}$	$1.1 \times 10^{-3}$	$5.7 \times 10^{-2}$	$2.9 \times 10^{-2}$	$2.8 \times 10^{-1}$
0.77	--	$4.3 \times 10^{-4}$	$4.2 \times 10^{-4}$	--	$4.4 \times 10^{-4}$	$2.3 \times 10^{-3}$	$4.2 \times 10^{-3}$	$5.6 \times 10^{-1}$	$5.7 \times 10^{-1}$	$8.0 \times 10^{-1}$
0.90	--	$1.5 \times 10^{-3}$	$2.4 \times 10^{-3}$	$2.1 \times 10^{-4}$	$3.4 \times 10^{-3}$	$6.4 \times 10^{-3}$	$1.7 \times 10^{-2}$	$6.6 \times 10^{-3}$	$5.9 \times 10^{-1}$	1.9
1.04	$1.1 \times 10^{-4}$	$3.2 \times 10^{-3}$	$6.9 \times 10^{-3}$	$3.6 \times 10^{-3}$	$1.3 \times 10^{-2}$	$1.8 \times 10^{-2}$	$4.2 \times 10^{-2}$	$6.4 \times 10^{-1}$	1.0	2.9
1.12	$2.4 \times 10^{-3}$	$5.8 \times 10^{-3}$	$1.5 \times 10^{-2}$	$1.4 \times 10^{-2}$	$2.9 \times 10^{-2}$	$3.0 \times 10^{-2}$	$6.8 \times 10^{-2}$	$9.4 \times 10^{-1}$	1.4	--
1.28	$5.7 \times 10^{-3}$	$1.2 \times 10^{-2}$	$2.7 \times 10^{-2}$	$2.7 \times 10^{-2}$	$6.1 \times 10^{-2}$	$6.3 \times 10^{-2}$	$1.1 \times 10^{-1}$	1.3	2.0	3.1
1.46	$1.4 \times 10^{-2}$	$2.1 \times 10^{-2}$	$3.8 \times 10^{-2}$	$4.9 \times 10^{-2}$	$1.1 \times 10^{-1}$	$1.2 \times 10^{-1}$	$2.0 \times 10^{-1}$	2.4	4.1	6.0
1.62	$1.6 \times 10^{-2}$	$3.0 \times 10^{-2}$	$7.5 \times 10^{-2}$	$8.2 \times 10^{-2}$	$1.40 \times 10^{-1}$	$1.3 \times 10^{-1}$	$2.8 \times 10^{-1}$	1.1	2.2	4.6
1.73	$2.4 \times 10^{-2}$	$4.5 \times 10^{-2}$	$8.0 \times 10^{-2}$	$1.09 \times 10^{-1}$	$1.80 \times 10^{-1}$	$2.0 \times 10^{-1}$	$3.1 \times 10^{-1}$	2.2	2.8	5.7
1.89	$4.3 \times 10^{-2}$	$5.5 \times 10^{-2}$	$1.2 \times 10^{-1}$	$9.8 \times 10^{-2}$	$2.40 \times 10^{-1}$	$2.9 \times 10^{-1}$	$3.5 \times 10^{-1}$	--	4.2	4.4
2.01	$6.9 \times 10^{-2}$	$8.0 \times 10^{-2}$	$1.5 \times 10^{-1}$	$1.5 \times 10^{-1}$	$3.0 \times 10^{-1}$	$4.8 \times 10^{-1}$	$4.4 \times 10^{-1}$	3.8	5.6	7.3
2.13	$3.7 \times 10^{-2}$	--	$1.1 \times 10^{-1}$	$1.4 \times 10^{-1}$	$2.4 \times 10^{-1}$	$2.7 \times 10^{-1}$	$4.0 \times 10^{-1}$	2.2	4.6	5.0

TABLE 3-8(B)  
 AVERAGE VALUES OF THE APPARENT SPECTRAL EMITTANCE OF FLASH FROM LARGE-CALIBER WEAPONS  
 (From Ref. 8e)

Wavelength ( $\mu$ )	155-mm Howitzer Charge M3	75-mm Howitzer	8-In. Howitzer	122-mm Howitzer Russian	105-mm Howitzer	90-mm Gun Propellant M15	75-mm Gun	85-mm Gun Russian	155-mm Howitzer Charge M4A1	90-mm Gun Propellant M6	8-In. Gun
	APPARENT SPECTRAL EMITTANCE ( $\frac{\text{watts}}{\text{cm}^2\mu}$ )										
0.99	$1.3 \times 10^{-4}$	$2.3 \times 10^{-3}$	$7.8 \times 10^{-3}$	$7.5 \times 10^{-3}$	$4.0 \times 10^{-3}$	$1.9 \times 10^{-2}$	$1.0 \times 10^{-2}$	$5.7 \times 10^{-2}$	0.74	0.76	3.2
1.11	$1.6 \times 10^{-3}$	$5.0 \times 10^{-3}$	$2.0 \times 10^{-2}$	$2.1 \times 10^{-2}$	$1.5 \times 10^{-2}$	$3.2 \times 10^{-2}$	$2.6 \times 10^{-2}$	$1.1 \times 10^{-1}$	1.2	1.0	4.5
1.26	$5.9 \times 10^{-3}$	$1.1 \times 10^{-2}$	$3.4 \times 10^{-2}$	$3.8 \times 10^{-2}$	$3.4 \times 10^{-2}$	$6.3 \times 10^{-2}$	$5.8 \times 10^{-2}$	$1.7 \times 10^{-1}$	1.3	1.4	5.5
1.41	$1.4 \times 10^{-2}$	$1.9 \times 10^{-2}$	$6.0 \times 10^{-2}$	$6.4 \times 10^{-2}$	$5.0 \times 10^{-2}$	$1.3 \times 10^{-1}$	$1.0 \times 10^{-1}$	$2.6 \times 10^{-1}$	2.7	3.2	7.8
1.52	$1.8 \times 10^{-2}$	$2.5 \times 10^{-2}$	$7.6 \times 10^{-2}$	$6.6 \times 10^{-2}$	$8.4 \times 10^{-2}$	$1.5 \times 10^{-1}$	$1.4 \times 10^{-1}$	$3.3 \times 10^{-1}$	1.8	2.9	5.7
1.66	$2.3 \times 10^{-2}$	$3.9 \times 10^{-2}$	$9.9 \times 10^{-2}$	$9.4 \times 10^{-2}$	$1.2 \times 10^{-1}$	$1.5 \times 10^{-1}$	$1.9 \times 10^{-1}$	$4.2 \times 10^{-1}$	1.4	1.6	6.8
1.79	$3.8 \times 10^{-2}$	$5.0 \times 10^{-2}$	$1.21 \times 10^{-1}$	$1.1 \times 10^{-1}$	$1.3 \times 10^{-1}$	$3.0 \times 10^{-1}$	$2.3 \times 10^{-1}$	$4.1 \times 10^{-1}$	3.2	4.1	5.8
1.91	$5.3 \times 10^{-2}$	$7.1 \times 10^{-2}$	$1.8 \times 10^{-1}$	$1.5 \times 10^{-1}$	$1.5 \times 10^{-1}$	$4.1 \times 10^{-1}$	$2.9 \times 10^{-1}$	$6.3 \times 10^{-1}$	3.3	4.3	9.4
2.04	$6.1 \times 10^{-2}$	$6.0 \times 10^{-2}$	$1.8 \times 10^{-1}$	$1.4 \times 10^{-1}$	$1.8 \times 10^{-1}$	$4.2 \times 10^{-1}$	$2.9 \times 10^{-1}$	$5.7 \times 10^{-1}$	3.6	6.1	9.0
2.17	$4.7 \times 10^{-2}$	$6.6 \times 10^{-2}$	$1.6 \times 10^{-1}$	$1.2 \times 10^{-1}$	$1.7 \times 10^{-1}$	$3.0 \times 10^{-1}$	$2.8 \times 10^{-1}$	$6.0 \times 10^{-1}$	1.7	3.0	5.7
2.26	$5.5 \times 10^{-2}$	$7.5 \times 10^{-2}$	$1.9 \times 10^{-1}$	$1.1 \times 10^{-1}$	$1.7 \times 10^{-1}$	$3.4 \times 10^{-1}$	$2.9 \times 10^{-1}$	$5.7 \times 10^{-1}$	1.2	1.8	5.1
2.35	$6.6 \times 10^{-2}$	$8.5 \times 10^{-2}$	$1.8 \times 10^{-1}$	$1.1 \times 10^{-1}$	$1.4 \times 10^{-1}$	$3.7 \times 10^{-1}$	$2.8 \times 10^{-1}$	$4.5 \times 10^{-1}$	1.6	2.3	6.5
2.44	---	$7.9 \times 10^{-2}$	$1.9 \times 10^{-1}$	$1.5 \times 10^{-1}$	$1.3 \times 10^{-1}$	$4.5 \times 10^{-1}$	$2.7 \times 10^{-1}$	$4.2 \times 10^{-1}$	4.0	5.1	7.9
2.55	$5.7 \times 10^{-2}$	$4.9 \times 10^{-2}$	$8.2 \times 10^{-2}$	$6.2 \times 10^{-2}$	$7.1 \times 10^{-2}$	$3.3 \times 10^{-1}$	$1.6 \times 10^{-1}$	$1.4 \times 10^{-1}$	1.6	3.7	1.5
2.60	$2.6 \times 10^{-2}$	$4.8 \times 10^{-2}$	$4.2 \times 10^{-2}$	$6.2 \times 10^{-2}$	$3.7 \times 10^{-2}$	$1.7 \times 10^{-1}$	$1.4 \times 10^{-1}$	$1.5 \times 10^{-1}$	1.5	1.9	2.1
2.70	$5.0 \times 10^{-2}$	$6.7 \times 10^{-2}$	$6.5 \times 10^{-2}$	$8.2 \times 10^{-2}$	$5.5 \times 10^{-2}$	$2.1 \times 10^{-1}$	$2.0 \times 10^{-1}$	$1.8 \times 10^{-1}$	2.4	3.7	3.1
2.77	$6.0 \times 10^{-2}$	$6.2 \times 10^{-2}$	$1.5 \times 10^{-1}$	$1.5 \times 10^{-1}$	$6.8 \times 10^{-2}$	$2.0 \times 10^{-1}$	$2.4 \times 10^{-1}$	$3.2 \times 10^{-1}$	4.7	6.2	6.5
2.82	$9.8 \times 10^{-2}$	$7.2 \times 10^{-2}$	$1.3 \times 10^{-1}$	$1.3 \times 10^{-1}$	$5.8 \times 10^{-2}$	$1.7 \times 10^{-1}$	$1.9 \times 10^{-1}$	$2.8 \times 10^{-1}$	5.8	8.9	8.3

TABLE 3-8(C)  
 AVERAGE VALUES OF THE APPARENT SPECTRAL EMITTANCE OF FLASH FROM LARGE-CALIBER WEAPONS  
 (From Ref. 8e)

Wavelength ( $\mu$ )	155-mm Howitzer Charge M3	75-mm Howitzer	8-In. Howitzer	105-mm Howitzer	75-mm Gun	90-mm Gun	85-mm Gun Russian	155-mm		8-in. Gun	
								Howitzer Charge M4A1	90-mm Gun Propellant M6		
	APPARENT SPECTRAL EMITTANCE $\left(\frac{\text{watts}}{\text{cm}^2 \mu}\right)$										
2.1	$5.2 \times 10^{-2}$	$5.9 \times 10^{-2}$	$1.6 \times 10^{-1}$	$2.4 \times 10^{-1}$	$1.40 \times 10^{-1}$	$3.7 \times 10^{-1}$	0.57	3.0	5.1	7.9	
2.19	$5.2 \times 10^{-2}$	$6.9 \times 10^{-2}$	$2.2 \times 10^{-1}$	$2.4 \times 10^{-1}$	$1.5 \times 10^{-1}$	$3.7 \times 10^{-1}$	0.64	1.4	2.5	6.4	
2.30	$7.5 \times 10^{-2}$	$8.8 \times 10^{-2}$	$2.6 \times 10^{-1}$	$2.3 \times 10^{-1}$	$1.8 \times 10^{-1}$	$4.4 \times 10^{-1}$	0.58	1.4	2.0	6.5	
2.40	$6.9 \times 10^{-2}$	$7.5 \times 10^{-2}$	$2.5 \times 10^{-1}$	$2.0 \times 10^{-1}$	$1.8 \times 10^{-1}$	$4.6 \times 10^{-1}$	0.54	2.6	3.1	7.7	
2.46	$1.1 \times 10^{-1}$	$1.1 \times 10^{-1}$	$2.6 \times 10^{-1}$	$2.1 \times 10^{-1}$	$2.7 \times 10^{-1}$	---	0.46	4.5	6.2	4.0	
2.54	$4.8 \times 10^{-2}$	$4.2 \times 10^{-2}$	$9.3 \times 10^{-2}$	$8.1 \times 10^{-2}$	$1.3 \times 10^{-1}$	$2.8 \times 10^{-1}$	0.13	1.2	2.5	0.84	
2.61	$6.7 \times 10^{-2}$	$6.4 \times 10^{-2}$	$1.4 \times 10^{-1}$	---	$2.2 \times 10^{-1}$	$2.5 \times 10^{-1}$	0.17	1.7	2.3	0.82	
2.69	$7.5 \times 10^{-2}$	$6.6 \times 10^{-2}$	$1.7 \times 10^{-1}$	$8.0 \times 10^{-2}$	$2.2 \times 10^{-1}$	$2.5 \times 10^{-1}$	0.16	2.3	3.3	1.9	
2.77	$7.0 \times 10^{-2}$	$9.1 \times 10^{-2}$	$2.4 \times 10^{-1}$	$1.1 \times 10^{-1}$	$2.2 \times 10^{-1}$	$2.7 \times 10^{-1}$	0.33	5.9	7.3	5.4	
2.85	$5.1 \times 10^{-2}$	$7.6 \times 10^{-2}$	$2.0 \times 10^{-1}$	$1.0 \times 10^{-1}$	$1.7 \times 10^{-1}$	$2.8 \times 10^{-1}$	0.31	5.8	9.1	6.2	
2.92	$4.3 \times 10^{-2}$	$6.3 \times 10^{-2}$	$1.5 \times 10^{-1}$	$7.1 \times 10^{-2}$	$1.7 \times 10^{-1}$	$1.9 \times 10^{-1}$	0.25	4.0	7.7	5.4	
2.98	$3.1 \times 10^{-2}$	$5.9 \times 10^{-2}$	$1.3 \times 10^{-1}$	$7.3 \times 10^{-2}$	$1.5 \times 10^{-1}$	$1.5 \times 10^{-1}$	0.23	2.9	5.1	4.3	
3.06	$7.3 \times 10^{-2}$	$5.2 \times 10^{-2}$	$8.1 \times 10^{-2}$	$6.8 \times 10^{-2}$	$1.2 \times 10^{-1}$	$2.5 \times 10^{-1}$	0.19	2.8	4.6	---	
3.14	---	$4.1 \times 10^{-2}$	$5.8 \times 10^{-2}$	$3.3 \times 10^{-2}$	$9.0 \times 10^{-2}$	$1.4 \times 10^{-1}$	0.19	2.1	2.7	5.0	
3.19	---	$2.9 \times 10^{-2}$	$4.4 \times 10^{-2}$	$3.1 \times 10^{-2}$	$9.6 \times 10^{-2}$	$1.0 \times 10^{-1}$	0.16	2.7	2.5	4.1	
3.27	---	$2.2 \times 10^{-2}$	$2.6 \times 10^{-2}$	$3.5 \times 10^{-2}$	---	$1.3 \times 10^{-1}$	0.14	1.7	3.3	5.2	
3.34	---	$1.5 \times 10^{-2}$	---	$5.5 \times 10^{-2}$	---	$1.1 \times 10^{-1}$	0.12	1.9	2.6	4.7	
3.40	---	$5.1 \times 10^{-2}$	---	$9.4 \times 10^{-2}$	---	$2.3 \times 10^{-1}$	0.23	2.3	2.1	4.6	

From an inspection of spectrometer records, the spectral emittance curves, and the photographs of flash it is apparent that secondary flashes were characterized by large values of emittance, long time durations, large flash areas, and large values of total energy; and intermediate flashes were characterized by low emittances, short time durations, low total radiation, and small flash areas.

The values of the projected areas of the flashes are listed in Table 3-7. It is of interest that the projected area of the flash from the 155-mm howitzer was smaller than that of both the 105- and 122-mm howitzers.

The apparent spectral emittance curves for both intermediate and secondary flash in Figure 3-10 (A to E) have peak values centered at 2.8 and 2.0 $\mu$ , which are characteristic of CO<sub>2</sub> and H<sub>2</sub>O emission. Apparent peaks at 2.45 $\mu$  are probably caused by atmospheric absorption at 2.6 $\mu$ .

The emittance curves for the secondary flashes also show that:

- (a) An additional peak occurred in each case at 1.42 $\mu$  which is characteristic of H<sub>2</sub>O emission.
- (b) The peaks at 2.8 $\mu$  were higher than those at 2.0 $\mu$  for the 90-mm gun and the 155-mm howitzer. This was not so for the 8-in. gun; but since the spectrometer was located further from the flash when the 8-in. gun was tested, atmospheric attenuation may be responsible for lowering the peaks at 2.0 $\mu$ .
- (c) There were indications that larger changes contributed to greater values of spectral emittance; however, this was not conclusive due to a number of variables, such as the parts of the

flashes observed, the direction of observation, and the distance from the flash to the spectrometer.

The spectrometer traces shown in Figures 3-11 (A to K) show typical variations of flash intensity with time for the weapons tested. The traces were separated into two groups that were made to deflect in opposite directions in order to enable the recording of large deflections.

The amplifiers were designed so that, for fixed background radiation, the traces would not underswing their base lines. Therefore, when underswing was observed, it was caused by the background radiation being interrupted by the smoke from the weapons. The spectral emittances were not corrected for background radiation because the effect did not influence values beyond 1.2 $\mu$ , the region of primary interest.

For intermediate flashes the spectrometer records can be split into two groups: guns and howitzers. The individual traces for the howitzers usually had two peaks, one being very distinct and the other distinct for some rounds and hardly noticeable in others. The individual traces for the guns generally had one peak.

The spectral emittance curves and emittance-time curves of the Russian 85-mm gun and 122-mm howitzer were comparable with those for the field artillery.

Table 3-7 shows that, at times, both secondary and intermediate flashes were produced by the same combination of weapon and propellant. When the spectrometer was set to record intermediate flash and an intermediate flash occurred, its presence was indicated on the intensity-time traces by a relatively small peak occurring before the large peak due to the secondary flash (see Record 2426, Figure 3-11(H), for an example).

(A) RECORD - 1868  
 (75mm Gun - Propellant M1)

(B) RECORD - 1876  
 (75mm Gun - Propellant M1)



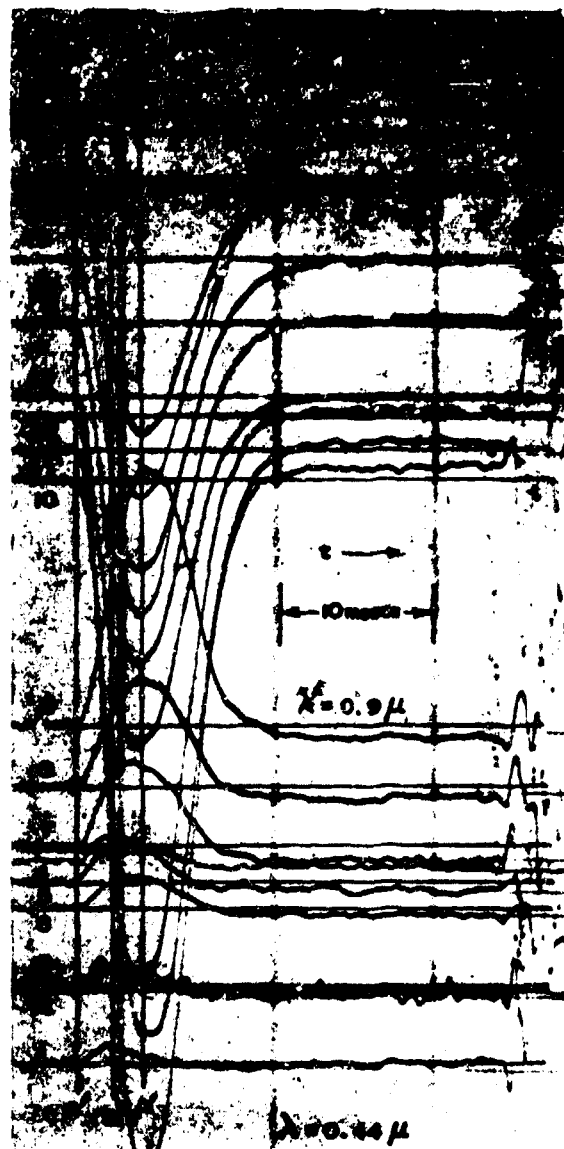
	TIME
OO' TO PEAK SIGNAL	2.7 msec
OO' TO 50% PEAK SIGNAL	4.9 msec
WAVELENGTHS 0.99 $\mu$ TO 2.84 $\mu$	

	TIME
OO' TO AA'	2.8 msec
OO' TO BB'	1.9 msec
WAVELENGTHS 0.44 $\mu$ TO 2.13 $\mu$	

FIGURE 3 - 11(A) - SPECTROMETER TRACES (FROM REF. 8\*)

(A) RECORD - 2477  
 (85mm Gun - Russian)

(B) RECORD - 2533  
 (85mm Gun - Russian)



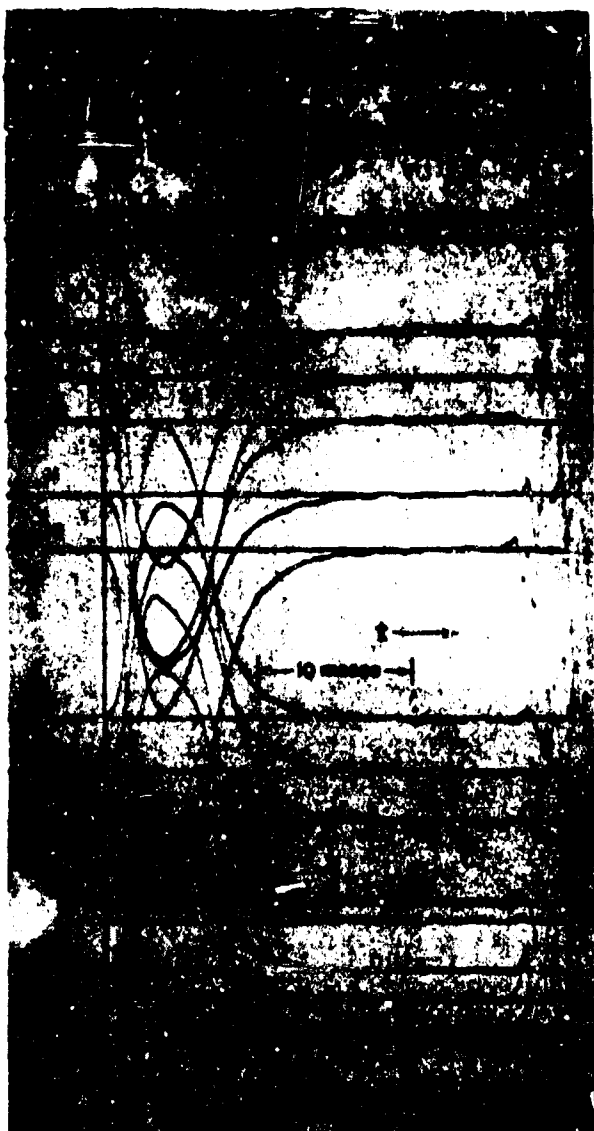
	TIME
OO' TO PEAK SIGNAL	4.5 msec
OO' TO 50% PEAK SIGNAL	7.5 msec
WAVELENGTHS 0.99 μ TO 2.84 μ	

	TIME
OO' TO AA'	4.2 msec
OO' TO BB'	2.1 msec
WAVELENGTHS 0.44 μ TO 2.13 μ	

FIGURE 3 - 11(B) - SPECTROMETER TRACES (FROM REF. 8e)

(A) RECORD - 2086  
(90mm Gun - Propellant M15)

(B) RECORD - 2108  
(90mm Gun - Propellant M15)



	TIME
00' TO PEAK SIGNAL	4.0 msecs
50' TO 50% PEAK SIGNAL	7.5 msecs

SPECTROMETER SETTING - 2456

	TIME
00' TO PEAK SIGNAL	4.0 msecs
50' TO 50% PEAK SIGNAL	7.5 msecs

SPECTROMETER SETTING - 2219

FIGURE 3 - 11(C) - SPECTROMETER TRACES (FROM REF. 8e)

(B) RECORD - 2035  
(90mm Gun - Propellant M6)



TIME FROM 00' TO PEAK SIGNAL 18.6 TO 24.1 msec

(A) RECORD - 2008  
(90mm Gun - Propellant M6)



TIME FROM 00' TO PEAK SIGNAL 17.9 TO 28.9 msec

FIGURE 3 - 11(D) - SPECTROMETER TRACES (FROM REF. 8e)

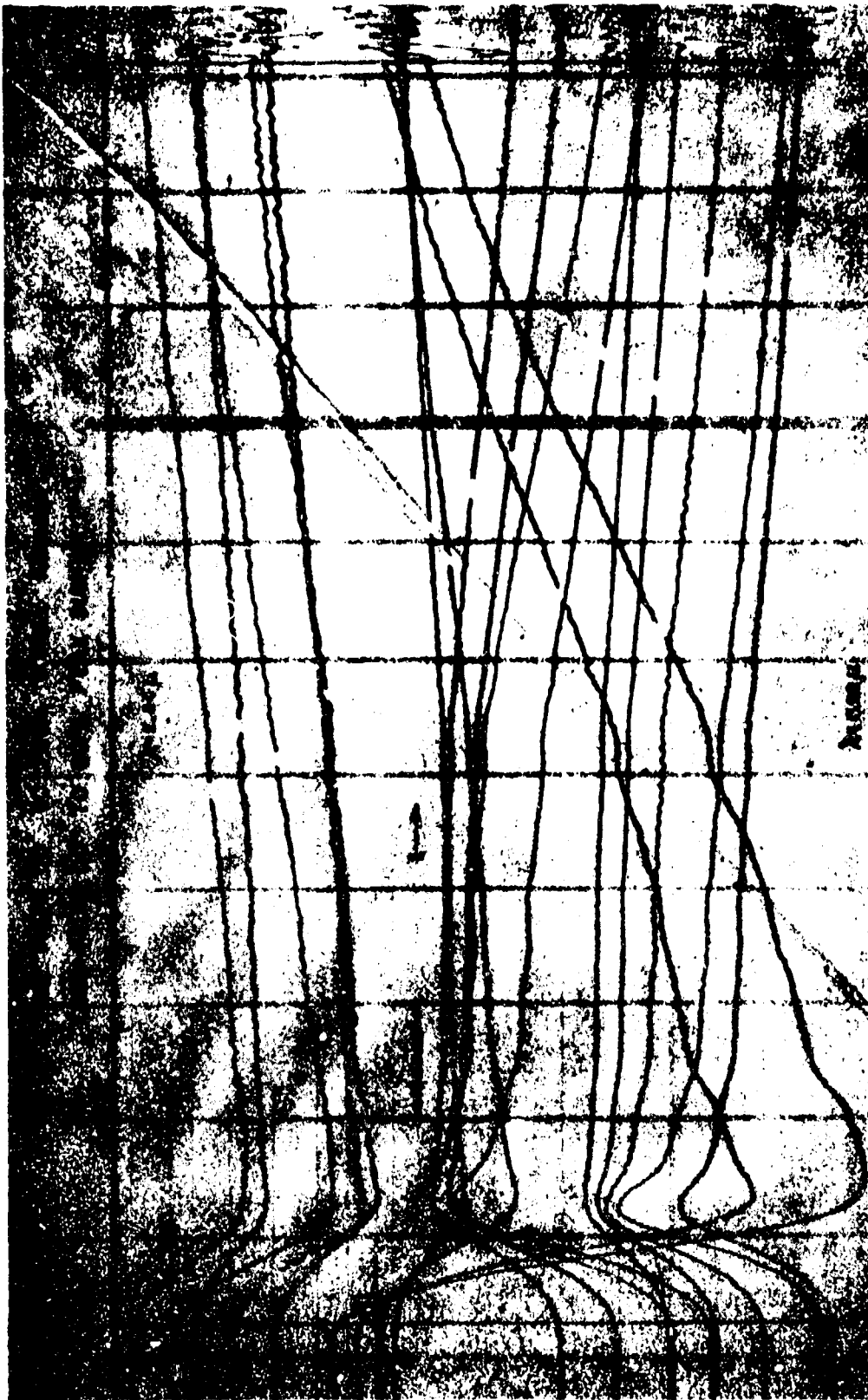


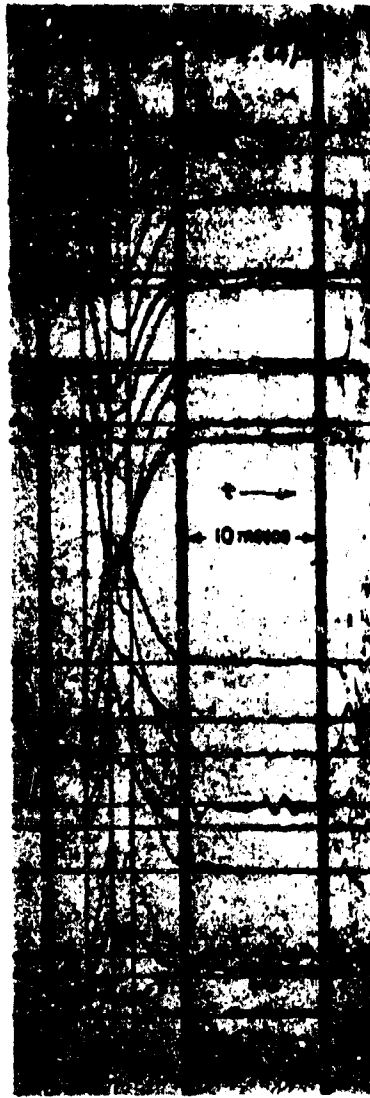
FIGURE 3—11(E)—SPECTROMETER TRACES (FROM REF. 8\*)  
8-IN. GUN

(A) RECORD - 1923  
(75mm Howitzer -  
Propellant M1)



	TIME
OO' TO PEAK SIGNAL (Traces 1 to 14)	1.9 msec
(Traces 16 to 18)	3.2 msec
OO' TO 50% PEAK SIGNAL (Traces 1 to 15)	3.9 msec
(Traces 16 to 18)	4.9 msec

(B) RECORD - 1925  
(75mm Howitzer -  
Propellant M1)



	TIME
OO' TO 1ST PEAK AA'	1.9 msec
OO' TO 2ND PEAK BB'	3.1 msec
WAVELENGTHS 0.99 $\mu$ TO 2.84 $\mu$	

(C) RECORD - 1959  
(75mm Howitzer -  
Propellant M1)

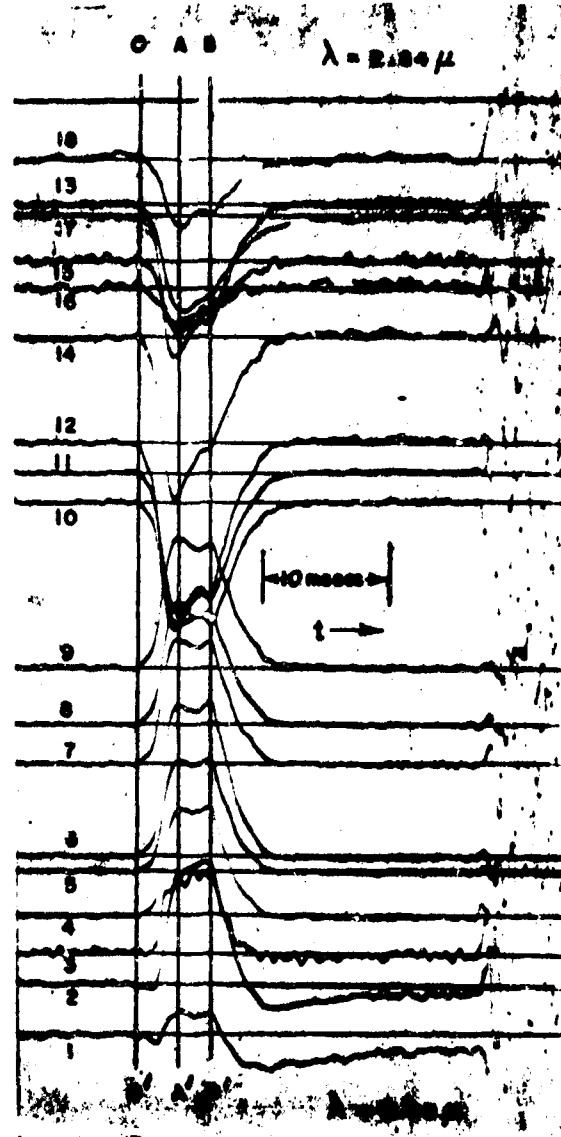
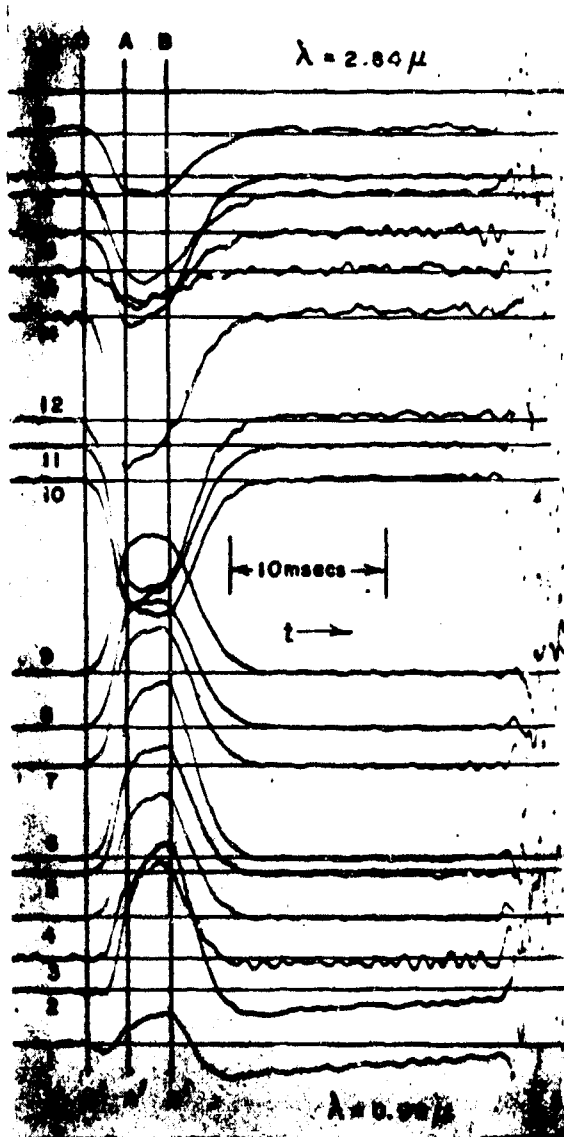


	TIME
OO' TO AA'	2.1 msec
OO' TO BB'	3.1 msec
WAVELENGTHS 0.44 $\mu$ TO 2.13 $\mu$	

FIGURE 3 - 11(F) - SPECTROMETER TRACES (FROM REF. 8e)

(A) RECORD - 2161  
 (105mm Howitzer - Propellant M1)

(B) RECORD - 2163  
 (105mm Howitzer - Propellant M1)



	TIME
OO' TO AA'	2.7 msec
OO' TO BB'	5.4 msec
OO' TO 50% PEAK SIGNAL AT AA'	7.3 msec
OO' TO 50% PEAK SIGNAL AT BB'	8.3 msec

	TIME
OO' TO AA'	2.8 msec
OO' TO BB'	5.4 msec
OO' TO 50% PEAK SIGNAL AT AA'	6.3 msec
OO' TO 50% PEAK SIGNAL AT BB'	7.1 msec

FIGURE 3-11(G) — SPECTROMETER TRACES (FROM REF. 8e)

(A) RECORD - 2424  
*(122mm Howitzer (Russian))*



	TIME
OO' TO AA	3.7 msec
OO' TO 50%	7.0 msec
PEAK SIGNAL	

WAVELENGTHS 0.99 $\mu$  TO 2.84 $\mu$

(B) RECORD - 2426  
*(122mm Howitzer (Russian))*



	TIME
OO' TO AA'	2.8 msec
OO' TO BB'	5.1 msec
OO' TO CC'	13 msec

WAVELENGTHS 0.99 $\mu$  TO 2.84 $\mu$

FIGURE 3 — 11(H) — SPECTROMETER TRACES (FROM REF. 8\*)

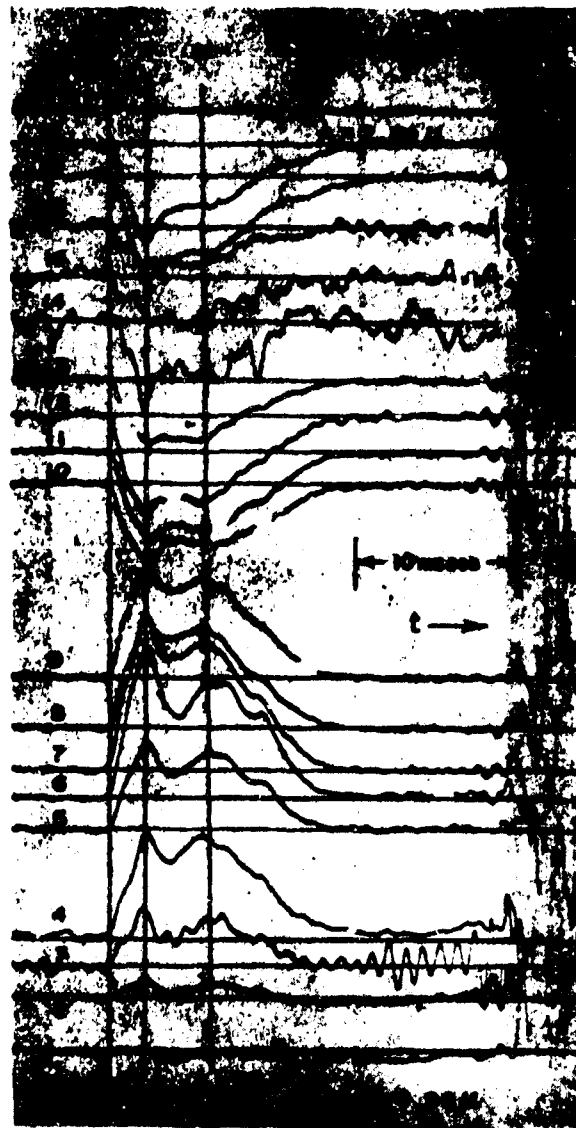
(A) RECORD-2220

(155 mm Howitzer — Propellant M1)



(B) RECORD-2221

(155 mm Howitzer — Propellant M1)



	TIME
OO' TO AA'	2.6 msec
OO' TO BB'	7.0 msec
OO' TO 50% PEAK SIGNAL	1.0 msec
WAVELENGTHS 0.99 $\mu$ TO 2.84 $\mu$	

	TIME
OC' TO AA'	2.4 msec
OO' TO BB'	6.4 msec
OO' TO 50% PEAK SIGNAL	11 msec
WAVELENGTHS 0.99 $\mu$ TO 2.84 $\mu$	

FIGURE 3 — 11(I) — SPECTROMETER TRACES (FROM REF. 8e)

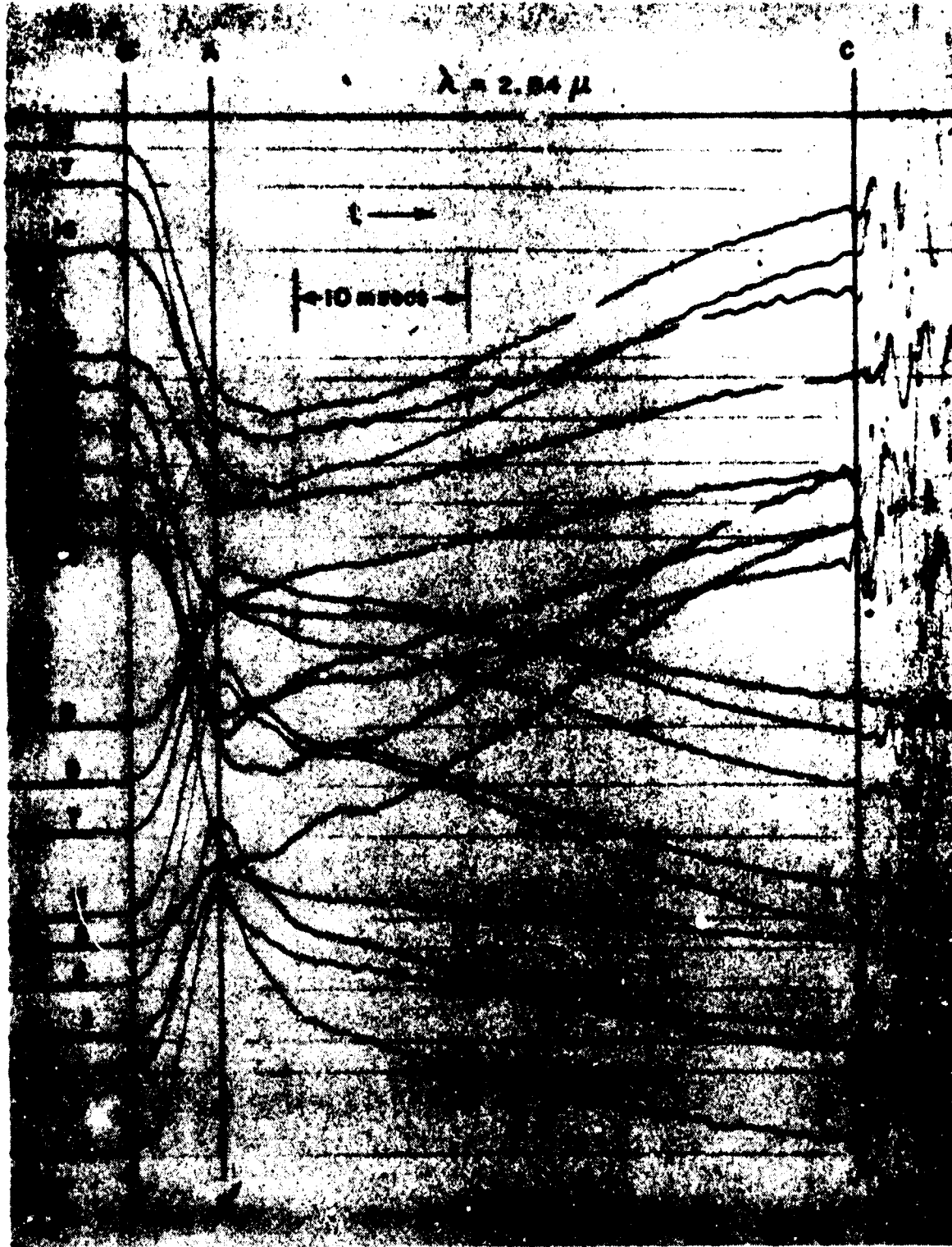


FIGURE 3 — 11(J) — SPECTROMETER TRACES (FROM REF. 8\*)  
155-MM HOWITZER — PROPELLANT M1 — — CHARGE M4A1



FIGURE 3 — 11(K) — SPECTROMETER TRACES (FROM REF. 80)  
8-IN. HOWITZER — PROPELLANT M1

## 3-6 SUMMARY

The infrared spectrum of secondary flash from a 155-mm M2 artillery weapons was observed at various distances from the weapon. It was found that the radiation transmitted through the atmosphere was most intense near  $2.9\ \mu$  for distances up to 500 ft, and that the position of maximum intensity changed to the vicinity of  $4.6\ \mu$  as the distance was increased to 1000 ft or more. This observation may have been influenced by the large aperture of the spectrograph, however, which permitted radiation reflected from the terrain to be viewed.

The radiation of suppressed and unsuppressed flash from a 155-mm gun was observed as a function of time at a number of wavelengths in the range 1 to  $3.6\ \mu$ . Both types of flash reached maximum intensity in approximately 10 msec; but, although the suppressed flash decayed almost as rapidly as it reached its peak value, the duration of unsuppressed flash approached 1000 msec. The peak values of spectral emittance varied between 1 and 7 (watts/cm<sup>2</sup> $\mu$ ) for unsuppressed flash and were 10 to 100 times smaller for suppressed flash. The spectra of both types of flash were characterized mainly by CO<sub>2</sub> and H<sub>2</sub>O emission.

For a number of weapons, calibrated spectral data were obtained which were used in computing spectral emittances of both intermediate and secondary flashes. Since no correction was made for atmospheric absorption of flash radiation, the values of spectral emittance computed from the spectrometer measurements were labeled apparent emittances. Furthermore, no correction was made for those intermediate flashes whose projected areas were too small to fill the field of view of the spectrometer.

The spectral emittance of unsuppressed flash from a 280-mm gun was recorded in the wavelength range between 0.6 and  $3.3\ \mu$ . Most of the maxima in the spectra were identified with CO<sub>2</sub> and H<sub>2</sub>O emission bands, and most of the minima were identified with

absorption by water vapor in the atmosphere. The apparent spectral emittance varied from nearly 0 to approximately 10 (watt/cm<sup>2</sup> $\mu$ ). Generally, the flash spectrum for the 280-mm gun was similar to, but somewhat more intense than, the spectrum for the 155-mm gun. Approximately 70 msec were required for flash from the 280-mm gun to reach maximum intensity, and the total duration of the flash was in the vicinity of 200 msec.

Other weapons for which spectral emittance data were obtained are 77-mm, 85-mm, 90-mm, and 8-in. guns and 75-mm, 105-mm, 122-mm, 155-mm, and 8-in. howitzers. Eight weapons were tested with charges which resulted in intermediate flashes, and three weapons were tested with charges yielding secondary flashes. The projected area of the intermediate flashes as viewed from the spectrometer ranged from 4 to 50 ft<sup>2</sup>. For the 90-mm gun and 155-mm howitzer the projected areas of secondary flash were 190 and 240 ft<sup>2</sup>, respectively; and for the 8-in. gun it was 1300 ft<sup>2</sup>. Observations with and without an infrared filter indicated that the boundaries of the flash regions emitting visible and infrared radiation were approximately the same.

While there were variations among the individual weapons, the general features of the spectral characteristics of the flash were similar to those described above for the 155-mm and 280-mm guns. For howitzers, the variation of flash intensity with time usually exhibited two peaks, one of them not always very distinct; the flash from guns generally exhibited one peak.

Generally, secondary flash was distinguished from intermediate flash in having larger values of emittance, longer duration, and much larger projected area. Intermediate flashes which filled the field of view of the spectrometer had total radiation rates of the order of 10<sup>4</sup> watts. The 90-mm gun and 155-mm howitzer had total radiation rates on the order of 10<sup>6</sup> watts, and the rate for the 8-in. gun was on the order of 10<sup>7</sup> watts.

## CHAPTER 4

### SPECIAL TOPICS

#### 4-1 VARIATION OF SPECTRA WITH TIME AS STUDIED WITH AN ORTHICON SPECTROGRAPH<sup>5(a)</sup>

The development of secondary flash with time was investigated with an orthicon spectrograph. For these studies, Ball M2 projectiles loaded with EX6333 propellant were fired in a caliber .50 gun with a 45-in. barrel. The oscilloscope trace of the resulting secondary flash was photographed with a high speed 16-mm movie camera at approximately 2800 frames per second, or about 3 frames per msec.

Figure 4-1 shows a typical series of traces taken at different times during the flash. Each scan of the orthicon target was completed in 1/60 sec; therefore, each trace represents the integrated intensity of flash radiation detected during the preceding 1/60 sec. Since no correction was made for variation in the sensitivity of the orthicon for different wavelengths, the relative intensities at different wavelengths are not truly represented.

The following observations may be made:

- (a) After 2 msec, only the red continuum with prominent potassium lines at approximately 7700 Å and possibly a weak band at a longer wavelength were visible.
- (b) One msec later the calcium hydroxide band at 6200-6300 Å appeared.\*
- (c) In the next frame, a fraction of a millisecond later, the sodium line at 5890 Å began to appear.
- (d) The next frame shows the beginning of the copper hydroxide bands at 5000-5500 Å.\*
- (e) No new bands were added after this point. The radiation at the blue end appeared to increase in intensity

more rapidly than the remainder until, at the end of about 11 msec, the trace appeared as shown in Frame E.

- (f) From this point there was a gradual decline in intensity of the traces beginning with the blue end of the spectrum until, at the end of about 25 msec, the trace exhibited little more than the potassium lines and some continuum at the long wavelengths, as shown in Frame F.

The apparent temperature dependence of the intensity of radiation from the emitters calcium hydroxide, copper hydroxide, potassium, and sodium — aside from the question of the amounts of each present — strongly suggested that the excitation was purely thermal. It is possible that the temperature of the flash at the start was such that only long-wavelength radiation could be excited. As the temperature increased, shorter wavelength bands appeared. Then, these disappeared as the gases cooled, leaving only the long-wavelength radiation. Such a dependence on temperature could reasonably have been expected in the case of potassium and sodium because the lines under consideration were the first of the principal series. In the case of calcium and copper compounds the energy states involved in the emission bands would have to be taken into account to determine such a relationship. It is possible that there was some excitation of higher energy states with emission too weak to register. If an emitter were present in sufficient amounts, it might possibly appear before another emitter that was more easily excited but present in smaller amounts.

---

\*Some of the bands initially thought to be those of CaO and CuO are now on the basis of newer measurements, thought to be those of CaOH and CuOH.<sup>31</sup>

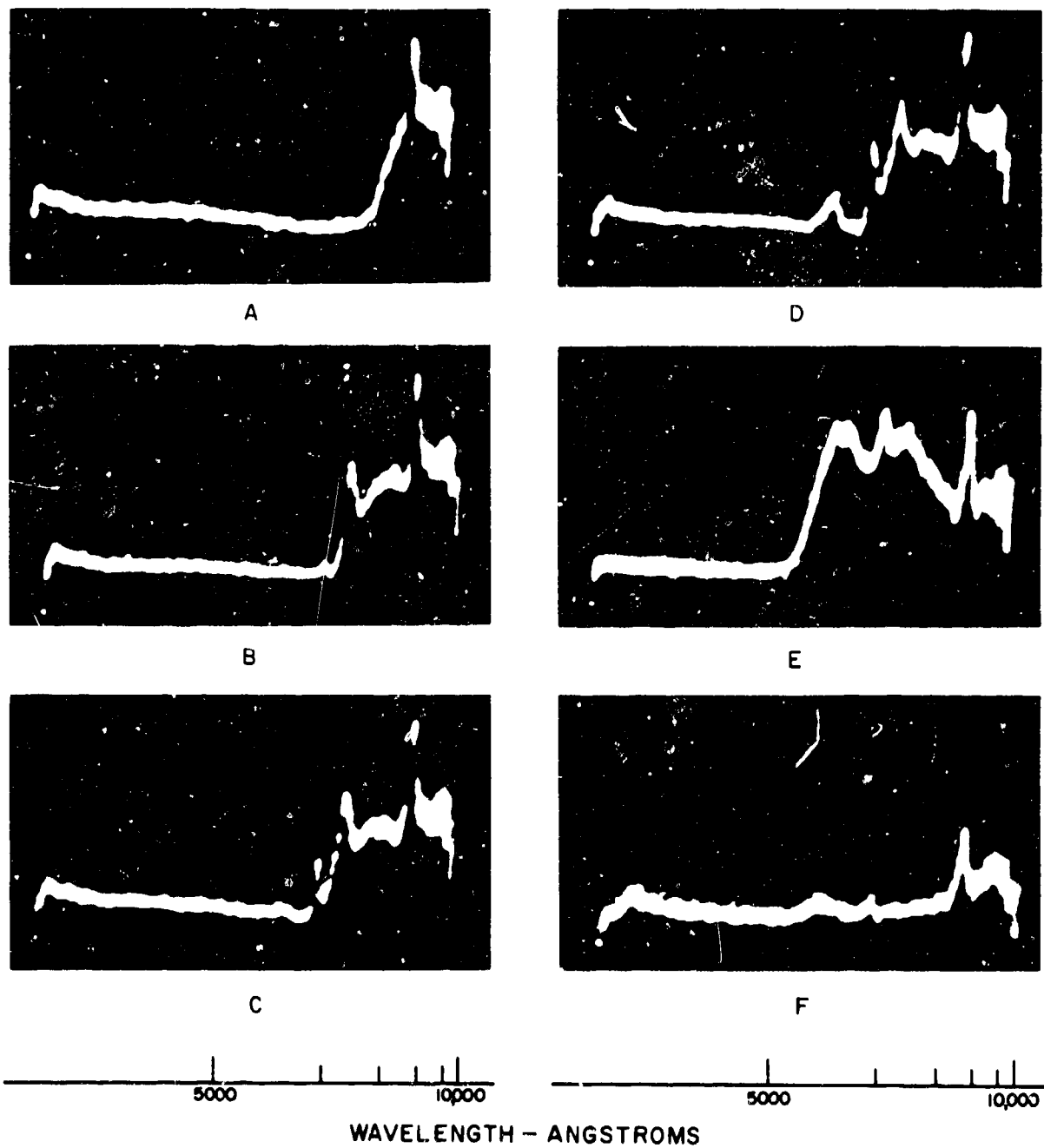


FIGURE 4-1 - VARIATION OF THE SPECTRAL DISTRIBUTION OF SECONDARY FLASH WITH TIME (FROM REF. 5a)  
FRAME TIMES WERE NOT INDICATED ON THE ORIGINAL, BUT SOME TIME  
INFORMATION IS GIVEN IN PAR. 4-1.

#### 4-2 VARIATIONS OF BREECH PRESSURE AND FLASH INTENSITY WITH TIME <sup>4(b)</sup>

The variation of breech pressure with time was observed by use of a piezoelectric detector. Its output was amplified and displayed on an oscilloscope by using one channel of a four-channel electronic switch. The second and third channels of the switch were connected to two photocells: one near the gun — adjusted to record weak intensities; the other some distance away — adjusted to record strong intensities. The fourth channel of the switch was connected to a microphone placed close to the gun muzzle. The microphone recorded the initial pressure wave and provided a signal nearly coincident in time with the exit of the projectile. The oscilloscope sweep on which these signals were recorded was triggered by the firing mechanism of the

gun. The weapon used was a caliber .50 gun having a barrel 79 in. long.

Information obtained by the above method appears in Figures 4-2 and 4-3 for typical rounds. Figure 4-2 corresponds to a round in which no secondary flash occurred. From left to right appear (a) a record of breech pressure vs time, (b) a record of intensity from muzzle glow as a function of time, and (c) a downward deflection indicating the microphone signal (projectile exit). In Figure 4-3, which shows a similar record for a round in which secondary flash occurred, the deflection corresponding to muzzle glow suddenly merged into a much larger deflection with the initiation of secondary flash. Trace D is the signal from the distant photocell showing the intensity of the secondary flash on a much reduced scale.

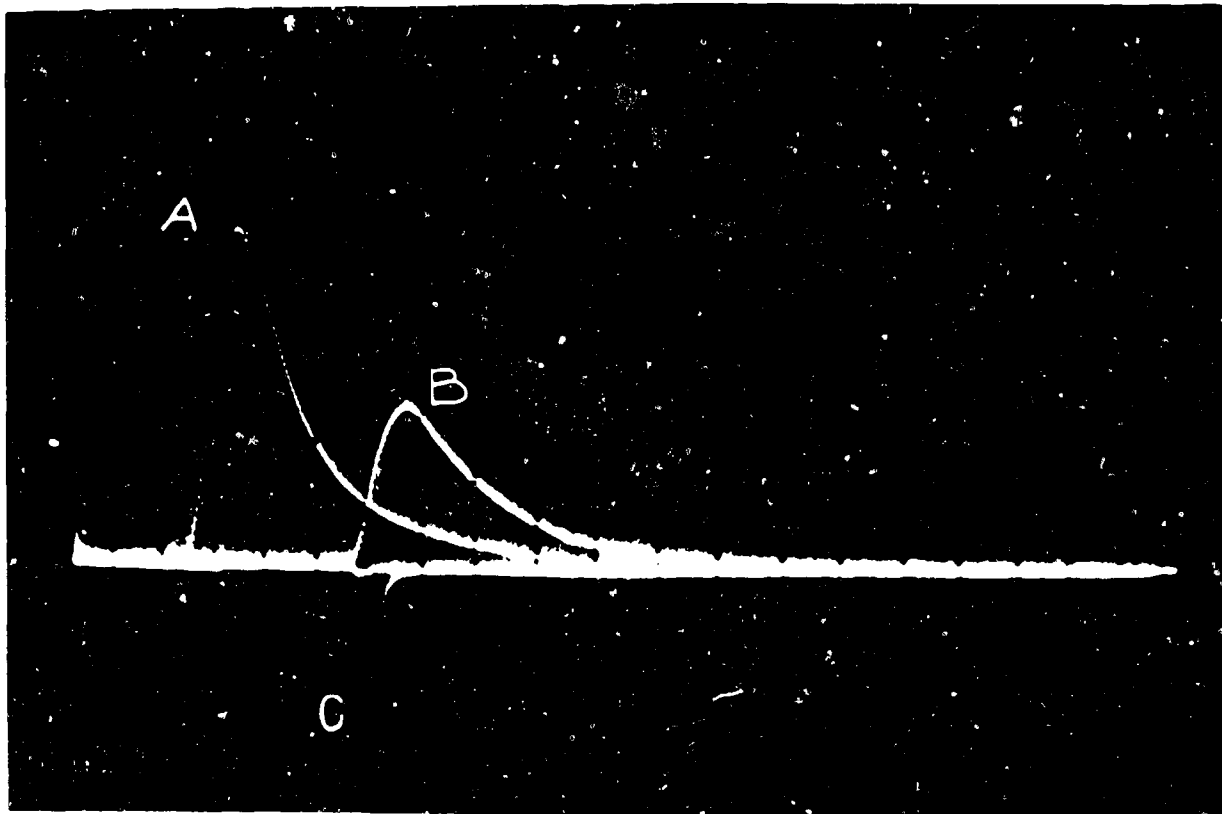


FIGURE 4-2 — VARIATION OF BREECH PRESSURE AND INTENSITY OF MUZZLE GLOW WITH TIME (FROM REF. 4b)

A — BREECH PRESSURE VS TIME  
 B — INTENSITY OF MUZZLE GLOW VS TIME  
 C — PROJECTILE EXIT  
 (MILLISECOND INTERVALS INDICATED)

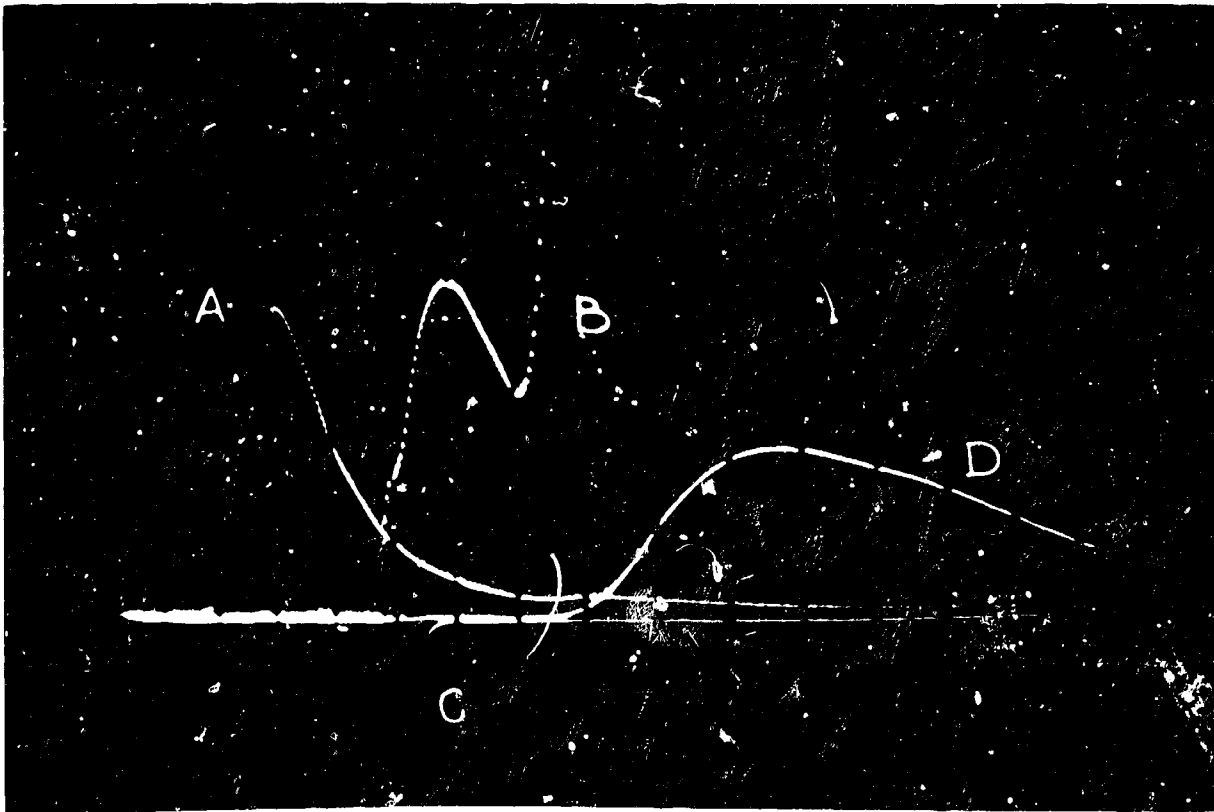


FIGURE 4-3—VARIATION OF BREECH PRESSURE AND FLASH INTENSITY WITH TIME (FROM REF. 4b)

- A — BREECH PRESSURE VS TIME
- B — INTENSITY OF MUZZLE GLOW VS TIME, AND BEGINNING OF SECONDARY FLASH
- C — PROJECTILE EXIT
- D — INTENSITY OF SECONDARY FLASH VS TIME (REDUCED AMPLITUDE)  
(MILLISECOND INTERVALS INDICATED)

#### 4-3 RADIATION AND TEMPERATURE MEASUREMENTS <sup>6(e)</sup>

##### 4-3.1 PROCEDURE

The effective temperature of a radiating gas mass can be determined if it is assumed that the radiating gas can be considered a gray body (having uniform emissivity over the entire spectrum). By comparing the curve for the observed spectral distribution with gray-body curves corresponding to different temperatures one can find a best fit and thus determine the effective temperature of the gas.

An example of such temperature determinations is given below for the secondary flash from a number of different types of rounds fired in the caliber .50 gun having

a 20-mm chamber. It is also shown how the values of intensity were corrected approximately for the effects of barrel wear, different propellant loads, and different flash temperatures in order to make them more nearly comparable. While it is useful to see what types of effects must be taken into account in the analysis of such data, the accuracy of these early measurements was probably insufficient to justify more than qualitative interpretation of the numerical results.\*

In the case described below the intensity data were obtained with the infrared monochromator using a photothermal detector.

\*For a discussion of the two-color method of temperature determination and the difficulties in obtaining accurate results see Ch. 54, Sect. IX, of Ref. 32.

Experience in the determination of the spectral distribution of energy in gun flash from the propellants tested showed that the best fitting gray-body curve could be obtained by matching them with the measured spectral distribution curves at wavelengths of 1.5 and 9.0  $\mu$ . The procedure that was followed, therefore, was to measure the spectral intensity at these wavelengths for several rounds (to minimize the variation from round to round) and to calculate the temperature from standard formulas\* on the assumption that the gas radiates as a gray-body.

#### 4-3.2 RESULTS

The results of the intensity measurements and the temperature calculations are shown in Table 4-1. The intensity measurements were placed on a more comparable basis by means of the following corrections.

a. Correction for Barrel Wear. This correction was required because a gradual, rather uniform increase in flash intensity occurred as the number of rounds fired in a barrel increased. For the data shown in Table 4-1, this increase due to barrel wear amounted to approximately 0.16 percent per round. For example, two separate groups of steel projectiles were fired with propellant PA-E-897. The average intensity corresponded to the intensity of round No. 9 for the first group and of round No. 74 for the second group. Therefore, at 1.5  $\mu$  the corrected intensities are:

$$2.11 \times \frac{100}{100 + 9 \times 0.16} = 2.08$$

$$2.3 \times \frac{100}{100 + 74 \times 0.16} = 2.10$$

b. Correction for Load. Because different propellant loads were used in the tests, an approximate correction was made to put the values of intensity on a more comparable basis. The load of 425 gr was chosen as standard, and all values of flash intensity were multiplied by the ratio of 425 to the actual load in grains.

c. Adjustment for Temperature. It is desirable to know how much of the effect of the graphite coating on the PA-E-897 propellant is produced by actual combustion of the carbon and how much is due to the presence of incandescent carbon or other particles. The two contributions were estimated by the method shown in the example which follows.

The intensity of the radiation at a wavelength of 1.5  $\mu$ , produced by the flash from PA-E-897 propellant fired with steel projectiles, was adjusted from its value at 1246°K to its effective value at a temperature of 1360°K, (see Table 4-1) as follows:

$$I_{1360k} = I_{1246k} \frac{\left[ \exp \left( \frac{14320}{1.5 \times 1246} \right) \right]^{-1}}{\left[ \exp \left( \frac{14320}{1.5 \times 1360} \right) \right]^{-1}}$$

$$I_{1360k} = 2.00 \times 1.9 = 3.80$$

The intensity ratio, 1.9, indicated that a 90-percent increase in intensity was effected by combustion of the graphite coating, resulting in the higher temperature of 1360°K. However, in Table 4-1 it can be seen that the *actual* corrected intensity for graphite-coated PA-E-897 propellant, using steel projectiles, is 3.98. Thus there was a total increase in intensity by a factor of  $3.98/2.00 = 1.99$ , or 99 percent, of which 9 percent must be attributed to an increase in emissivity at a temperature of 1360°K.\*\*

#### 4-3.3 CONCLUSIONS \*\*

Examination of temperature radiation curves (gray-body curves) based on the results shown in Table 4-1 indicated the following:

(a) The addition of graphite to the PA-E-897 propellant (steel projectiles) caused the flash intensity to be approximately

\*See *Radiation law, Wien's* in the Glossary, and Ch. 54, Sect. IX, of Ref. 32.

\*\*See comment on accuracy in par. 4-3.1, at end of second paragraph.

TABLE 4-1  
SUMMARY OF FLASH TEMPERATURE MEASUREMENT DATA  
(From Ref. 6e)

(All values of intensity are in arbitrary units.)

Projectile	Propellant	Load (grain)	Round No.	Measured Flash Intensity	Intensity Corrected for Barrel Life		Average of Intensity Corrected for Barrel Life	Calculated Temperature (°K)	Average of Intensity Corrected to	
					1.5μ	9.0μ			1360 °K	1246 °K
Steel	PA-E-897	445	3-15	1.5μ	9.0μ	1.5μ	9.0μ	1246	1.5μ	9.0μ
				2.11	0.213	2.08	0.210		3.80	0.248
				2.09		0.224	2.00		0.214	
Steel	PA-E-897	445	64-83	2.35	0.267	2.10	0.238	1362		
Steel	PA-E-897 (Graphite coated)	450	17-36	4.39	0.282	4.12	0.270	1362		
Steel	EX6333	435	37-63	4.28	0.310	4.51	0.287	1363		
Ball M2	PA-E-897	425	99-123	1.78	0.233	1.51	0.198	1205	3.80	0.243
Ball M2	PA-E-897	425	174-203	1.99	0.258	1.53	0.198			
2.09		0.224	2.00	0.214						
Ball M2	PA-E-897 (Graphite coated)	430	124-148	5.18	0.334	4.24	0.273	1360		
Ball M2	EX6333	390	149-173	4.03	0.30	3.19	0.237	1325	4.19	0.270

doubled. The increase in intensity was mostly due to a rise of approximately 100°K in flash temperature, but a smaller contribution was due to increased emissivity at the higher temperature.

(b) The addition of graphite to the PA-E-897 propellant (Ball M2 projectiles) caused the flash intensity to increase by 150 percent due to a temperature rise of 155°K and by an additional 26 percent due to increased emissivity, making a total increase of 176 percent.

(c) The EX6333 and graphited PA-E-897 propellants gave a flash with essentially the same temperature (approximately 1360°K), with the exception that the EX6333 propellant gave a temperature of 1325°K when used with Ball M2 projectiles. This was probably due to the low charge of 390 grains used in these rounds.

(d) The intensity of radiation from the flash of the EX6333 propellant (steel projectiles) was somewhat greater than that from the graphited PA-E-897 propellant (steel projectiles). Since the effective gas temperatures were practically the same for these two propellants, the higher intensity resulting from use of EX6333 propellant was probably due to increased emissivity.

#### 4-4 MEASUREMENTS OF FLASH TEMPERATURE BY THE LINE REVERSAL TECHNIQUE<sup>5(c),18</sup>

The temperature of intermediate and secondary flash from several caliber .50 weapons was measured by the line reversal technique. In accordance with this method, a lens was used to focus the image of a tungsten lamp onto the center of the flash region. Radiation from the flash and the light source was focused by means of another lens onto the slit of the spectrograph. The electrical output generated in the detectors was fed to an oscilloscope. The temperature of the comparison source (tungsten lamp) was determined with a Leeds and Northrup Optical Pyrometer.

The basis of the line reversal technique is the following. If the atomic lines of the element studied are in temperature equilibrium with a flash which is of a lower temperature

than that of the comparison source, absorption of source radiation will be detected on the oscilloscope. If the comparison source is at a lower temperature than the element in the flash, emission will be detected. Therefore, the equilibrium temperature of the element under study is the temperature of the comparison source when neither emission nor absorption is detected on the oscilloscope.

Observations were made with the following combinations of wavelength and detector: (a) the sodium doublet at 5890 and 5896 Å, using a photomultiplier tube detector; (b) the potassium doublet near 7700 Å, using a lead sulfide detector; and (c) the water band at approximately 9400 Å, using a lead sulfide detector.\* The results of the temperature measurements are shown in Table 4-2.

Examination of the temperatures listed in Table 4-2 indicates, as expected, that the special caliber .50 gun chambered for 20-mm cases had a low flash temperature (approximately 1200°K) with a barrel length of 85 inches. When the barrel was shortened to 45 in. and  $K_2SO_4$  was added to prevent secondary flash, the temperature of the intermediate flash increased to approximately 1550°K. When the shortened barrel was fired without  $K_2SO_4$  added to the charge, secondary flash with a temperature of approximately 2200°K was obtained. The caliber .50 machine gun with standard rounds produced an intermediate flash with temperature comparable to that of the special gun with 85-in. barrel.

It is difficult to analyze the differences among the three temperature measurements (potassium line, sodium line, and water vapor band) for each case without having information concerning the accuracy of the measurements. It is possible that the differences may be accounted for mostly by measurement errors. Those who performed the measurements apparently regarded the experimental errors as sufficiently small so

\*A measurement of the temperature of secondary flash using the sodium doublet and a lead sulfide detector yielded the same value as that obtained when the photomultiplier detector was used.

TABLE 4-2  
FLASH TEMPERATURE MEASURED BY THE LINE REVERSAL METHOD  
(From Ref. 5c)

Gun	Exp't	Barrel Length (in.)	Charge (grain)	Type of Flash	Flash Temperature (°K)		
					Potassium Line (Note 1)	Sodium Line (Note 2)	Water Vapor Band (Note 1)
Caliber .50, chambered for 20-mm cases.	A	85	410	Intermediate	1250	1250	1150
	B	45	410 (5% K <sub>2</sub> SO <sub>4</sub> added)	Intermediate	1650	1510	1510
	C	45	410	Secondary	2200	2130 (Note 3)	2250
Caliber .50, HB Browning machine gun	D	36	(Std. Round)	Intermediate	1320	1320	1150

- Notes. 1. A lead sulfide photoconductive cell was used to detect the radiation from the potassium doublet (7665 and 7699 Å) and from the water vapor band near 9400 Å.
2. A photomultiplier tube was used to detect the radiation from the sodium doublet (5890 and 5896 Å).
3. The same value of temperature (2130 °K) was obtained when the lead sulfide detector was used in place of the photomultiplier.
4. Listed values are based on the brightness temperature of the tungsten filament comparison source at 0.665 μ. The values that were given in References 5(c) and 18 were erroneously based on the actual temperature of the filament.

that the observed temperature differences could be considered significant. They interpreted the data as indicating that potassium and sodium line temperatures were equal when potassium atoms were not involved in chemical reactions (Experiments A and D), but that the potassium line temperature exceeded the sodium line temperature when the potassium atoms were involved in chemical reactions (Experiments B and C). Thus, they were led to the conclusion that, due to their participation in chemical reactions associated with the suppression of secondary flash, potassium atoms are excited to an energy exceeding that corresponding to temperature equilibrium with their surroundings.

#### 4-5 MEASUREMENTS OF FLASH TEMPERATURE AS A FUNCTION OF TIME <sup>5(b)</sup>

The orthicon spectrograph\*, after being modified for single sweep operation, was used to apply the line reversal method of temperature measurement<sup>21</sup> to gun flash. Use was made of the unresolved potassium doublet at 7665 and 7699 Å, which will be referred to as the 7700-Å line. The image of an incandescent tungsten strip filament was focused by means of a lens onto the center of the flash region. Radiation from this image and the flash itself was then focused by a second lens onto the slit of the orthicon spectrograph. Thus, the spectral radiation curve from the source was presented continuously on the oscilloscope screen. A diaphragm in the objective lens of the spectrograph limited the field of view of the system, so that light from both the source and the flash just filled the entire area. Temperatures were determined with a Leeds & Northrup Optical Pyrometer focused on the image of the tungsten filament. Since the spectral emissivity of tungsten varies only slightly in the region between the red utilized by the pyrometer and the 7700-Å line, the brightness temperature indicated by the pyrometer was taken as the temperature under consideration. When the flash appeared, if the radiating potassium atoms were in equilibrium with a temperature state lower than that of the source, an absorption line at 7700 Å would

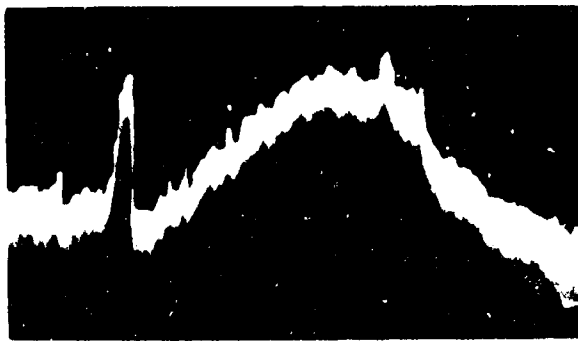
be observed. When the temperature of the flash was equal to that of the comparison source, the absorption by and emission from the potassium atoms were in equilibrium, and no characteristic radiation appeared at 7700 Å. When the flash temperature was greater than the source temperature, the potassium doublet appeared in emission. The value of temperature so determined represented an average value for the flash region in the vicinity of the image of the comparison source. The method was subject to the limitations common to the line reversal technique for measuring temperature.<sup>21</sup>

The temperature determinations were made with a scanning rate of 1000 cycles/sec. (The duration of each scan was 63 μsec.) The resulting oscilloscope traces were photographed on 35-mm film rotated on a drum camera. The arrangement permitted 33 traces to be recorded on a single film strip. Since each individual trace required only 63 μsec for its completion, the traces appeared distinctly separated on the film strip.

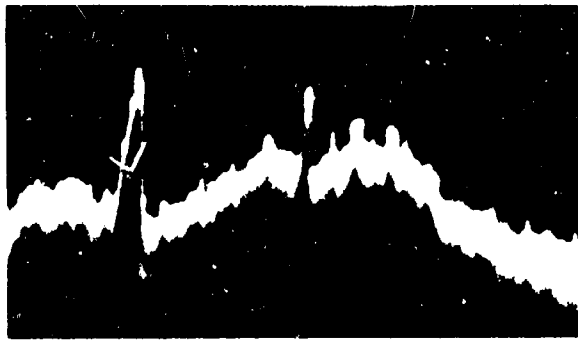
In experiments involving the firing of rounds with a 425-grain load of propellant EX6451 in the special caliber .50 test gun (see Appendix A-2) the potassium doublet reached almost maximum intensity in 1 msec, the green copper oxide band being the last to appear.\*\* The intensity remained practically constant for several milliseconds thereafter; but after 11 or 12 msec the trace showed a noticeable decrease, especially in the green region. The potassium doublet was the last to disappear. Figure 4-4 shows six consecutive traces for the above firing conditions, with the comparison source set at a temperature of approximately 1900°K. It can be seen that the 7700-Å line appears in emission on every frame except Frame F, where it

\*By orthicon spectrograph we refer to the large-aperture spectrograph using an orthicon tube to produce an oscilloscope display of the spectra. See Appendices A-4 and A-6.

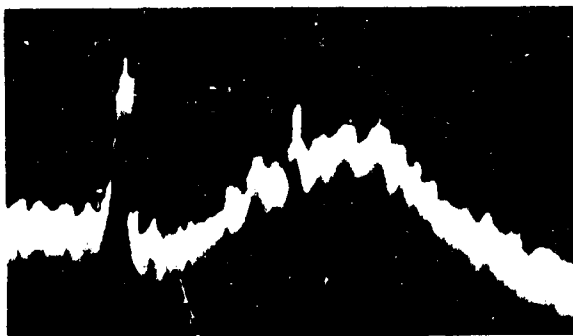
\*\*See footnote to par. 2-3.1.



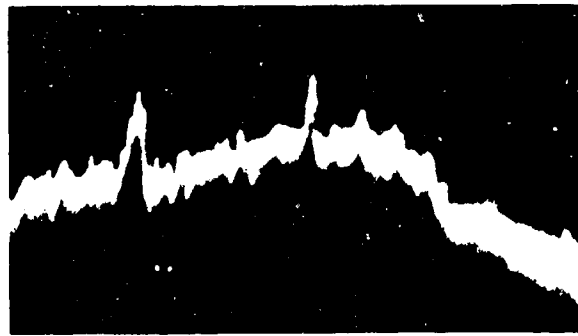
A-1msec



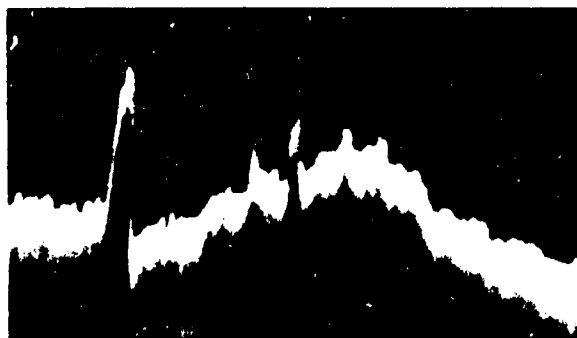
D-4 msec



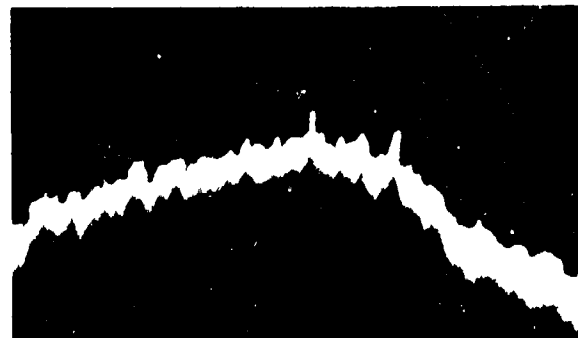
B-2 msec



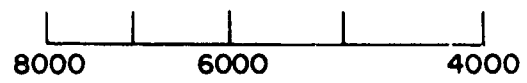
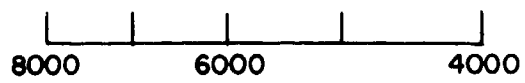
E-5 msec



C-3 msec



F-6 msec



WAVELENGTH (Å)

FIGURE 4-4—SPECTRAL DISTRIBUTION OF SECONDARY FLASH SUPERIMPOSED ON CONTINUOUS BACKGROUND FROM TUNGSTEN FILAMENT AT 1900°K (FROM REF. 5b)

appears slightly reversed. Thus, the temperature at 6 msec was taken to be approximately 1900°K. Figure 4-5 shows the appearance of Trace B—2 msec after the initial appearance of visible radiation—for comparison temperature settings of 1900°, 2035°, 2155°, 2275°, 2390°, 2500° and 2585°K.\* From these curves it can be seen that the peak temperature at about 2 msec after visible radiation began to appear was approximately 2600°K, since the 7700 A line is matched or slightly reversed in this temperature range (see Traces F and G).

The temperature curve plotted in Figure 4-6 was obtained from determinations of temperature for each millisecond, up to 6 msec after visible radiation appeared. Note that the maximum temperature was reached in approximately 2 msec, whereas maximum radiation intensity occurred in the third or fourth millisecond. However, it must be remembered that the temperature was determined by the reversal of the potassium line, a method which is based on the assumption that temperature equilibrium exists. If the system were not in equilibrium, the temperature indicated by the potassium line would be expected to be higher than the temperature of the gas surrounding the potassium particles. The fact that maximum temperature and maximum radiation intensity were observed at different instants suggests that the system was not in equilibrium. This was also suggested by the temperature measurements discussed in par. 4-4.

#### 4-6 SUMMARY

The development in time of the secondary flash spectrum from a caliber .50 gun, studied with an orthicon spectrograph, suggested that the excitation of the emitters was purely thermal. All the lines and bands that were observed appeared during the first few milliseconds in the order of decreasing wavelength: K (7700 A), CaOH (6200-6300 A), Na (5890 A), CuOH (5000-5500 A). While these emitters appeared, the wavelength of maximum continuum radiation shifted from the red end of the spectrum toward the blue end. The intensity of radiation began to decay after approximately 10 msec, beginning at the blue end. At about 25 msec, only the potassium lines and red continuum remained.

This spectral development may have been caused by the temperature rising initially and then gradually falling.

Simultaneous recording of breech pressure and flash intensity for a caliber .50 gun showed that the peak breech pressure was attained about 2 msec before the projectile emerged from the muzzle. The initiation of radiation from muzzle glow was practically coincident with emergence of the projectile, it reached its peak value in a little over 1 msec and gradually decayed over a period of several milliseconds. When secondary flash occurred, it started about 2 msec after projectile emergence. Nearly 4 msec later it reached a peak intensity far exceeding that of muzzle glow; then decayed gradually for a total duration of more than 10 msec.

On the assumption that the gas radiated as a gray-body, the temperature of secondary flash from a caliber .50 gun was estimated for several types of rounds from measurements of the intensity of radiation at 1.5 and 9.0 $\mu$ . The computed temperatures varied approximately between 1200 and 1360°K. When adjusted for barrel wear, propellant load, and flash temperature, the values of flash intensity indicated that the observed increase of intensity with temperature was largely due to thermal effects but also included a contribution due to increased emissivity at the higher temperatures.

The temperature of intermediate and secondary flash from two caliber .50 weapons was determined also by the line-reversal technique at three wavelengths, using potassium and sodium lines and a water vapor band. The special caliber .50 gun chambered for 20-mm cases, with an 85-in. barrel, had an intermediate flash temperature of approximately 1200°K. When the barrel was shortened to 45 in. and secondary flash was suppressed by the addition of K<sub>2</sub>SO<sub>4</sub> to the charge, the temperature of intermediate flash increased to over 1500°K. Secondary flash obtained with this gun, by eliminating the use

\*Note that in Figure 4-4 and 4-5 no well defined potassium absorption lines at 7700 A were obtained. This was also true when very high comparison temperature sources such as photo-flash lamps (approximately 3500°K) were used. A consideration of the actual mechanism of operation of the orthicon tube under single-sweep conditions indicated that this difficulty was instrumental.

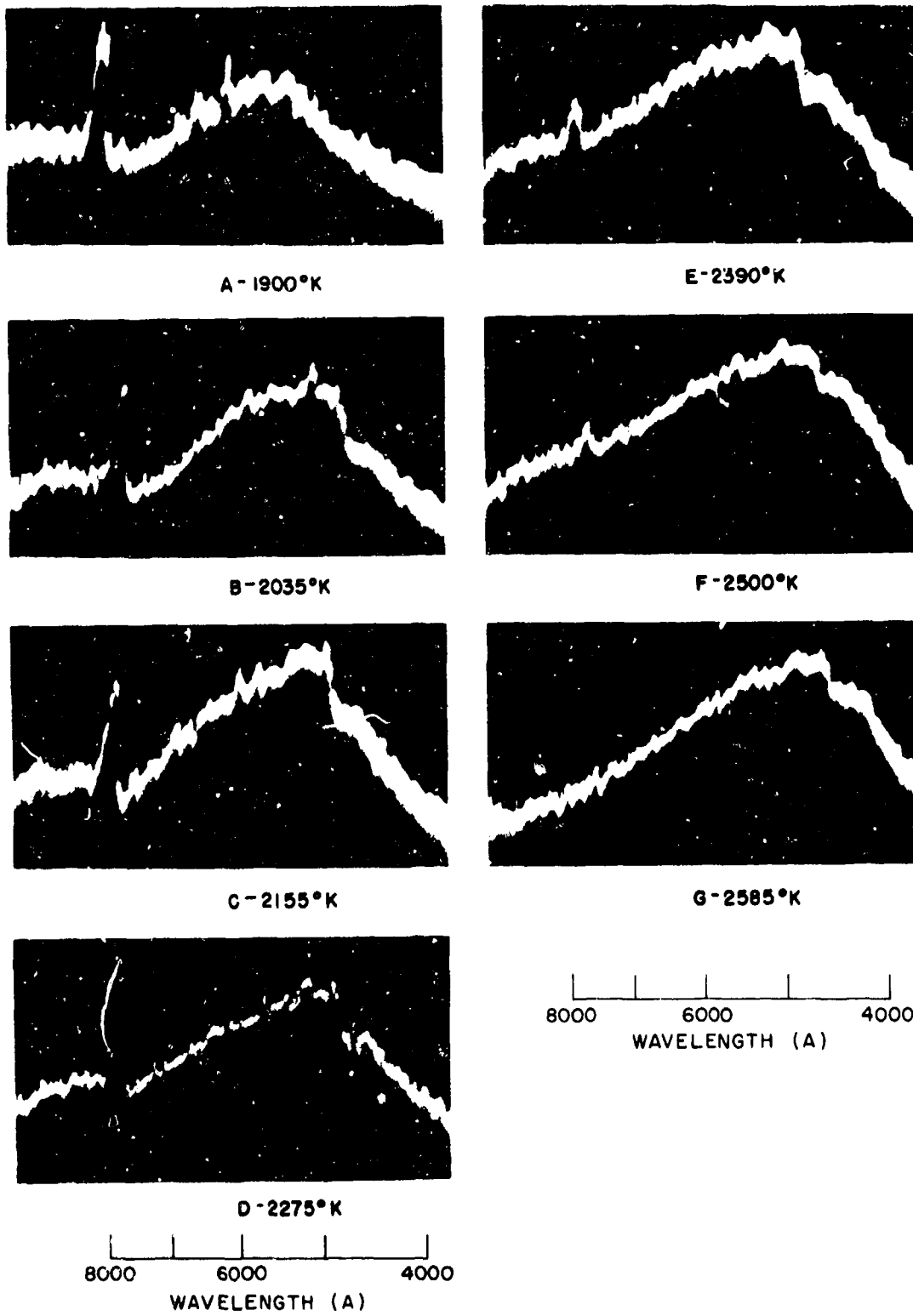


FIGURE 4-5 — SPECTRAL DISTRIBUTION OF SECONDARY FLASH SUPERIMPOSED ON CONTINUOUS BACKGROUND FROM TUNGSTEN FILAMENT AT VARIOUS TEMPERATURES (FROM REF. 5b)

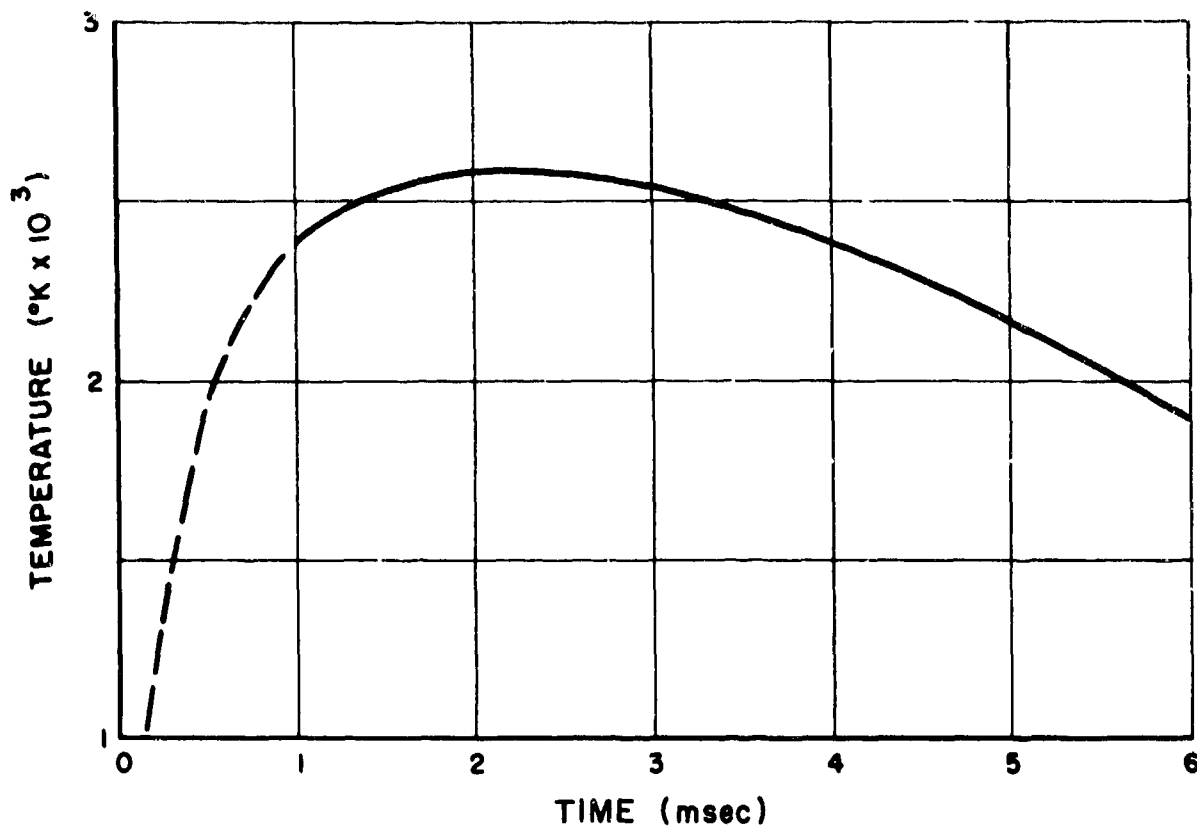


FIGURE 4-6—VARIATION IN TEMPERATURE OF SECONDARY FLASH WITH TIME (FROM REF. 5b)

of  $K_2SO_4$ , had a temperature of approximately  $2200^\circ K$ . The intermediate flash from a caliber .50 machine gun with a 36-in. barrel, using standard rounds, had a temperature comparable to that of the special caliber .50 gun with an 85-in. barrel. Differences between potassium- and sodium-line temperatures suggest that, when they were involved in chemical reactions, the potassium atoms were excited to an energy exceeding that corresponding to temperature equilibrium with their surroundings.

The temperature of secondary flash from the special caliber .50 gun was determined

as a function of time. By use of the line-reversal technique and the orthicon spectrograph, the spectrum was scanned at the rate of 1000 times per second. The temperature was observed to reach a peak value of  $2600^\circ K$  in approximately 2 msec after visible radiation appeared. Then it decreased gradually, reaching  $1900^\circ K$  at the end of 6 msec. The observed intensity of radiation reached its peak value 1 or 2 msec after the indicated temperature peaked, suggesting that the system was not in temperature equilibrium.

## REFERENCES

1. R. Ladenburg, *Report on Muzzle Flash*, BRL Report No. 426, Aberdeen Proving Ground, Md., 1943.
2. R. Ladenburg, *Suppression of Muzzle Flash from Caliber .30 Machine Gun M1919 A4*, BRL Memorandum Report No. 404, Aberdeen Proving Ground, Md., 1945.
3. R. Ladenburg, *Studies of the Muzzle Flash and its Suppression*, BRL Report No. 618, Aberdeen Proving Ground, Md., 1947.
4. C. T. Chase, et al, *Activities in Connection with Basic and Technical Work on the Flash of Military Propellants Leading to the Development of Ideal Propellants*, The Franklin Institute, Phila., Pa.
  - a. Monthly Progress Report 1886-9, 3 March 1947 (AD-492 321)\*.
  - b. Monthly Progress Report 1886-10, 7 April 1947 (AD-492 322).
  - c. Final Report No. 325, F. I. Project 1886, 9 June 1947.
  - d. Quarterly Progress Report 1886-9, 29 February 1948.
  - e. Final Report F-1886, 27 October 1948.
5. A. W. Horton, J. T. Agnew, et al, *Basic and Technical Work on Military Propellants*, The Franklin Institute, Phila., Pa.
  - a. Quarterly Progress Report P-2092-3, 3 January 1948.
  - b. Quarterly Progress Report P-2092-6, 31 March 1949.
  - c. Final Report F-2092-15, 31 December 1949.
6. J. T. Agnew, et al, *Activities in Connection with Basic and Technical Work on the Infrared Radiation from the Flash of Military Propellants*, The Franklin Institute, Phila., Pa.
  - a. Monthly Progress Report 1897-5, 25 November 1946 (AD-492 327).
  - b. Monthly Progress Report 1897-6, 15 February 1947 (AD-492 328).
  - c. Monthly Progress Report 1897-7, 15 May 1947 (AD-492 329).
  - d. Monthly Progress Report 1897-9, 15 November 1947.
  - e. Monthly Progress Report 1897-10, 15 February 1948.
7. J. T. Agnew, et al, *Detection of Infrared Radiation for Military Applications*, The Franklin Institute, Phila., Pa.
  - a. Quarterly Progress Report P-1897-19, 14 May 1950.
  - b. Quarterly Progress Report P-1897-20, 14 August 1950.
  - c. Final Report F-1897-21, 14 October 1950.
8. L. S. Herczeg, *Investigation of the Spectral Emittance of Military Propellants*, The Franklin Institute, Phila., Pa.
  - a. Interim Report I-2258-1, 10 July 1952 (AD-2 329).
  - b. Annual Report A-2258-1, September 1952 (AD-3 490).
  - c. Quarterly Report Q-2258-1, 14 December 1952 (AD-3 489).
  - d. Quarterly Report Q-2258-6, 14 March 1954.
  - e. Final Report F-2258, 31 August 1954 (AD-66 009).
9. J. T. Agnew, *Long Range Research Leading to the Development of Superior Propellants*, The Franklin Institute, Phila., Pa.
  - a. Progress Report P-2152-3, 31 March 1950.
  - b. Progress Report P-2152-9, 30 September 1950.
10. E. R. Stephens, *Long Range Research Leading to the Development of Superior Propellants*, The Franklin Institute, Phila., Pa.
  - a. Progress Report P-2216-3, 3 March 1951.
  - b. Progress Report P-2216-6, 7 June 1951.
  - c. Progress Report P-2216-9, 7 September 1951.
  - d. Progress Report P-2216-12, 15 January 1952.

\*AD numbers in parentheses identify reports available from Defense Documentation Center, Cameron Station, Alexandria, Virginia, 22314.

## REFERENCES (Cont.)

11. Stephens, Wachtell, and Carfagno, The Franklin Institute, Phila., Pa.
  - a. Interim Report I-2364-1, *Physical Suppression of Gun Muzzle Flash*, 1 September 1953 (AD-21 736).
  - b. Final Report F-2364, *Long Range Research Leading to the Development of Superior Propellants; Part I, Gun Muzzle Flash*, 15 March 1954 (AD-31 199).
12. Carfagno, Wachtell, and Stephens, *Physical Suppression of Gun Muzzle Flash and Howitzer Flash Tests (U)*, Interim Report I-2442-2, The Franklin Institute, Phila., Pa., 1 February 1955 (AD-65 812), (Confidential)\*.
13. S. P. Carfagno and G. P. Wachtell, *Emergence of Muzzle Gases Between Suppressor Bars*, Interim Report I-A1828-5, The Franklin Institute, Phila., Pa., 31 January 1958 (AD-300 766).
14. S. P. Carfagno and G. P. Wachtell, *Research and Development on Ignition of Propellants and Muzzle Gases (U)*, Final Report F-A1828, The Franklin Institute, Phila., Pa., June 1958 (AD-300 955), (Confidential)\*.
15. S. P. Carfagno and O. N. Rudyj, *Relationship Between Propellant Composition and Flash and Smoke Produced by Combustion Products (U)*, Final Report F-A2132, The Franklin Institute, Phila., Pa., 13 December 1960 (AD 321 118) (Confidential)\*.
16. S. P. Carfagno, *Handbook on Gun Flash (U)*, The Franklin Institute, Phila., Pa., November 1961 (AD 327 051) (Confidential)\*.
17. Gillam, Fisher, and Young, *Smoke and Flash in Small Arms Ammunition*, Midwest Research Institute, Kansas City, Missouri, 1948.
18. H. Young, Ed., *Smoke and Flash in Small Arms Ammunition (U)*, Midwest Research Institute, Kansas City, Missouri, 1945. (Confidential)\*.
19. R. W. B. Pearse and A. G. Gaydon, *The Identification of Molecular Spectra*, 1st. Ed., Chapman & Hall, Ltd., London, 1941, p. 105.
20. W. E. Forsythe, Ed., *Measurement of Radiant Energy*, McGraw Hill, New York, 1937, pp. 9 and 13.
21. A. G. Gaydon and H. G. Wolfhard, *Flames - Their Structure, Radiation and Temperature*, Chapman & Hall, Ltd., London, 1953, Ch. X.
22. M. J. E. Golay, *A Pneumatic Infrared Detector*, Rev. of Sci. Inst., V. 18, 357-362, 1947.
23. Agnew, Franklin and Benn, *A Ten Channel Infrared Spectrograph*, Opt. Soc. Am. J., V. 41, pp. 76-79, (1951).
24. J. T. Agnew, *Combustion Studies Using the Golay Photothermal Detector with an Infrared Monochromator*, ASME Trans., V. 71, 107-114, 1949.
25. J. T. Agnew et al, *Combustion Studies with the Orbicon Spectrograph*, Opt. Soc. of Am. J., V. 39, 409-410, 1949.
26. Benn, Foote, and Chase, *The Image Orbicon in Spectroscopy*, Opt. Soc. of Am. J., V. 39, 529-532, 1949.
27. W. C. Michels, Ed. in Chief, *The International Dictionary of Physics and Electronics*, 2nd Ed., Van Nostrand Co., inc., Princeton, N. J., 1961.
28. ST 9-152, *Ordnance Technical Terminology*, U. S. Army Ordnance School, Aberdeen Proving Ground, Md., June 1962.
29. F. A. Jenkins and H. E. White, *Fundamentals of Optics*, 2nd Ed., McGraw Hill, New York, 1950, p. 30.
30. R. G. Bernhard and E. W. McCallion, *Background and Small-Arms Radiation Measurements for an IR Ground - Fire Locator (U)*, Report No. LWL-CR-01P65 (Aerojet Report No. 143), Aerojet Von Karman Center, Azusa, California, 31 March 1966. (Confidential)\*
31. R. Mavrodineanu and H. Boiteux, *Flame Spectroscopy*, John Wiley and Sons, Inc., New York, 1965.
32. F. G. Brickwedde, Ed., *Temperature, Its Measurement and Control in Science and Industry*, V. 3, Part I, Reinhold Publishing Corp., New York, (1962).

\*Confidential documents are in Group IV, downgraded at three-year intervals and declassified after twelve years.

## GLOSSARY

**Aperture.** An opening through which radiation may pass, such as the open area of a lens or slit in an optical system.

**Aperture stop.** The opening in an optical system that limits the size of the bundle of rays which may pass from a point on the object to a point on the image.

**Black body.** An ideal body which would absorb all radiation falling upon it. The spectral energy distribution of such a body is described by Planck's radiation formula. A black body can be approximated by an enclosure having a small opening.

**Black-body radiation.** Radiation having a spectral distribution of energy which depends only on the temperature of the radiator, according to the Planck radiation formula.

**Breech.** The rear part of the bore of a gun, especially the opening that permits insertion of the projectile.

**Caliber.** The diameter of a projectile or the diameter of the bore of a gun, often based on a nominal value. (Unless otherwise indicated, in this handbook the caliber is given in inches.)

**Continuum.** See Spectrum, continuous.

**Dispersion.** The spatial separation of the components of radiation according to wavelength, as with a prism.

**Ektron detector.** The Registered Trade Name of Eastman Kodak Company for a photoconductive detector of infrared radiation, consisting basically of a coating of lead sulfide or lead selenide on a glass or other dielectric base.

**Emissivity.** The ratio of the radiation emitted by a surface to the radiation emitted by a black body at the same temperature and under similar conditions.

**Emittance.** The power radiated per unit area of a surface. When specified per unit wavelength range it is called the spectral radiant

emittance, and it is called the total radiant emittance when integrated over all wavelengths.

**Globar.** A ceramic rod consisting largely of silicon carbon which can be heated to an almost white heat in air without rapid deterioration. It radiates almost like a black body.

**Gray body.** A radiator whose spectral emissivity is independent of wavelength and whose radiation intensity therefore bears a constant ratio to that of a black body at the same temperature.

**Gun.** A weapon consisting essentially of a tube or barrel for throwing projectiles, usually by the force of an explosive. It is distinguished from other weapons of this general type in having a relatively long barrel (usually more than 30 calibers), relatively high muzzle velocity, and the capability of being fired at low angles of elevation.

**Howitzer.** A projectile-firing weapon with bore diameter greater than 30 mm. The bore length is usually between 20 and 35 calibers, and the maximum angle of elevation is about 65 degrees. The howitzer is used to fire projectiles in curved trajectories, the range of which can be altered by the use of several propelling charges or zones.

**Intensity of radiation.** Energy flowing through unit area (perpendicular to the direction of propagation) per unit time.

**Muzzle.** The end of the barrel of a gun from which the projectile emerges.

**Orthicon.** A television-type pick-up tube in which a low velocity electron beam scans a photoactive mosaic which has electrical storage capability.

**Photoconductive detector.** Apparatus used to detect and/or measure radiant energy by the change in the electrical resistance of a material such as lead sulfide (doped with the proper amount of certain impurities).

## GLOSSARY (Cont.)

Radiation law, Planck's. The spectral radiant emittance of a black body can be expressed by the following formula

$$W_{\lambda} = C_1 / \left[ \lambda^5 (e^{C_2/\lambda T} - 1) \right]$$

The spectral emittance  $W_{\lambda}$  will have units of (watt/cm<sup>2</sup>μ) if

$$C_1 = 3.741 \times 10^4 \text{ watt } \mu^4/\text{cm}^2, \text{ (NBS, 1960)}$$

$$C_2 = 14330^\circ \text{ K}\mu, \text{ (NBS, 1960)}$$

T = absolute temperature of the black body, °K

λ = wavelength, μ

Radiation law, Wien's. An empirical law which is almost identical with Planck's radiation law at short wavelengths, and is simpler to use, is the following

$$W_{\lambda} = C_1 / \left[ \lambda^5 (e^{C_2/\lambda T} - 1) \right]$$

The symbols have the same meanings as those given above for Planck's radiation law.

Spectrograph. An instrument used to produce a record of a spectrum. It includes the apparatus for separating the radiation into a spectrum and for recording the spectrum.

Spectrometer. An instrument used to determine the wavelength distribution of radiation, usually including apparatus for intensity as a function of wavelength.

Spectrum. A visual display, photographic record, or plot of the distribution of the intensity of radiation of a given kind, usually as a function of its wavelength or frequency.

Spectrum, band. The type of spectrum produced by molecules, characterized by groups (bands) of closely spaced spectrum lines.

Spectrum, continuous. Radiation characterized by a continuous variation of intensity with wavelength, distinguished from line or band spectra. Radiation due to thermal agitation of atoms or molecules produces a continuous spectrum.

Spectrum, infrared. The portion of the electromagnetic spectrum which comprises radiation within the wavelength region extending from the visible red at about 0.75 μ to about 300 μ.

Spectrum, line. The spectrum associated with changes in the energy states of atoms, characterized by emission or absorption of radiation at discrete wavelengths.

Spectrum, ultraviolet. The portion of the electromagnetic spectrum that extends from the violet portion of the visible spectrum at 0.39 to 0.40 μ to shorter wavelengths, as far as about 0.02 μ.

Spectrum, visible. The portion of the electromagnetic spectrum, extending from about 0.38 μ to about 0.70 μ, which is capable of producing a visual sensation in the human eye.

Wave number. The reciprocal of the wavelength of a harmonic wave. Sometimes,  $2\pi/\lambda$  is used instead of  $1/\lambda$ .

## APPENDIX A

### INSTRUMENTATION

#### A-1 INTRODUCTION

Most of the spectral studies reported in this handbook were conducted between ten and twenty years ago. In analyzing the results, therefore, it is necessary to bear in mind the limitations of the apparatus that was available at that time. In this appendix an attempt is made to provide, within the limits of available information, a description of the instruments that is reasonably adequate for evaluating the data reported.

#### A-2 SPECIAL CALIBER .50 TEST GUN

The gun used in most of the spectral studies was a caliber .50 gun, chambered to take 20-mm cases which were necked down for caliber .50 projectiles. The gun was designed at The Franklin Institute for high-pressure work. The tube had an outside diameter of 1-5/8 in. and a length of 45 in., of which 40 in. were rifled. It had 8 lands,

*NOTE: All Dimensions in Inches*

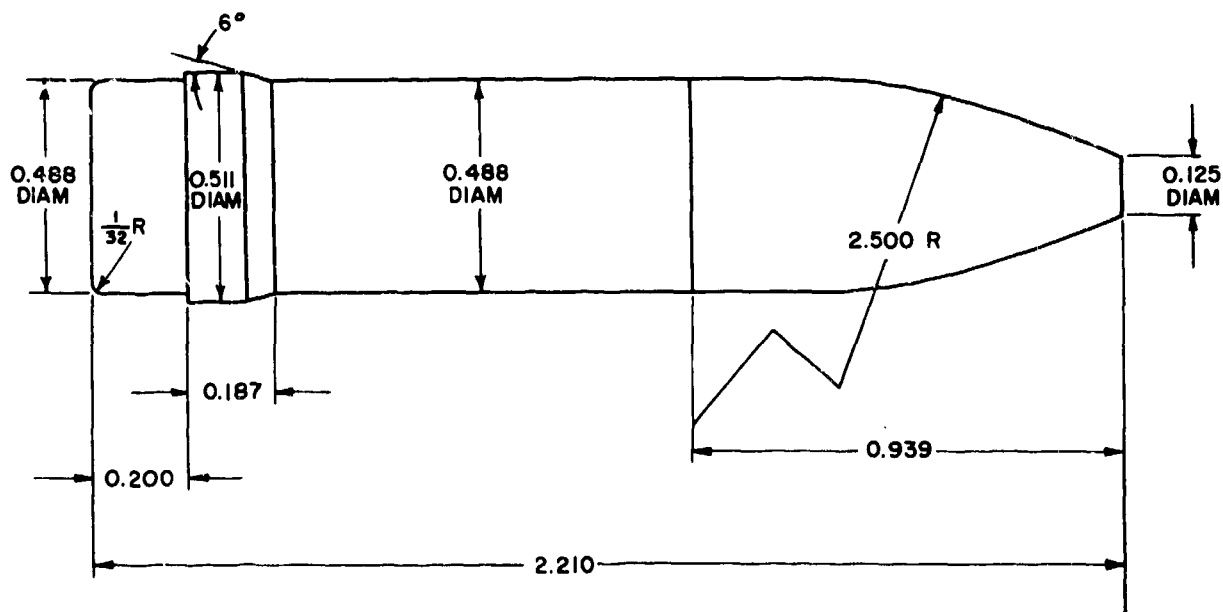


FIGURE A-1—SPECIAL ARTILLERY-TYPE, BANDED STEEL PROJECTILE

and the groove depth was 0.010 in., twice the depth in the standard caliber .50 Browning machine gun. To obtain the 85-in. length used for some tests, the rifled portion of a tube was coupled and clamped to another tube. Although it was called a caliber .50 gun, the bore diameter was actually 0.490 in. In addition to Ball M2 projectiles, special artillery-type, banded steel projectiles of the design shown in Figure A-1 were used.

#### A-3 COMMERCIAL INSTRUMENTS <sup>4(c)</sup>

Much of the equipment used for the study of flash spectra at The Franklin Institute was developed by the researchers themselves; descriptions are given in the following subparagraphs of this appendix. Prior to the development of special equipment, however, some of the work was conducted with commercial instruments. These included the following:

- a. Large Littrow spectrograph.
- b. Hilger medium quartz spectrograph (this was reported to be the most useful of the commercial spectrographs available).
- c. Hilger glass, constant-deviation spectrograph.
- d. Small Hilger spectrograph.
- e. Leeds and Northrup microphotometer, used for automatic recording of plate density.
- f. Gaertner spectrogram comparator for determination of wavelength of spectrum lines and sharply defined bands. When lines or bands were diffuse or broad, a modification of this instrument was used for measuring the position of maximum density.
- g. Fastax high speed 16-mm movie camera.

#### A-4 THE IMAGE ORTHICON TUBE <sup>4(a)</sup>

The image orthicon tube used in the spectroscopic studies was the RCA Type 2P23, which was a recently developed television pick-up tube at the time of the studies. Its function is to convert an optical image into an electrical signal. Its advantages were that it was more sensitive than available photographic emulsions and that its sensitivity extended farther into the infrared than any stable emulsions then available. The orthicon also had the advantage that spectra could be obtained at several times during a single flash, thus showing its development in time.

Presentation of the signal was made by means of an oscilloscope, the electron beam of which was synchronized in the horizontal direction with the scanning electron beam of the image orthicon. The signal amplitude appeared as a vertical deflection on the oscilloscope screen, giving a plot of intensity versus wavelength. This plot was photographed for a permanent record. To obtain the variation of spectra with time, the tube was scanned more than once during a single flash; and the succeeding intensity-wavelength plots were displaced vertically on the oscilloscope screen.

A-2

Originally, the circuitry was such that each scan of the orthicon target required 1/60 sec for completion; therefore, each trace represented the integrated intensity of the preceding 1/60 sec interval of the flash. Subsequently, the orthicon circuits were adapted for *single sweep* operation so that a given portion of the orthicon target could be scanned at predetermined times — the interval between scans being much longer than the duration of each scan. <sup>5(a), 5(b)</sup>

#### A-5 INFRARED MONOCHROMATOR WITH PHOTOTHERMAL DETECTOR <sup>6(a)</sup>

This instrument consisted of a low-dispersion monochromator used with a photothermal detector developed by the U. S. Army Signal Corps. It made it possible to determine the spectral distribution of gun flash from the visible portion of the spectrum to 25  $\mu$ . The radiant energy was dispersed by either a sodium chloride or a potassium bromide prism, then collimated and focused onto the detector.

The design of the infrared monochromator is shown in Figure A-2. The two small sections of the same large parabolic mirror, used respectively for collimation ( $M_1$ ) and for focusing ( $M_4$ ), were essentially equivalent to two small off-axis parabolic mirrors. As can be seen in Figure A-2, the radiation entered slit  $S_1$ , striking parabolic mirror  $M_1$ . From there, parallel rays traveled to the 60° prism of sodium chloride. The prism and mirror  $M_2$  were arranged according to the Wadsworth<sup>29</sup> type of mounting, such that the rays that passed through the prism at the angle of minimum deviation were reflected from plane mirror  $M_2$  in a direction making an angle with the incident rays of twice the angle between the perpendicular to the prism base and a line parallel to the face of  $M_2$ . Hence, for this monochromator, the total deviation of the rays that passed through the prism at the angle of minimum deviation was 90°.

Parallel rays were reflected from mirror  $M_2$  onto plane mirror  $M_3$  and were again deviated through 90° to mirror  $M_4$ , which would ordinarily refocus them at the slit  $S_1$ ; but plane mirror  $M_5$  was interposed in their path to deflect the rays through slit  $S_2$ , which

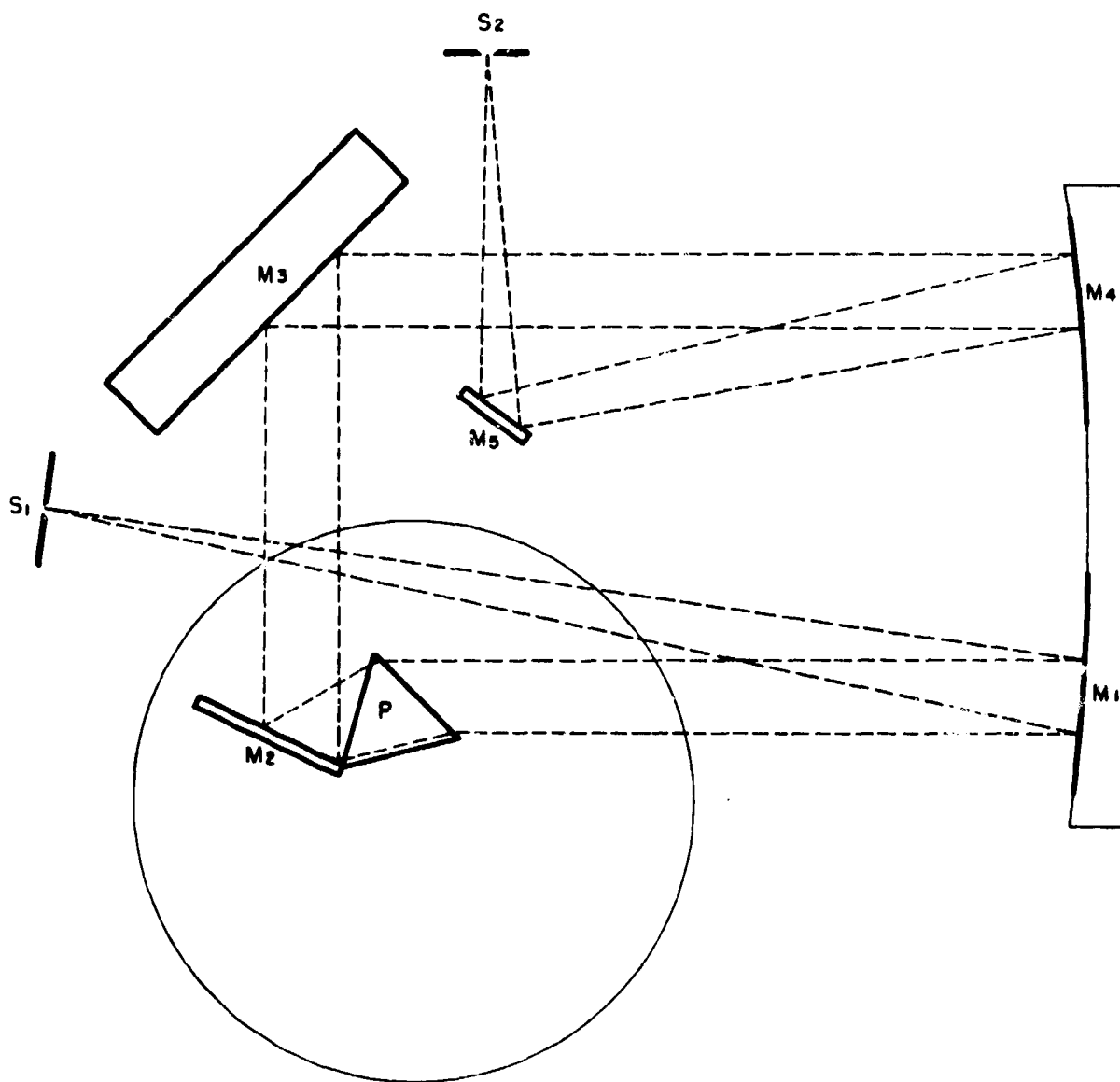


FIGURE A-2—SCHEMATIC DIAGRAM OF MONOCHROMATOR (FROM REF. 6a)

was mounted on the photothermal detector. The signal from the detector was amplified electronically and fed to the vertical plates of an oscilloscope, and the resultant pattern on the oscilloscope screen was photographed.

An air-tight cover for the apparatus served the purpose of providing a dry atmosphere for the salt prism. During tests,

radiation was allowed to enter slit S<sub>1</sub> by opening a gate in the cover.

Calibration of the monochromator over the range between 0.5 and 20  $\mu$  was carried out by means of several prominent mercury lines (Hg arc) as well as by means of the radiation from a blackened brass cylinder at 1000°F.

### A-6 LARGE-APERTURE SPECTROGRAPH FOR VISIBLE AND NEAR-INFRARED RADIATION. 4(a)

This spectrograph was designed to increase the light gathering power of the spectrographic equipment, especially to facilitate observation of the relatively weak (primary and intermediate) components of flash. The sensitivity was further increased by replacing the photographic plate with an image orthicon tube.

The plan of the spectrograph-orthicon assembly is shown in Figure A-3. The various components were mounted on a surface plate to insure rigidity and freedom from warping. The slit could be quickly removed and replaced. Five fixed slits of width 10, 25, 50, 100, and 200  $\mu$  were available. In addition, a *pinhole slit* was provided for use when a point source was desired to facilitate alignments of the apparatus. Just behind the slit, there was a shutter which could be operated either manually or electrically. Both the collimator and the objective were compound lenses (shown in the diagram as simple lenses), corrected for the usual lens aberrations. The f/4 collimator has a focal length of 12 mm.

After traversing the collimator the parallel beam of light was dispersed by two 60-deg prisms which had the following characteristics:

- Glass — extra dense flint
- Index of refraction (sodium light) — 1.649
- Length — Prism 1 — 77 mm  
Prism 2 — 91 mm
- Height — 50 mm

The prisms were so mounted that the yellow mercury lines at 5770-5791 A passed through at minimum deviation.

After dispersion by the prisms, the light was brought to a focus on either the photographic plate or the orthicon cathode by the f/2.5 objective lens, which had a focal length of 178 mm.

A plane front-surface, aluminum-coated mirror could be used — as shown in Figure A-3 — to deflect the beam to the sensi-

tive surface of the orthicon tube. The mirror was positioned by two dowel pins to insure reproducibility of position.

The optical parts were enclosed in a light-tight box with suitable baffles to exclude stray light. A graflex camera-back and a plate-holder (3-1/4 in. x 4-1/4 in.) were adapted for use as the spectrograph camera. The camera was attached to the main body of the spectrograph by flexible bellows which permitted adjustment for optimum focus.

The length of the spectrum, from 4000 to 10,000 A, was approximately 1-3/8 inches. The image orthicon was designed for an image length of at least 1-1/2 in., which was sufficient to include space at each end of the spectrum for the provision of a zero-intensity base line on the recording oscilloscope.

### A-7 TEN-CHANNEL INFRARED SPECTROMETER 7(a), 7(b)

This spectrometer utilized two sodium chloride prisms mounted in a double Wadsworth arrangement.<sup>29</sup> A bank of ten exit slits were situated in the focal plane, and the radiation passing through the various slit openings was conducted to Golay photo-thermal detectors by means of ten silver tubes. Lead sulfide photoconductive cells were used because of their availability and good frequency response. The production of a satisfactory surface on the inside of the silver tubes was obtained by drawing a series of swaging plugs very slowly and steadily through tubes which had been previously highly polished by the manufacturer. The final passage through the tube was made with a highly polished steel ball bearing. Signals from the ten detectors were presented simultaneously on one oscilloscope screen by means of a ten-channel electronic switch.

A schematic diagram (plan view) of the optical system is shown in Figure A-4. An off-axis parabolic mirror  $M_1$  is used to collimate the incident radiation. The collimated beam is then reflected to the first prism by a plane mirror  $M_2$ . Upon emergence from the second prism the beam was split into two parts by mirrors as shown in Figure A-5.

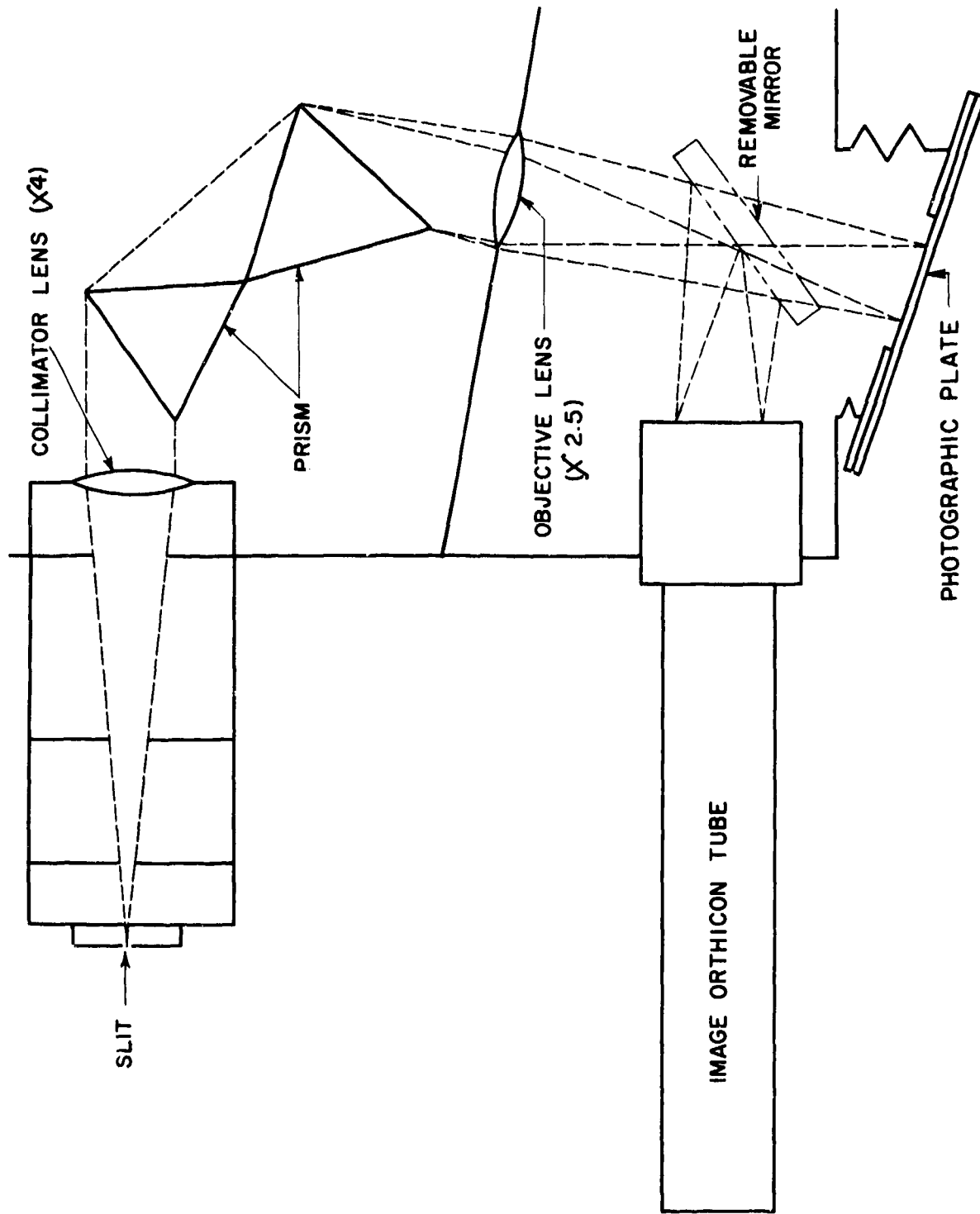


FIGURE A — 3 — SCHEMATIC DIAGRAM OF LARGE APERTURE SPECTROGRAPH (FROM REF. 4a)

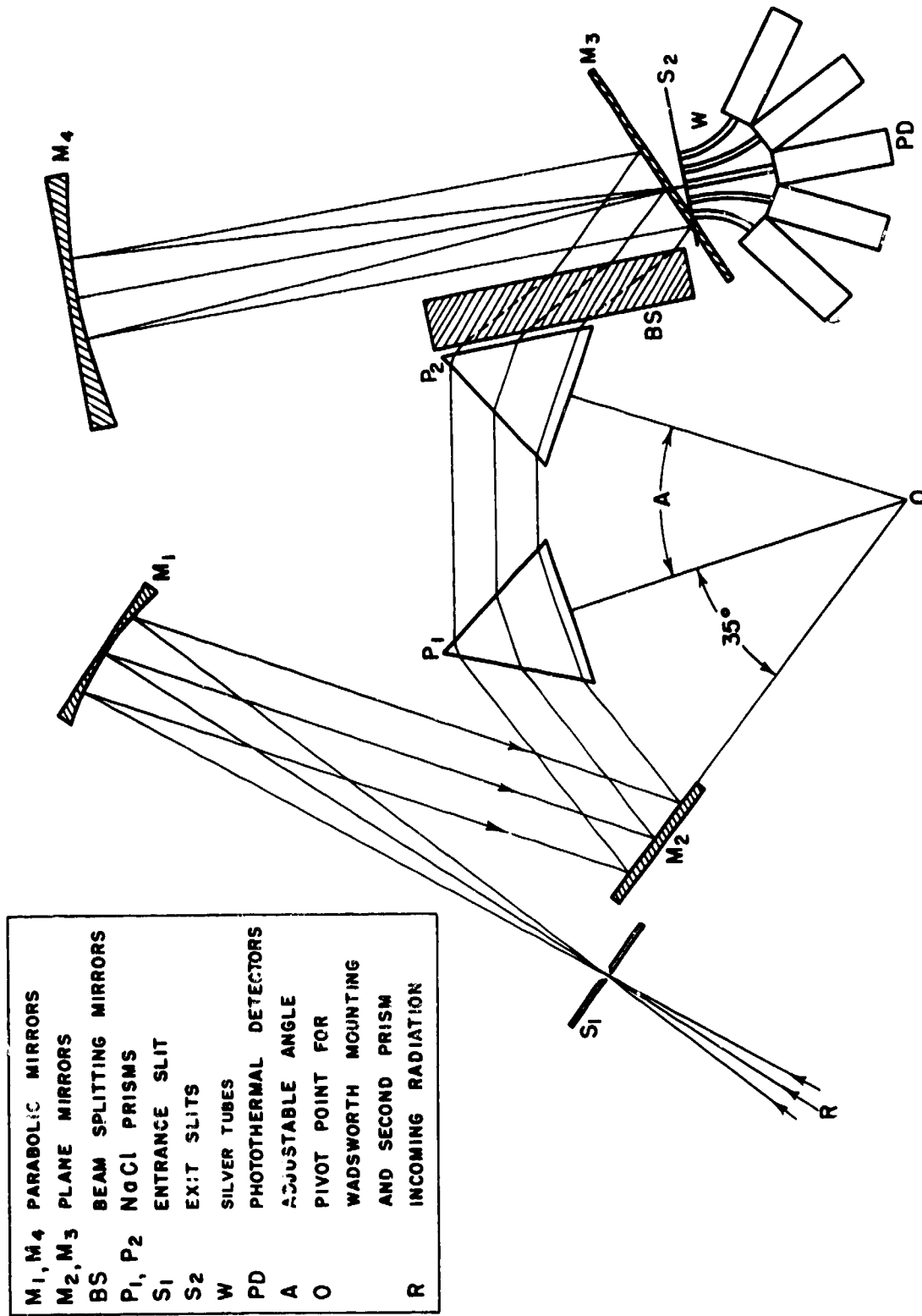
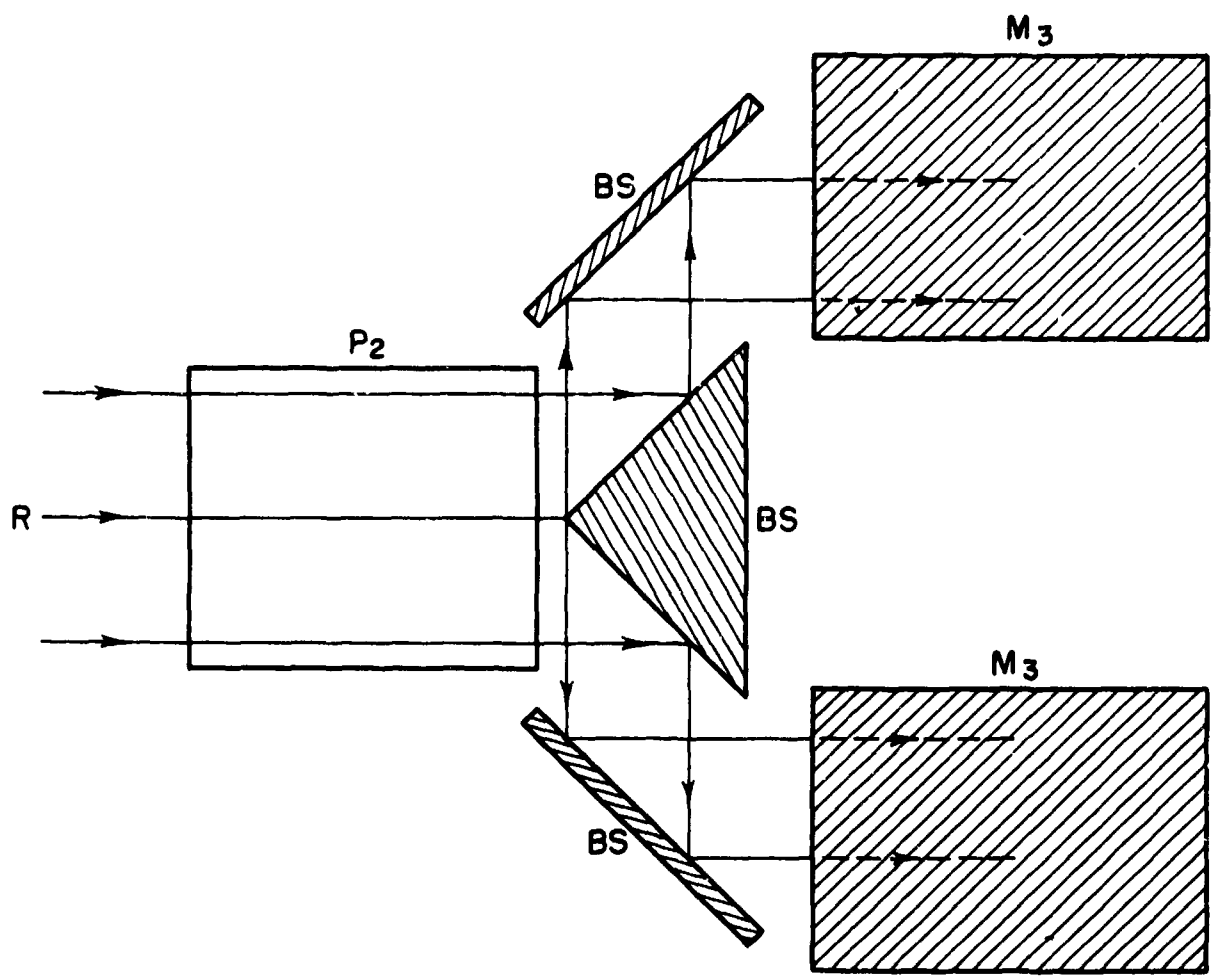


FIGURE A-4—OPTICAL SYSTEM OF INFRARED SPECTROGRAPH (REF. 7a)  
(PLAN VIEW)



P <sub>2</sub>	NaCl PRISM
BS	BEAM SPLITTING MIRRORS
M <sub>3</sub>	PLANE MIRRORS
R	RADIATION

FIGURE A-5 — BEAM SPLITTING MIRRORS FOR INFRARED SPECTROGRAPH (FROM REF. 7a)  
(ELEVATION)

These beam-splitting mirrors, shown as BS, were mounted as a unit on the prism table so that their position relative to the second dispersing prism remained unchanged as the prisms were rotated. The two beams were then reflected by the two coplanar mirrors  $M_3$  to an 8-in. diameter, 13-in. focal length on-axis parabolic mirror  $M_4$ . Due to lack of space, the mirrors  $M_3$  could not be mounted as Wadsworth mirrors; instead, they were mounted directly on the base plate of the spectrograph in a fixed position. Since the prism tables were to be rotated only through a small angle, it was felt that such an arrangement would be entirely satisfactory. Finally, mirror  $M_4$  focused the two beams on the slit block  $S_2$  which lay between the two parts of mirror  $M_3$ . Thus, none of the incident radiation was lost.

All the slits were placed in two rows on the slit block, symmetrically just above and below the optical axis. The silver tubes were arranged to make the radiation enter them as nearly axially as possible to avoid the higher attenuation that otherwise occurred within the tubes. When the collimating mirror was suitably diaphragmed to exclude approximately the upper and lower tenth of the beam, the ratio of the intensities through the various channels remained constant to within a few percent as the aperture was decreased.

The entire spectrograph was shock-mounted to avoid damage to the equipment during transportation to various places where observations were to be made.

Calibration curves were obtained by locating the mercury arc emission lines at 1.014, 1.13, 1.37 and 1.69  $\mu$ ; the characteristic absorption bands of atmospheric water vapor and carbon dioxide at 2.67 and 4.25  $\mu$ ; and, of furfural at 5.92, 6.39, 6.8, 7.16, 7.82, 8.66 and 9.27  $\mu$ . It was found that the calibration was a function of ambient temperature, probably due to variations in coefficients of thermal expansion of the many metal parts in the instrument. The final calibration was made at 90°F which was maintained by a thermostatically controlled bank of heaters on the sub-structure of the cast iron surface plate forming the base of the spectrograph. The temperature of 90°F was

chosen as being above any that would be reached under normal operating conditions.

In addition to the wavelength calibration an attempt was made to determine the relative signal amplitude of the various channels. The purpose of this calibration was to account for the following attenuation factors:

- (a) Detector sensitivity;
- (b) Attenuation due to propagation through the silver tubes;
- (c) Attenuation due to the optical system.

As a fraction of the most sensitive channel, No. 9, the following relative sensitivities were obtained: <sup>7(b)</sup>

Channel	Relative Sensitivity
9	1.000
5	0.710
7	0.546
10	0.514
4	0.510
8	0.491
2	0.352
6	0.153
1	0.132
3	0.100

In general, an attempt was made to arrange the detectors and waveguides in combinations that would give high sensitivity in regions of the spectrum where weak radiation was expected, and vice versa.

#### A-8 MODIFIED TEN-CHANNEL INFRARED SPECTROMETER <sup>8(a), 8(b)</sup>

The optical system of a modified version of the spectrometer described in Appendix A-7 is shown in Figure A-6. The Golay detectors of the original instrument were replaced because their frequency response was not high enough for recording flash as a function of time. They were replaced by an assembly of Ektron cells consisting of 10 elements, each 1 mm wide and spaced 1/2 mm apart. The use of these cells reduced the

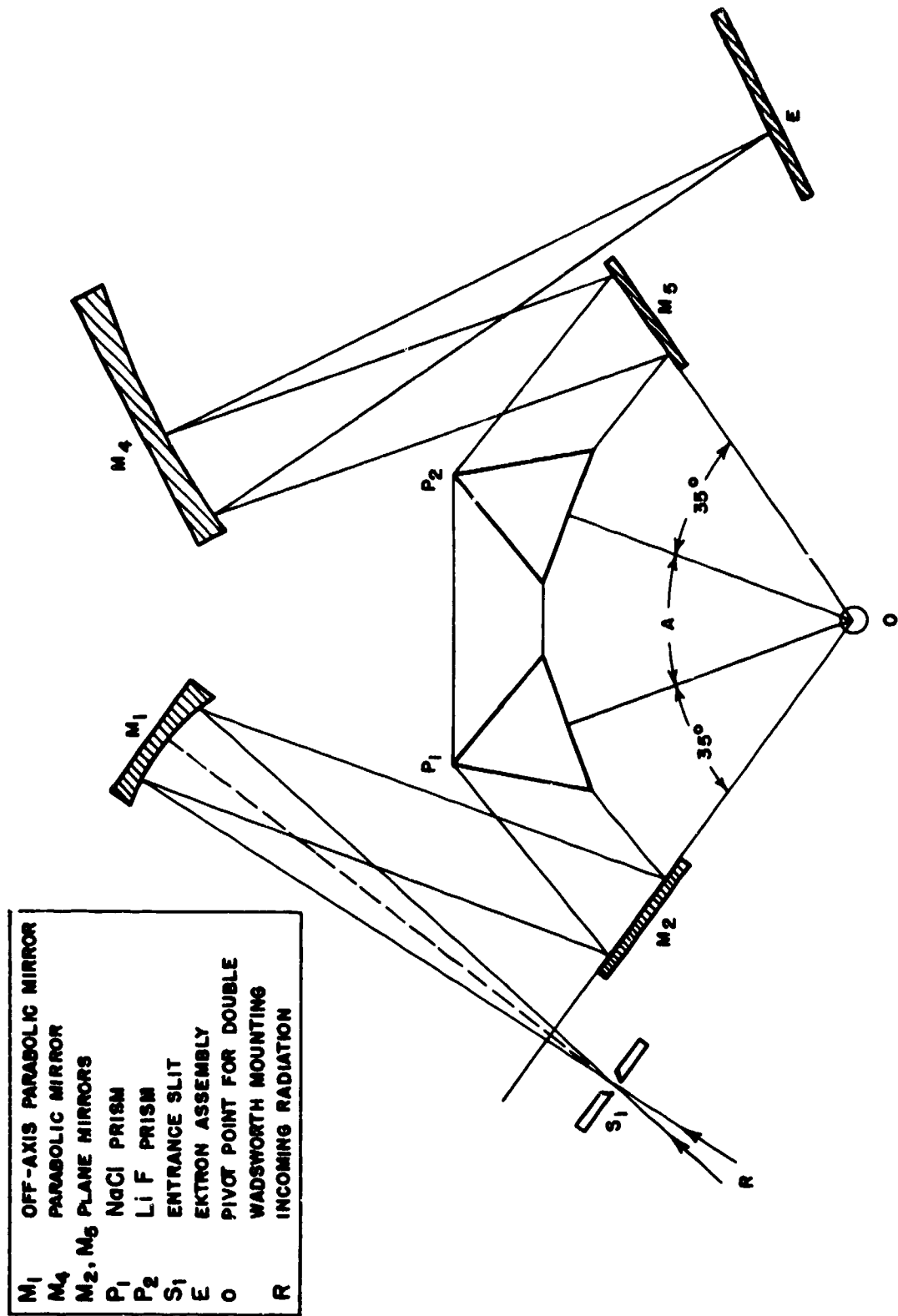


FIGURE A-6—OPTICAL SYSTEM OF THE MODIFIED TEN-CHANNEL SPECTROMETER (FROM REF. 86)

spectral range of the instrument since they are not sensitive beyond  $3.6\ \mu$ , but their convenient size allowed simplification of the optical system.

This spectrometer was used to obtain the data on the spectral emittance of a 155-mm gun shown in Figures 3-3 and 3-5 of par. 3-3. Subsequently, the wavelength band-pass falling on each Ektron cell was reduced by placing a limiting aperture in front of the Ektron cell assembly. Each slit was 0.010 in. wide and they were spaced 0.050 in. apart. The linear dispersion of the instrument was also altered slightly. Subsequent to these changes, additional observations of flash from a 155-mm gun were made as described in par. 3-4.

#### A-9 EIGHTEEN-CHANNEL INFRARED SPECTROMETER <sup>8(c), 8(e)</sup>

The optical parts of the spectrometer are shown in Figure A-7. The radiation entering slit  $S_1$  was collimated by mirror  $M_1$ . This radiation was reflected by mirror  $M_2$  onto prism  $P_1$  (LiF). After traversing the prism, the radiation was reflected by  $M_3$  and

focused by the parabolic mirror  $M_4$  onto the 18-element detector. The elements of this assembly were  $1/2$  mm wide, and they were spaced  $1/4$  mm apart. These were typical Ektron detectors, having a  $200\ \mu$ sec time constant and a 2 megohm resistance.

The average wavelength band that the spectrometer passed in the region between 1 and  $3.5\ \mu$  was: (a)  $0.07\ \mu$  when the  $50\text{-}\mu$  slit was used to observe secondary flashes, and (b)  $0.14\ \mu$  when the  $500\text{-}\mu$  slit was used to observe intermediate flashes.

The radiation falling on each element of this assembly was transformed into electrical energy, which was then amplified by 18 individual amplifiers. The electrical outputs from the power amplifiers drove individual galvanometers in an 18-channel recording oscillograph (Consolidated Engineering 5-114-P4). The frequency response of the entire system — including the Ektron detectors, amplifiers and recording oscillograph — was flat from  $1/2$  to 500 cycles/sec.

A block diagram of the detecting and recording system of the 18-channel spectrometer is shown in Figure A-8.

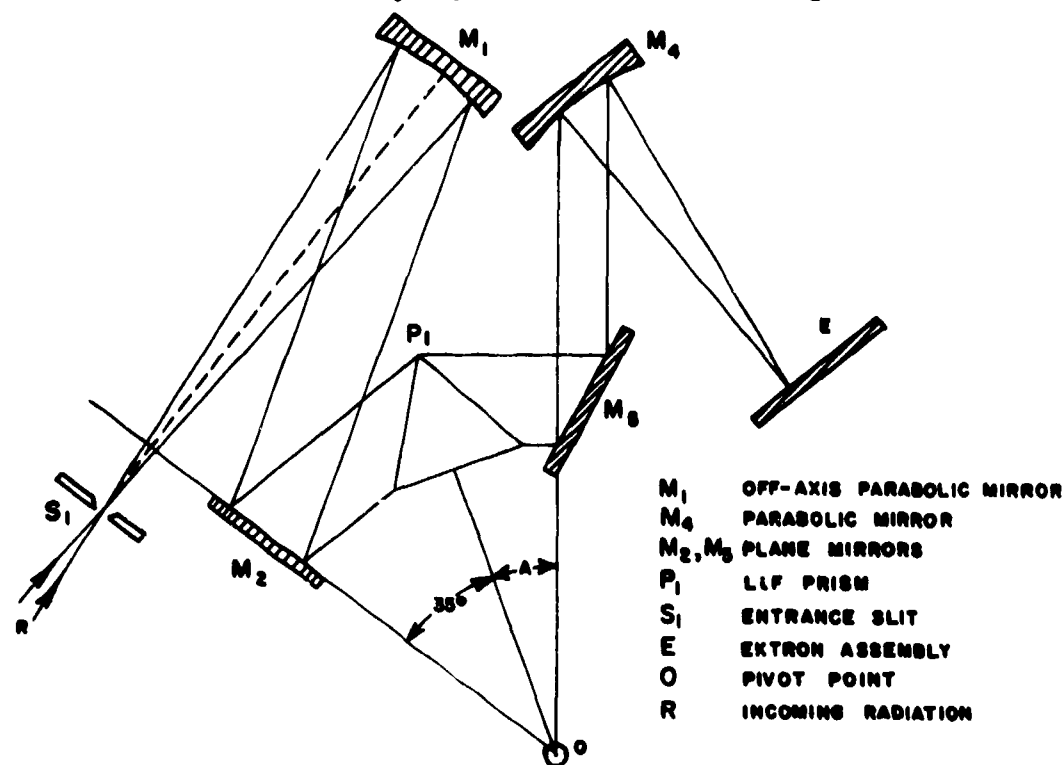


FIGURE A-7—OPTICAL SYSTEM OF THE 18-CHANNEL SPECTROMETER (FROM REF. 8e)

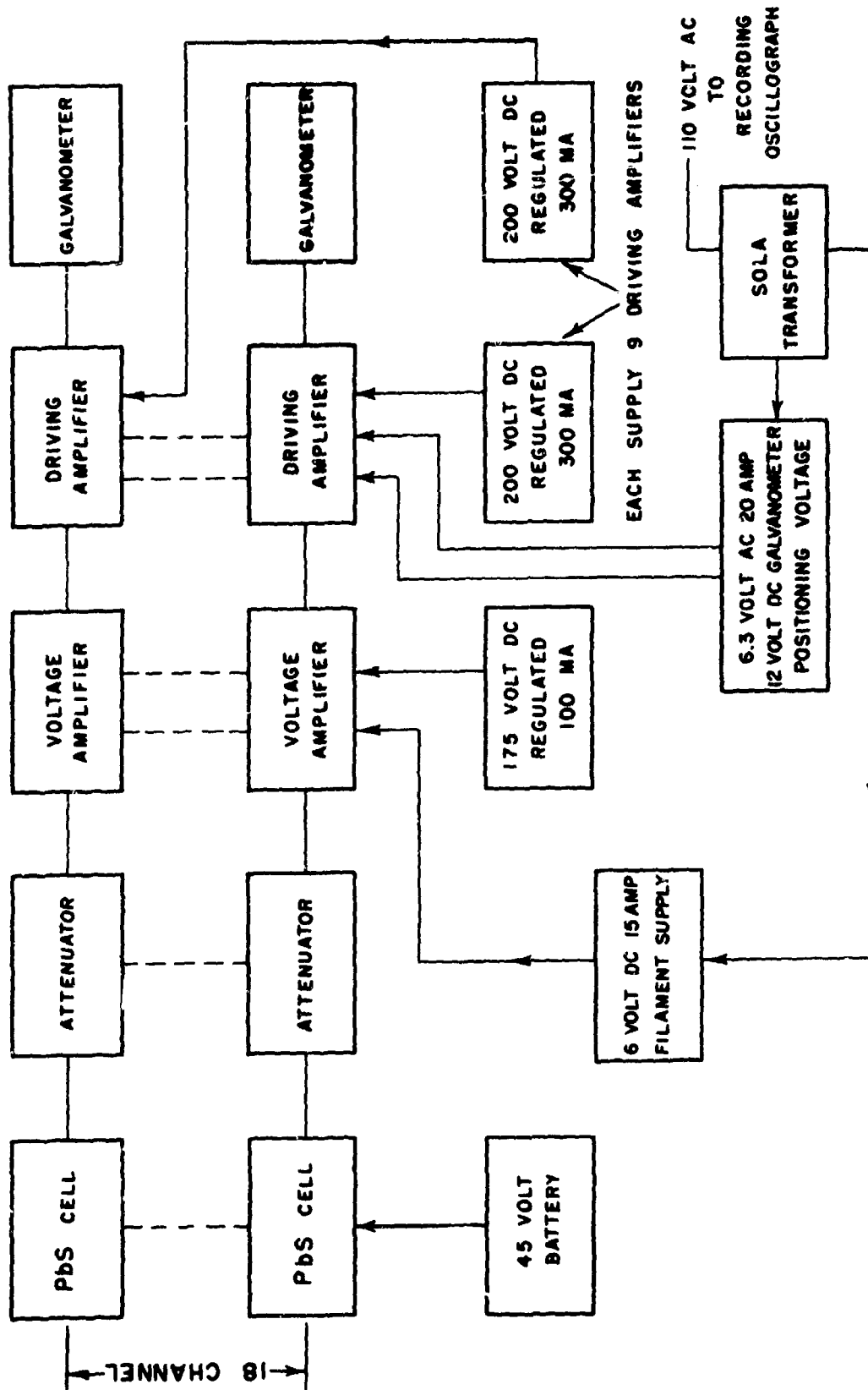


FIGURE A-8 — BLOCK DIAGRAM OF THE DETECTING AND RECORDING SYSTEM OF THE 18-CHANNEL SPECTROMETER (FROM REF. 8c)

**APPENDIX B**  
**COMPUTATIONS FOR DATA IN FIGURE 3-1**

The procedures for reducing relative spectral intensity data for secondary flash produced by a 155-mm gun in order to plot the curves in Figure 3-1 are described in this Appendix.

Table B-1 is a complete summary of the data obtained at the actual wavelengths used in the tests. The symbols used in Table B-1 have the following significance:

$I_{200}^{obs}$  = observed relative intensity at the 200-ft position.

$I_{500}^{obs}$  = observed relative intensity at the 500-ft position.

$I_{500}^{calc}$  = calculated relative intensity at the 500-ft position, corrected for aperture.

$I_{1350}^{obs}$  = observed relative intensity at the 1350-ft position.

$I_{1350}^{calc}$  = calculated relative intensity at the 1350-ft position, corrected for aperture and atmospheric absorption.

$\alpha_{300}$  = absorption of the atmosphere corresponding to a distance of 300 ft, as determined by the formula:

$$\frac{I_{200}^{obs}}{I_{500}^{calc}} = e^{\alpha_{300}}$$

$\alpha_{200}$  = absorption of atmosphere corresponding to a distance of 200 ft, as determined by the formula:

$$\alpha_{200} = \frac{2}{3} \alpha_{300}$$

$I_0$  = relative intensity at the source, as determined by the formula:

$$I_0 = I_{200} e^{\alpha_{200}}$$

$k$  = absorption coefficient of the atmosphere as defined by the formula:

$\alpha = kd$ , where  $d$  is the distance in feet.

The data in Table B-1 are plotted in Figure 3-1. The actual data points are indicated, and the smooth curves were obtained by calculation of intermediate points. The bases for calculation and construction of the curves were as follows:

Curve B, corresponding to a distance of 200 ft, was constructed first—with primary consideration being given to the known prominent absorption and emission bands of water vapor and carbon dioxide and the resolving power of the spectrograph effected by the use of a 750- $\mu$  entrance slit. Curve D for the distance of 500 ft was constructed with the same consideration in mind.

A correction was then applied to the data obtained at a distance of 500 ft to account for the decreased aperture relative to the aperture at the 200-ft distance. Calculations based upon the observed size of the flash indicated that, with the spectrograph in the 200-ft position, the aperture was 57.9 percent filled. A similar calculation for the 500-ft position gave a value of 18.8 percent. Thus, it was necessary to multiply the values of intensity on Curve D by  $57.9/18.8 = 3.08$  in order to obtain comparable values. Curve C in Figure 3-1 is simply Curve D multiplied by this factor.

TABLE B-1  
 RELATIVE INTENSITY OF RADIATION FROM SECONDARY FLASH  
 PRODUCED BY 155-mm GUN AS A FUNCTION OF WAVELENGTH AND DISTANCE  
 FROM SOURCE (From Ref. 7b)

Wavelength ( $\mu$ )	$I_{200}^{obs}$	$I_{500}^{obs}$	$I_{500}^{calc}$ = $I_{500}^{obs} \times 3.08$	$I_{200}^{obs}/I_{500}^{calc}$	$\alpha_{300}$ = $k(500-200)$	$\alpha_{200}$ = $k(200-0)$	$I_o$	$I_{1350}^{obs}$	$I_{1350}^{calc}$
1.00	1.68								
1.10	4.43								
1.30	9.03	0.90	2.77	3.26	1.182	0.788	19.85		
1.64	15.77	1.69	5.20	3.03	1.109	0.740	33.03	0.27*	
2.00	37.67	4.45	13.71	2.75	1.012	0.675	73.98	0.48	0.035
2.62	25.25	2.64	8.13	3.11	1.135	0.757	53.83		
2.74	98.60	7.02	21.61	4.56	1.519	1.014	271.8		
3.22	54.38	6.85	21.09	2.58	0.948	0.632	102.4		
3.44	16.92	2.57	7.92	2.14	0.760	0.507	28.09		
3.86	7.70	1.40	4.31	1.79	0.582	0.388	11.35		
3.94	10.21	1.17	3.60	2.86	1.051	0.701	22.17		
4.60	39.66	5.5**	16.85	2.34	0.852	0.568	70.0	0.72	
4.64	41.13	6.36	19.58	2.10	0.742	0.495	67.45	1.81* 1.00	0.107
5.10	20.78	2.53	7.79	2.67	0.982	0.656	40.02		
5.47	2.94	0.31	0.95	3.10	1.132	0.757	6.28		
5.80	0.65								
6.20	0.43								
6.34	0.18								
6.62	0.30								
6.92	0.89								
7.0	0.94								
7.16	1.91								
7.50	3.51	0.56	1.73	2.03	0.708	0.472	5.64		
8.10	3.80	0.59	1.82	2.09	0.737	0.492	6.22		
8.32	3.98	0.52	1.60	2.49	0.912	0.608	7.32		
8.62		0.46	1.42						
9.12	1.70								
9.3	1.69								
9.56	0.87								

\*With supercharged round.  
 \*\*From Curve D, Figure 3-1.

By having values for  $I_{200}^{obs}$  and  $I_{500}^{calc}$ , it was then possible to calculate  $I_o$ , the intensity at the source, by means of the relation

$$I_o = I_x e^{kx} \quad (B-1)$$

where

$k$  = the absorption coefficient of the atmosphere at a particular wavelength

$x$  = the distance between the source and the detector

$I_o$  = the source intensity

and

$I_x$  = the intensity at distance  $x$

Thus,

$$I_o = I_{200}^{obs} e^{200k} \quad (B-2)$$

$$I_o = I_{500}^{calc} e^{500k} \quad (B-3)$$

and

$$\frac{I_{200}^{obs}}{I_{500}^{calc}} = e^{(500 - 200)k} = e^{300k} \quad (B-4)$$

Since  $k$  was assumed constant, the symbol  $\alpha_{300}$  was substituted for  $300k$  and the relationships used to calculate  $I_o$  were

$$\frac{I_{200}^{obs}}{I_{500}^{calc}} = e^{\alpha_{300}}$$

$$\alpha_{200} = 2/3 \alpha_{300}$$

and

$$\frac{I_o}{I_{200}^{obs}} = e^{\alpha_{200}}$$

This allowed the calculation of the values of  $I_o$  and the construction of Curve A in Figure 3-1.

The values of  $I_{1350}^{calc}$  were calculated on the basis of the values of  $I_{200}^{obs}$  and  $I_{500}^{calc}$ , with proper correction being made for atmospheric absorption and the increased field of view at 1350 ft.

It can be seen in Table B-1 that a wide discrepancy exists at 2.0 and 4.64  $\mu$  between the values of  $I_{1350}^{obs}$  and  $I_{1350}^{calc}$ . It did not seem likely that such wide discrepancies as indicated (12.63X at 2.0  $\mu$  and 9.35X at 4.64  $\mu$ ) were due to either experimental or analytical inaccuracies. The most logical explanation appeared to be on the basis of a definite physical effect, such as reflection of radiation from the grassy field between the gun and the spectrograph. <sup>7(b)</sup>

**APPENDIX C**  
**TABLE OF PROPELLANT PROPERTIES**

TABLE C-1

<u>Propellant</u>	<u>M6</u>	<u>E.X6332</u>	<u>EX6333</u>	<u>DMR4996*</u>	<u>Glazed Cordite N</u>
<b>Composition (% by weight)</b>					
Nitrocellulose	87	88.29	88.47	88.29	
(% Nitrogen in Nitrocellulose)	13.2	13.15			19.0
Guncotton and Chalk					18.75
Nitroglycerins		0.65	0.57	0.65	
Diphenylamine	1			9.7	
Dinitrotoluene	10	8.96 (Coating)	9.29 (Coating)		
Picrite					54.7
Centralite					7.25
Chalk					0.20
Graphite					0.25
Potassium Sulfate		0.59		0.59	
Residual Solvent			0.88		
Moisture	0.6		0.79		
Total Volatiles	4		1.67		
Moisture and Volatile Ash			0.80		Not greater than 0.30
<b>Physical Properties</b>					
Specific Gravity					Not less than 1.630
Calorific Value (cal/gm.)					758
<b>Grain Dimensions (in.)</b>					
Length		0.0838	0.0831	0.0840	0.086
Diameter		0.0704	0.0677	0.0691	
Diameter of Perforation		0.0084	0.0086	0.0074	
Web (average)		0.0310	0.0295	0.0309	
External Diameter					0.0696
Internal Diameter					0.0146
Annulus					0.0275

\*DMR is an abbreviation for Improved Military Rifle.

